2023-05-01

Assessing Technology Options to Reduce the Carbon Intensity of Bioethanol Production

Oke, Kafayat Adesewa

UNIVERSITY OF CALGARY

Assessing Technology Options to Reduce the Carbon Intensity of Bioethanol Production

by

Kafayat Adesewa Oke

A THESIS

SUBMITTED TO THE FACULTY OF GRADUATE STUDIES

IN PARTIAL FULFILMENT OF THE REQUIREMENTS FOR THE

DEGREE OF MASTER OF SCIENCE

GRADUATE PROGRAM IN CHEMICAL ENGINEERING

CALGARY, ALBERTA

MAY, 2023

Abstract

Significant reductions in carbon dioxide (CO_2) emissions are required to mitigate the effects of climate change. For hard-to-abate sectors like transportation, the use of biofuels is playing and will play a growing role in decarbonization. While much research has focused on the environmental benefits of second-generation biofuels, technological advances could apply to the production of the most widely used biofuel in transport today: first-generation bioethanol. This could reduce its carbon intensity in the short term, thereby increasing its competitiveness as a transportation fuel and opening new possibilities for its usage as a feedstock for chemicals before alternative technologies, such as electric vehicles and lignocellulosic-based biofuel, can be deployed at scale.

This thesis evaluates two technology options for their potential to reduce the carbon intensity of corn ethanol using Aspen Plus® simulation coupled with techno-economic and life cycle assessment. The first option is the capture of fermentation emissions and oxycombustion capture of fossil fuel-based emissions for steam utility provision in the ethanol production step of the life cycle. In lieu of this, the electrification of process heat provision through the integration of heat pumps is investigated.

Capturing the emissions has the potential of removing up to 99.6% of total emission, which is 187 ktCO_2 annually in a 40 MGY dry grind ethanol mill, at an additional purchased equipment cost of $15.5M, with the composition of the compressed CO_2 meeting a pipeline transport requirement. In the alternative electrification scenario, there is a 63% reduction from 7.55MJ/L in the base plant heat demand, with a 259% increase in electricity demand at an additional purchased equipment cost of $8.7M. LCA and TEA results showed a net reduction of the life cycle carbon intensity by 84% to 8.9 gCO_2eq/MJ when both biogenic and fossil CO_2 are captured

at the cost of 95 USD/t_{CO2}. There is almost no change to life cycle emissions in the electrification case due to the relatively high carbon intensity of the current US electricity grid. However, the life cycle carbon intensity can be reduced by 113% to -7.1 gCO_2eq/MJ when zero-emission renewable electricity is introduced with all technology interventions.

Preface

Acknowledgements

Dr. Sean McCoy: words fail me to express how incredibly grateful I am for the chance to work with your research group at the University of Calgary. I am a better academic today through your insightful and enlightening discussions, constructive feedback, and indefatigable support. Thank you very much.

My research collaborators, John Dees, Hannah Goldstein, A.J Simon, Daniel Sanchez, and Wenqin Li: I appreciate your perceptive inputs and discussion of this topic; they were essential in completing this thesis.

My MRG teammates, past and present, Abdalla, Ayesha, Ben, Fathelrahman, Haoming, Keju, Niyi, Meshach, Precious, Shima, and Stacy: thanks for the encouragement and readiness to discuss whenever needed.

Dearest Nasir: my sincere gratitude for your unwavering support and love through this journey. One could not have hoped for a better spouse.

Kaysan and Naheed: my precious little ones, I am grateful for you.

My family and friends, new and old: I am happy to know you, ese lopolopo.

This research was undertaken with funding from the Canada First Research Excellence Fund.

Table of Contents

List of Tables

List of Figures

List of Symbols, Abbreviations, and Nomenclature

AACE	Association for the Advancement of Cost Engineering
ACTL	Alberta Carbon Trunk Line
APEA	Aspen Process Economic Analyzer
ARS	Agricultural Research Service
ASU	Air Separation Unit
BGY	Billion Gallons per Year
BTU	British Thermal Unit
CAPEX	Capital Expenditure
CCS	Carbon Capture and Storage
CCUS	Carbon Capture, Utilization and Storage
CEPCI	Chemical Engineering Plant Cost Index
CH_4	Methane
CHP	Combined Heat and Power
CI	Carbon Intensity
CO_2	Carbon Dioxide
COP	Coefficient of Performance
CPU	CO_2 Purification Unit
DAC	Direct Air Capture
DDGS	Dried Distillers Grains with Solubles
EOR	Enhanced Oil Recovery
ETBE	Ethyl tertiary-butyl ether
EtOH	Ethanol
GHG	Greenhouse Gases
GREET	Greenhouse gases, Regulated Emissions, and Energy use in Technologies
HHV	Higher Heating Value
IEA	International Energy Agency
kWh/t	Kilowatt-hour per tonne
L	Litres
LCA	Lifecycle Assessment
LCFS	Low Carbon Fuel Standard

LHV	Lower Heating Value
LLNL	Lawrence Livermore National Laboratory
LUC	Land Use Change
MAC	Marginal Abatement Cost
MEA	Monoethanolamine
MESP	Minimum Ethanol Selling Price
MGY	Million Gallons per Year
MJ	Mega Joules
MTBE	Methyl tert-butyl ether
MVR	Mechanical Vapor Recompression
M$	Million USD
O_2	Oxygen
OPEX	Operating Expenditure
PET	Polyethylene terephthalate
ppb	Parts per Billion
ppm	Parts per Million
Q	Heat
RED	Renewable Energy Directive
RER	Renewable Energy Ratio
RFA	Renewable Fuels Association
RFS	Renewable Fuel Standard
SER	Specific Energy Requirement
SUV	Sports Utility Vehicle
TEA	Techno Economic Assessment
TPD	Tonnes per day
USDA	United States Department of Agriculture
VOC	Volatile Organic Compounds
W	Work input

Chapter 1 Bioethanol: An Alternative Fuel

One of the most significant challenges of this century is the mitigation of anthropogenic climate change. This problem is caused primarily by emissions produced in energy provision for industry, transportation, and power generation [1]. Therefore, utilizing resources efficiently, investing in the generation of alternative energy sources, and continuing to develop new technologies—emphasizing greenhouse gas (GHG) emission reduction—are all necessary to meet the world's rising energy demand while addressing the climate challenge. Using renewable fuels, such as ethanol, in the transportation sector is one of such alternative energy option.

1.1 The Chronicle: "Fuel of the Future"

Ethanol or ethyl alcohol is an organic compound with chemical formula C_2H_5OH (abbreviated EtOH). It is a flammable, clear, volatile liquid with a distinct smell, produced naturally by fermenting sugars or hydrating ethylene. The former is termed bioethanol, i.e., derived from biomass-based sources. Even though humans have employed bioethanol since prehistorical times as intoxicating alcoholic beverages, its use as a fuel in the USA dates to the 19^{th} century.

The first internal combustion engine to be patented in the US in 1826 was designed by Samuel Morey to run on a blend of ethanol and turpentine. In 1860, the German engineer Nicolaus August Otto (the inventor of the modern four-cycle internal combustion engine, 1876) developed another internal combustion engine that ran on an ethanol fuel blend [2]. Henry Ford deemed ethanol the "fuel of the future'' [3], and his 1908 Model T was a 'flex-fuel' vehicle, meaning it could run on a mixture of ethanol and gasoline. However, ethanol's popularity was diminished by the prohibition law (18^{th} Amendment) of the 1900s as well as the colossal supply, low cost, and efficiency of petroleum products. During both World Wars and the 1973 oil crisis, the shortage of petroleum products supply coupled with adverse environmental concerns involving

octane enhancer, leaded gasoline, has renewed interest in biofuel production. The first US pilot bioethanol production began operation in 1979 [4].

1.2 The Controversy: Food vs. Fuel

The gradual but inevitable depletion of fossil energy sources and the associated adverse environmental impacts of fossil energy extraction and use has driven the search for cleaner alternative fuel sources. The International Energy Agency (IEA) estimated that in 2021, transportation and power generation (electricity and heat) contributed more than two-thirds of all CO_2 emissions from fuel combustion, which is consistent with trends over the past decade [5]. Our drive to reduce these emissions has meant that growth in renewable energy such as solar, wind, and hydropower for electricity generation is at an 'all-time high'. It was reported that their usage alongside nuclear power avoided 220 Mt of emissions in 2021 [5]. Despite the growing popularity of electric vehicles, record sales in 2021 had little effect on emissions because conventional SUV sales increased by an equal amount [5]. Therefore, renewable liquid fuels may yet play a critical role in decarbonizing light-duty vehicle transport due to the maturity and cost-effectiveness of the internal combustion engine [6], [7].

The primary culprit contributing to global warming is carbon dioxide (CO_2), which can be reduced by using biofuels instead of traditional fossil fuels. This reduction comes about because plants fix an equivalent mass of CO_2 into biomass during their growth cycle as is released during biofuel combustion, making biofuels carbon neutral—at least in principle. Ethanol is the predominant biofuel globally, although others are commercially available or in development, such as biogas, biodiesel, biohydrogen and biobutanol [8]. One of the benefits of ethanol as a transportation fuel is that the existing gasoline distribution infrastructure can be leveraged for its distribution and another is its capacity to lessen engine knocking. It can be blended with

gasoline, 10 vol% in E10 and used in existing cars, up to 85 vol% in E85 if a flex fuel vehicle is used.

Apart from its usefulness as a transportation fuel, it is one of the most widely utilized substances in industrial and consumer goods manufacturing [9]. It is a predecessor of other compounds including but not limited to acetaldehyde, acetic acid, ethylene, glycol, dyes, detergents, ethyl acetate, ethyl chloride, ethyl ether, butadiene, ethylene dibromide, plastics and plasticizers, soap and cleaning preparations, explosives, paint, lacquers, varnish, antifreeze [10], [11].

One of the primary drawbacks of first-generation ethanol (and other 1st generation biofuels) is the feedstocks from which it is made, i.e., starchy, or sugary crops that are also used as human and animal food. The use of these crops for biofuel is a contentious issue because of its effects on biodiversity, land use, and competition with food crops and prices [12], [13]. While, in principle, a biofuel such as ethanol should be carbon neutral, it is not when impacts of land use change, inputs of fuel and fertilizer in agriculture, and energy in production are considered. Nonetheless, the life cycle (i.e., from "cradle-to-grave" or "well-to-wheels") carbon intensity of corn ethanol has decreased in time due to advancements in agriculture and the use of energy-efficient technology in biorefineries [14]–[19]. Although lignocellulosic (non-food) biomass is abundant and could be used to produce second-generation ethanol, thus avoiding some of the drawbacks of food crops, conversion of cellulose to glucose remains technically challenging and expensive [20], [21]. Major obstacles include the unpredictability of feedstock, logistics, R&D investment in cost-effective pre-treatment, unit integration, and solid legislative support [21].

Production of biofuels has associated emissions and energy requirements, which must be evaluated to ensure that they deliver a climate benefit over their life cycle. For example, in a study by Wang *et al.* 2012, relative reductions in the lifecycle GHG emissions, including land

use change (LUC) associated with ethanol produced from corn, sugarcane, corn stover, switchgrass and miscanthus, relative to gasoline (94 gCO_2e/MJ) are 34%, 51%, 96%, 88% and 108%, respectively [19]. Furthermore, according to Lee *et al*. [15], ethanol fuel's carbon intensity (CI) has fallen by about 23% from 2005 to 2019. Therefore, additional improvements in the CI of ethanol support its continued use as an alternative fuel source, particularly when made from non-food crops.

1.3 The Global Market: Production Trends

Global ethanol production reached over 27 billion gallons (103 billion litres) in 2021 [22], which is more than double the production in 2007 [23]. Table 1-1 shows the production data from 2016 to 2021. Although 2021 output is a 3% increase from 2020 data in the wake of the COVID-19 pandemic, the number is approximately 2 billion gallons (7.6 billion litres) lower than 2019's. Nevertheless, ethanol had the world's largest share (70%) of biofuel production in 2019 [24]. Global production is expected to increase to 37 billion gallons (140 billion litres) in 2031 [25]. USA is the world's leading ethanol producer in 2021, followed by Brazil. Both countries accounted for 82% of global output in the same year. European Union, China and India are third, fourth and fifth, respectively. India defeated Canada for fifth place two years in a row. Currently, corn feedstock makes up around 59% of the ethanol generated, followed by sugarcane (22%), molasses (2%), wheat (2%), and other grains (cassava or sugar beets) for the remaining 15% [25]. Table 1-2 overviews the top six ethanol-producing nations and regions' biorefinery count, blend mandate and predominant feedstocks in 2021.

Ethanol blending with gasoline's nomenclature is between E0, i.e., containing 0 vol% ethanol plus 100 vol% gasoline and vice versa for E100. Therefore, E10 contains 10 vol% ethanol and 90 vol% gasoline, E15 contains 15 vol% ethanol and 85 vol% gasoline, etc.

Table 1-1: Global fuel ethanol production by country (2016–2021) in million Gallons [22]

Region	2016	2017	2018	2019	2020	2021
United States	15,413	15,936	16,091	15,778	13,941	15,015
Brazil	6,840	6,730	8,060	8,860	8,100	7,430
European Union	1,190	1,250	1,300	1,350	1,280	1,350
China	730	850	810	1,010	930	860
India	260	230	430	460	540	860
Canada	460	460	460	497	429	434
Thailand	330	380	390	430	390	350
Argentina	240	290	290	290	210	260
Rest of World	587	644	709	655	650	711
Total	26,050	26,770	28,540	29,330	26,470	27,270

Table 1-2 Top five ethanol-producing countries/regions' data for 2021

Country/ Region	Biorefinery count	Nameplate Capacity (*10^6 m^3)	Primary Feedstock	Blend level	Reference
USA	208	66.42	Corn	E10	[26], [27]
Brazil	362	54.5	Sugarcane	E27	[28]
EU	55	6.36	Sugar beets/ other grains	E10	[29]
China	22	7.72	Cassava/Biomass/ other grains	E10	[30]
India	231	4.3	Molasses	E10	[31]
Canada	12	1.88	Corn/Wheat	E10	[32]

1.4 Policy Drivers

Climate protection goals, energy security, health concerns and the elimination of harmful exhaust emissions from light-duty transport have been the cornerstone of various environmental policies worldwide [25]. These policies have helped in the ethanol industry's growth. This section discuses the current directives for biofuel production for the top three global ethanol producer.

1.4.1 USA

Tetraethyl lead was added to gasoline to boost its octane rating beginning in the 1920s. Octane rating is a measure of a fuel to resist "knocking", which occurs when a fuel ignites prematurely in an internal combustion engine, thereby reducing its efficiency and ultimately causing irreversible damage. While other known octane sources included alcohols like ethanol and aromatic hydrocarbons like benzene, tetraethyl lead was chosen because of its lower production costs [33]. The Environmental Protection Agency (EPA) was established after Congress approved the Clean Air Act in 1970 to regulate tailpipe emissions of carbon monoxide (CO), volatile organic compounds (VOCs) and nitrogen oxides (NOx). The EPA started phasing down leaded gasoline in 1973 and, finally, an outright ban in 1996 for on-road vehicles due to the detrimental health impacts of lead emissions [33].

Methyl tert-butyl ether (MTBE) promptly replaced lead as an octane booster for gasoline because of the advantage of using existing infrastructure and produced from gasoline refinery by-products. Furthermore, to attain air quality goals, the Clean Air Act Amendment of 1990 required the use of reformulated gasoline to increase the fuel's oxygenate content, thereby combusting completely [34]. MTBE was banned as an oxygenate because of underground water contamination in 2006 [35]. Ethanol replaced MTBE, and virtually all gasoline sold for motor

fuel in USA today contains ethanol as both oxygenate (to reduce emissions of CO and particulate matter) and octane booster [36].

Additionally, the energy crisis of the 1970s, the Organization of the Petroleum Exporting Countries (OPEC) oil embargo and the Iranian revolution, prompted ethanol's advocacy to promote energy independence. The Energy Tax Act of 1978 gave ethanol a 40 cents/gallon subsidy, facilitating the industry's launch [37].

Nearly 30 years later, the Energy Policy Act of 2005 enacted the Renewable Fuel Standard (RFS), which requires transportation fuel sold in the United States to contain a minimum volume of renewable fuels [38]. The goal of this act was to improve domestic energy security as well as to achieve climate goals. It required 4 billion gallons (15.1 billion litres) annual use of renewable fuel with motor fuel by 2006 and 7.5 billion gallons (28.4 billion litres) by 2012. The Energy Independence and Security Act (EISA) of 2007 expanded the RFS to use 36 billion gallons (136 billion litres) by 2022, with 15 billion gallons (56 billion litres)/year (BGY) from corn ethanol and 22 BGY (80 billion litres) from advanced cellulosic [35], [39]. This mandate has subsequently significantly increased ethanol production from 175 million gallons (662 million litres) in 1980 to 4 billion gallons (15.1 billion litres) in 2005 to over 15 billion gallons (57 billion litres) in 2021 [26], [40]. Figure 1-1 shows the upward trend in USA historical fuel ethanol production.

Other policies in the US include California’s Low Carbon Fuel Standard (LCFS), which focuses on reducing the carbon intensity of fuels used within California [41]. The LCFS program provides several credit generation opportunities to incentivize the production and use of low-carbon fuels in California, with fuels sold with a carbon intensity above the target generating deficits and below the target generating credits. Over the past five years, the LCFS price rose

from around \$100/tCO_2e to over \$200/tCO_2e in early-2020, and has fallen back to around \$100/tCO_2e in early 2023 [42].

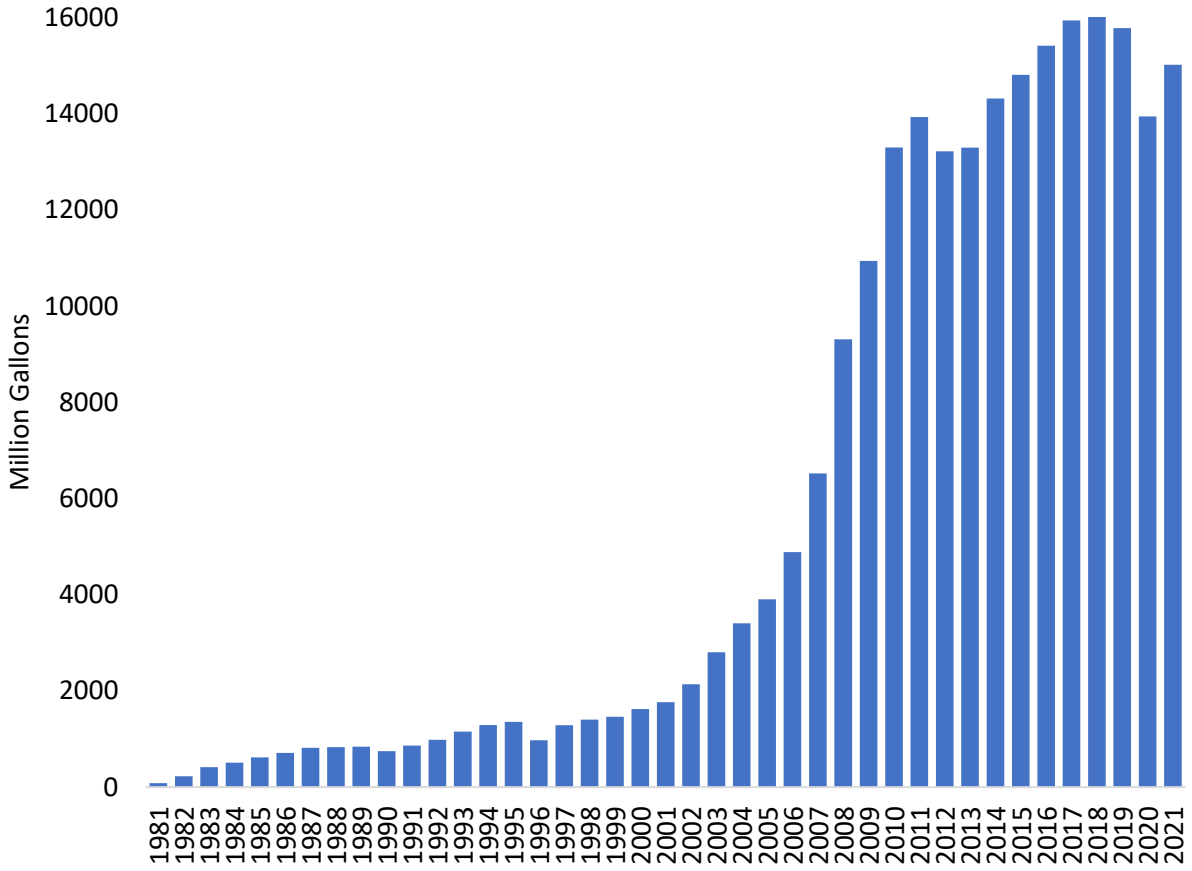

Figure 1-1: Historical US fuel ethanol production (source EIA data [43])

Additionally, the US Internal Revenue Code's Section 45Q, which was first adopted in 2008, offers a tax credit for CO_2 storage. The Inflation Reduction Act 2022 expanded and extended the 45Q tax credit, offering up to \$85 per tonne of CO_2 that is permanently stored and \$60 per tonne of CO_2 used for enhanced oil recovery (EOR) or other industrial purposes [44]. Previously, 45Q eligibility projects were required to capture 500,000 or more metric tons of CO_2 per year, but this was reduced to 18,750 for power plants, 12,500 for industrial facilities and 1,000 tons per year for Direct Air Capture (DAC) facilities [44]. Because, as will be discussed, ethanol plants

generate substantial amounts of high-concentration CO_2 during fermentation, they are well-positioned to benefit from both the LCFS and 45Q policies.

1.4.2 Brazil

The world's most advanced and comprehensive biofuel programme is in Brazil [45]. Brazil is a pioneer in ethanol production and a “biofuel superpower” [46]. In response to the 1970s oil crisis, Brazil launched the National Alcohol Program - Programa Nacional do Álcool or “Pró-Álcool” in 1975, focusing on the ethanol generation from sugarcane [47]. Since then, the Brazilian government has mandated anhydrous ethanol blending in gasoline-operated light-duty vehicles in varying volumes from 10% in 1977 to 15% in 1982, 22% in 1992, 25% in 2014 and finally, the current 27% today [28], [47]. E100 is the only other liquid fuel utilized by Brazil's light-duty fleet [28]. The present Brazilian “National Biofuels Policy” is the RenovaBio program, formalized in 2017, which focuses on setting annual targets for reducing carbon intensity, biofuel certification based on effectiveness in reducing GHG emissions, and decarbonization credits [28]. Flex-fuel vehicles (FFVs), which can run on varying ethanol concentrations, were introduced to the Brazilian market in 2003 has dominated the Brazilian market [19], [47]. The Brazilian light vehicle fleet is estimated to have 36.67 million cars in July 2022, with 30.8 million being flex-fuel vehicles [28]. Tax incentives are also available, as well as credit lines to fund sustainable agricultural practices and GHG reduction programs [28].

1.4.3 European Union (EU)

In 2009, the EU created the Renewable Energy Directive (RED). RED is a comprehensive policy for the generation and promotion of renewable energy sources in the EU. The directive mandated that 20% of the energy used within the EU must come from renewable sources. Under RED, biofuels in the EU must reduce their GHG emissions by an increasing minimum: 35% in 2009,

50% in 2017, and 60% for new biofuel facilities that begin production in 2017 [48], [49]. It expects at least 10% of its transport fuels to come from renewables by 2020. The Directive underwent a significant recast in 2018 called Renewable Energy Directive II (RED II), with a revised target of at least 32% renewable energy by 2030 [50]. There is also a binding aim of 14% from the transportation sector and a GHG saving threshold of 65% for plants starting after 2021 [51].

1.5 Carbon Intensity: gCO_2e/MJ

The term "carbon intensity" (CI) of a fuel refers to the climate impact of the GHG emissions resulting from a transportation fuel's production and consumption. It is commonly measured in grammes of CO_2-equivalent per megajoule or British thermal unit, i.e., gCO_2e/MJ or gCO_2e/BTU. Ideally, and in this thesis, it includes the impacts of GHG emissions linked to the extraction of resources, production and transportation of the fuel, and consumption of a unit of energy in the form of transportation fuel. It is usually estimated using life cycle assessment (LCA) methods.

The life cycle is commonly considered from the "cradle-to-grave" or, in the transportation context, "well-to-wheels" (see Figure 1-2) i.e., from feedstock production (planting the agricultural produce: corn, wheat, sugarcane, cellulosic, waste) to processing and transporting of feedstock to biorefinery to ethanol production and finally to usage (combusting the fuel itself).

Prior to the early 2000s, the estimated CI of corn ethanol (without land use change) ranged from 99 gCO_2e/MJ in 1990 to 58 gCO_2e/MJ in 2005 [17]. Over the years, substantial efforts have been made to decrease the CI of corn ethanol. For example, installing on-site wind turbines and solar arrays to generate electricity, using combined heat and power systems, and procuring biogas to replace fossil natural gas are all efforts by ethanol producers to achieve net-zero emissions.

Additionally, some facilities are working on carbon capture, utilization, and sequestration (CCUS) initiatives [26].

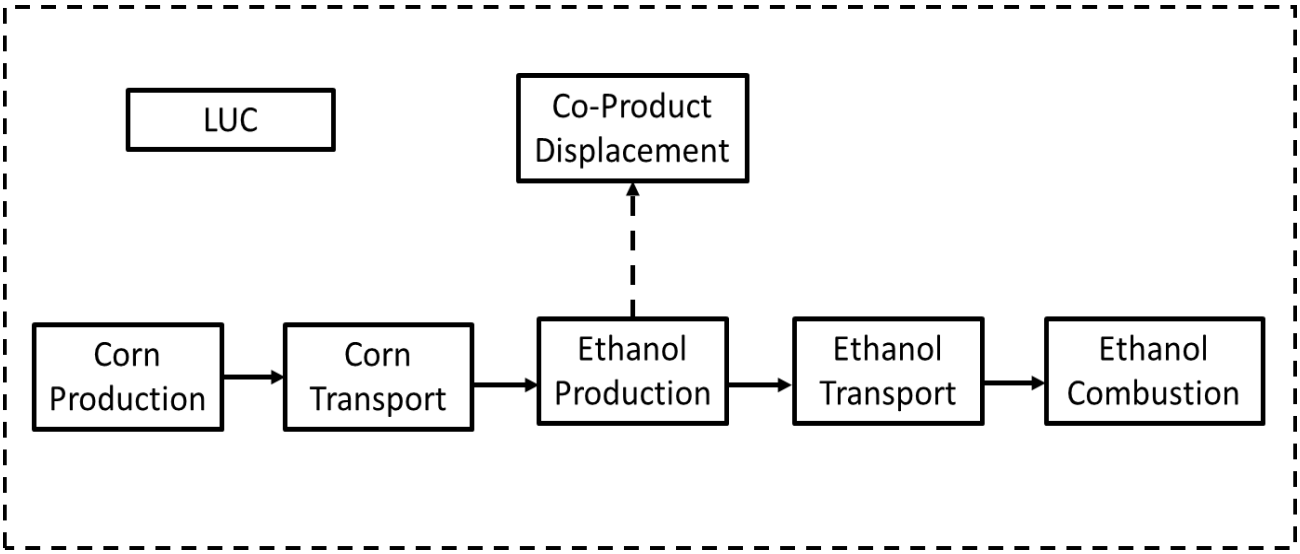

Figure 1-2; Lifecycle stages from wells to wheels: LUC – Land use change

Mueller and Kwik, 2012, also demonstrated that cutting-edge energy and processing technologies at the biorefinery level, including intricate heat integration, combined heat and power technologies, variable frequency drives, sophisticated milling technologies, various combinations of front and back-end oil separation, and innovative ethanol and coproduct recovery, could decrease the energy footprint of the corn ethanol production process [16].

1.6 Energy Balance of Ethanol

Energy balance is the ratio of the energy a fuel delivers to the energy input into its production. The term "energy return on energy investment, EROI" is frequently used to describe this metric. Over the past two decades, documentation shows increased corn ethanol's energy balance. The calculations include energy used in corn production, corn transport, ethanol conversion in biorefineries, ethanol transportation and farm machinery. It was estimated on average as 1.34 by

Shapouri *et al.* 2002 [52], 1.9-2.3 by Shapouri *et al.* in 2010 [53], 2.6-2.8 by Renewable Fuels Association (RFA) in 2016 [54] and 2.8-3.0 by RFA in 2021 [55]. Table 1-3 shows the survey data for various parameters such as ethanol yield, energy use and balance. Brandt [56] suggested that a minimum EROI of 5 is required for a functioning modern society. Therefore, there is still a margin for improvement for ethanol.

Table 1-3: Energy use and corn ethanol energy balance 2000 - 2022

	Shapouri *et al.* 2002 [52]	Mueller 2008 [57]	Shapouri *et al.* 2010 [53]	Gallagher *et al.* 2016 [18]	Mueller & Kwik 2013 [16]	RFA 2016 [54]	RFA 2022 [55]
No of plants	17	73	18	18	84	60	60
Plant type	-	DDGS+ WDGS	DDGS	DDGS	DDGS+ WDGS	DDGS+ WDGS	DDGS+ WDGS
Year of data	2001	2008	2008	2008	2012	2016	2021
Thermal energy use for ethanol conversion BTU/gal	36,000	26,202	29,412	29,421	23,862	24,409	23,755
Electricity use (kWh/gal)	1.09	0.73	0.757	0.757	0.75	0.67	0.6
Corn Yield (gal/bu)	2.64-2.68	2.78	2.76	2.76	2.82	-	-
Average Energy balance	1.34	-	1.9-2.3	2.1-2.3	2.6-2.7	2.6-2.8	2.8-3.0

*DDGS= Dried Distillers Grains with Solubles; WDGS= Wet Distillers Grains with Solubles

1.7 Research Goals

The primary aim of this thesis is to create parts of an inventory for the lifecycle analysis and techno-economic assessment of corn ethanol, ultimately answering these questions:

- How much emission reduction is achieved through the identified technology, and which is preferred?
- Is net zero emission achievable for corn ethanol?
- What is the marginal abatement cost (MAC) and minimum ethanol selling price (MESP) for the assessed technologies?

1.7.1 Scope of Work

Farming and ethanol refining are the two main areas to concentrate on to reduce the CI of corn ethanol because they account for 95% of ethanol's life-cycle GHG emissions [59]. Setting aside LUC and co-product credits, the US ethanol industry's ethanol refining stage contributes 45% of corn ethanol's life-cycle GHG emissions [15]. Therefore, this work focuses on mitigating emissions from the corn ethanol production step (see Figure 1-3) to improve its CI because of this potential. Corn ethanol is selected based on a large proportion of its use in the US (the largest producer) and global ethanol production. Two technological approaches have been identified to reduce emissions from the production stage of the ethanol life cycle: carbon capture and storage (CCS) and electrification. Fermentation of glucose in starchy food and combustion of fuel naturally releases CO_2 and shown in equations 1.1 and 1.2.

$$C_6H_{12}O_6 \xrightarrow{yeast} 2C_2H_6O + 2CO_2 \quad 1.1$$

$$CH_4 + 2O_2 \rightarrow 2H_2O + CO_2 \quad 1.2$$

There are two CCS options in ethanol production: capture of high-purity CO_2 produced in the fermentation step and the capture CO_2 from the combustion of fossil fuels to produce process heat (see Figure 1-3). A more detailed base plant description is given in (Section 2.1). As an alternative to the capture of CO_2 from combustion, fossil fuel demand can be reduced by

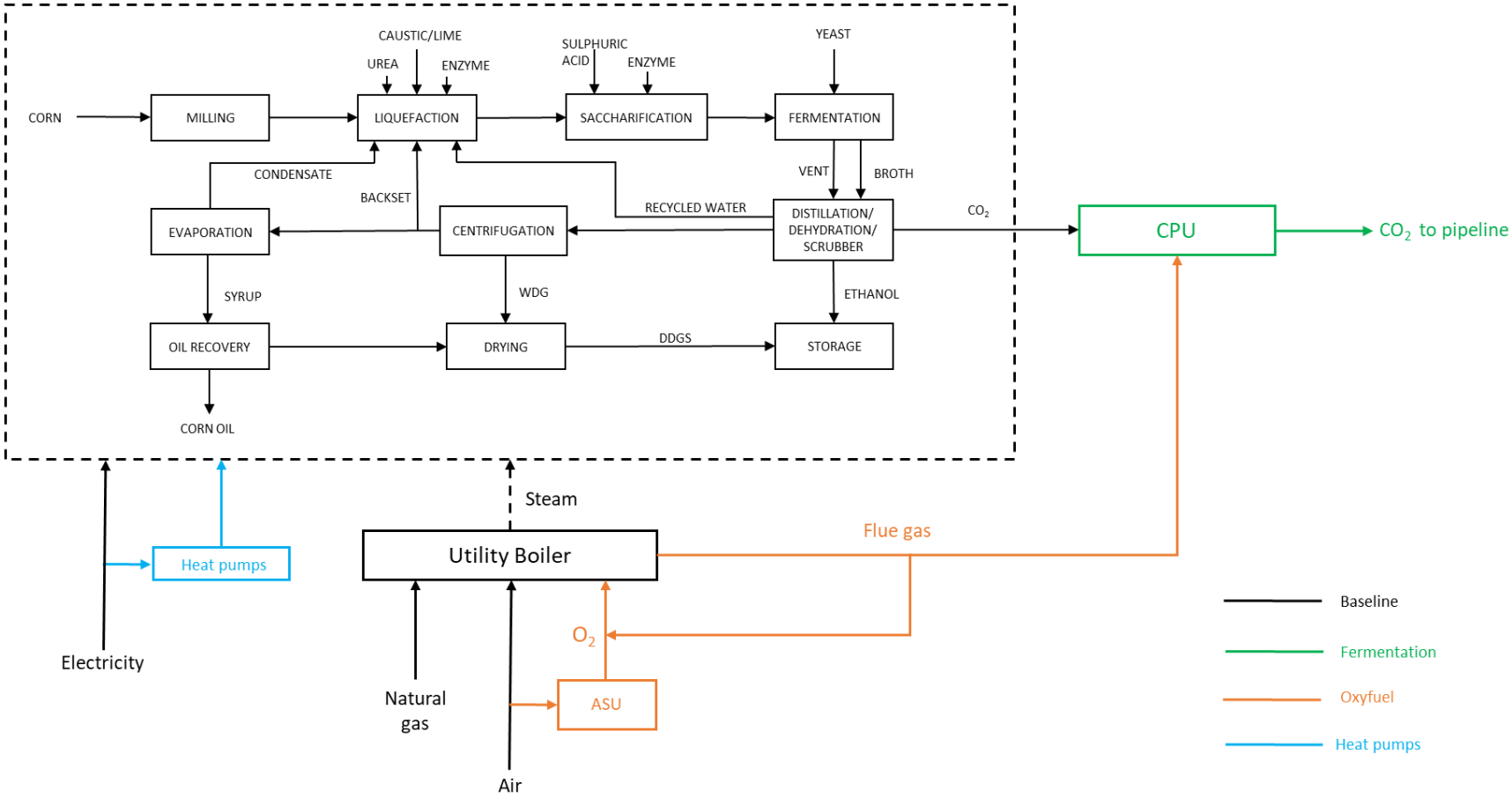

Figure 1-3: Process flow of dry grind corn to ethanol production (adapted from McAloon et al.[60]); Air Separation Unit (ASU); CO_2 Purification Unit (CPU)

introducing heat pumps to recover and reuse low-grade waste heat in the plant. This work is on ethanol production process modelling, improvement, and modification. The resulting performance information is used to perform a life cycle assessment, focusing on GHG impacts and techno-economic assessment of ethanol production. It should be noted that this work is specific to the dry-grind ethanol production process, which is the predominant route to fuel ethanol production in North America today, although the same method could be applied to other biofuel production processes.

1.7.2 Thesis Outline

After introducing the subject matter in this first chapter, literature findings, detailed process modelling, and cost estimation of the CCS option are discussed in the second. The third chapter evaluates and models the heat recovery process in the electrification case as well as associated costs. The results of LCA and TEA are shown in the fourth chapter. Finally, the last chapter discusses, concludes, and recommends future work.

1.7.3 Statement of Contribution

This thesis is part of a highly collaborative work with researchers at the University of California, Berkeley (UCB) and Lawrence Livermore National Laboratory (LLNL). The first part of this analysis on the CCS technology option for bioethanol production was published [61]. The work described in this thesis is specifically on process modelling of the technological add-ons to the ethanol-producing facility with a focus on process improvement and energy efficiency; thereby, creating parts of the LCA inventory, as well as the equipment cost calculation of such additions. The final LCA and TEA results presented in this thesis builds upon models by Dees *et al* [61].

Chapter 2 Carbon Capture Integration

The carbon mitigation potential of integrating carbon capture with ethanol production is assessed in this chapter. The goal is to capture CO_2 emissions from fermentation and fossil combustion for utility provision, thereby reducing overall emissions. However, integrating carbon capture technology (specifically oxyfuel combustion) has associated parasitic energy requirements which must also be estimated.

Various studies have investigated options to improve the energy efficiency or reduce the CI of ethanol production. Karuppiah *et al.* 2008, assessed a model optimization of dry grind ethanol plant with heat integration that reduced energy consumption up to 54.6% from the 10.6 MJ/L baseline [62]. They developed a mathematical model of mass and energy balances, thermodynamic equations, and constraint representative of a 61.29 million gallon per year (232 million litres) ethanol plant. De Kam *et al*. [63] studied the possibility of generating electricity and supplying domestic process heat from corncobs and syrup co-products. Their study employed integrated gasification using a twin fluidized bed steam gasification configuration based on the SilvaGas process to produce syngas. They concluded that the renewable energy ratio (RER), a variation of EROI), is 3 times that of a typical fossil fuel, i.e., natural gas-fired ethanol plant (RER; 1.7), while generating 30.4 MW_e of power and 50 million gallons (190 million litres) of ethanol per year. This is an improvement from their previous study [64], which yielded an RER range of 2.7 - 4.7 for different configurations. Zheng *et al.* also computed the thermal efficiencies (53-78%) for dry grind ethanol plants with biomass integrated gasification combined cycle (BIGCC) and natural gas combined cycle (NGCC) generating 20-30 MWe output power while meeting process heat needs of the plant [65].

From the LCA perspective, Wang *et al.* 2007 studied the GHG emissions of different corn ethanol plants configurations with LCA inventory from the GREET (Greenhouse gases, Regulated Emissions, and Energy use in Transportation) model. The work concluded that using Dried Distillers Grains with Solubles (DDGS) coproduct as process fuel (instead of animal feed) leads to 24% reduction in GHG emissions compared with current 2007 plant (79,000 gCO_2e/MMBTU), while 41% reduction was reported for wood chips [66].

Additionally, Kaliyan *et al.* [67] explored replacing grid electricity with integrated biomass fuel and found a significant reduction in the GHG emissions by replacing fossil fuels with co products - DDGS, corn stover and syrup in different conversion methods. A reduction of base case CI (Midwest dry-grind corn ethanol plant fueled with natural gas 56.4 gCO_2e/MJ) is 10 - 31% for process heat, 41 - 66% for combined heat and power (CHP), and 119 - 131% for BIGCC depending on the biomass fuel. In the BIGCC cases, more electricity is exported to the grid compared with the CHP cases. A further reduction of 32% is achieved when CO_2 from fermentation is captured and sequestered. Furthermore, Zheng *et al.* determined the life-cycle GHG emission reduction for conventional corn ethanol compared to base plant (56.4 gCO_2e/MJ) as 127% for BIGCC with syrup and corn stover fuel, 139% for BIGCC with corn stover fuel; and 89% for NGCC [65]. Their study, however, did not account for indirect land use change effects. Likewise, Pereira *et al.* 2019 harmonized assumptions from three publicly available LCA tools; BioGrace (EU), GHGenius (Canada), and GREET (U.S.), along with the Virtual Sugarcane Biorefinery (VSB), a Brazilian platform for analyses of sugarcane ethanol. For sugarcane, corn, and wheat ethanol, the CI varied between 16 - 45, 43 - 62 and 45 – 68 gCO_2eq/MJ, respectively. Harmonization varied the results between 3% and 8%. Lee *et al.* also explored the potential to use captured CO_2 to generate additional ethanol and concluded that the source of electricity has a significant impact on the CI,

even though ethanol production could increase by more than 37% without additional corn grain feedstock [68]. Finally, Lee *et al.* summarized the improvements in the corn ethanol production industry over 15 years in the USA that reduced GHG emissions [15]. Collectively, these studies indicate a pertinent role for fuel choices, improved process modification and energy efficiency in biorefineries and outline additional environment benefits of corn ethanol. All these studies expect Karuppiah *et al.* [62] did not estimate the cost of implementing these modifications. This is the first study to investigate the use of oxycombustion technology (process modelling, environmental and economics) to capture fossil emissions (as well as biogenic emissions) in an ethanol mill.

2.1 Base Plant Description

In a dry grind process (described by McAloon *et al.* [60]) with corn as the feedstock, as shown in Figure 1-3, corn grains are cleaned to remove debris and ground to increase surface area. Next, the milled corn is mixed with process condensate, alpha-amylase enzyme, lime, and urea in the liquefaction step. Starch is broken down to maltose/oligomers by alpha-amylase, lime for pH control, and urea provides nitrogen for yeast during fermentation. The resulting liquid mash is mixed with recycled thin stillage. During saccharification, glucoamylase hydrolyses the oligomers to glucose and sulphuric acid is used for pH control. Next, the glucose is fermented with yeast and converted to a beer mixture of ethanol, water, solids, and CO_2. CO_2 from fermentation is scrubbed and sent to either vent or recovery. The first distillation step in the beer column recovers nearly all the ethanol with less than 0.1 wt% in the bottoms, primarily water and non-fermentable solids. The second column purifies the ethanol further to near azeotropic concentration of about 91 wt%. The top product feeds the molecular sieves, increasing ethanol concentration to over 99 wt%. The whole stillage from the beer column is sent to a centrifuge, producing thin stillage (dissolved solids) and wet distiller's grains (WDG). A portion of thin

stillage is sent as backset while the remaining fraction is sent to the evaporator, which concentrates the syrup to 55 wt%. The heat of condensation from the second column powers the four-effect evaporator. Corn oil is extracted from the syrup (condensed distillers soluble) and the rest is mixed with the WDG. The final mixture is dried in either a steam or direct fired gas dryer to 9 wt% moisture known as distiller's dried grains with solubles (DDGS) and typically sold as animal feed. A thermal oxidizer treats the volatile organic compounds present during drying process. Typically, the ethanol is denatured by adding a small amount of gasoline.

2.2 Carbon Capture and Storage (CCS)

Carbon capture and storage (CCS) is a method of mitigating emissions from fossil fuel use (and cement production) in which CO_2 is captured from large point sources such as powerplants (and, potentially, from the air, through direct air capture), transported to a location suitable for its geological storage, and the CO_2 is injected into a geological formation where it is expected to be permanently retained.

There are three primary routes to capturing CO_2 (see Figure 2-1). In pre-combustion capture, carbon is removed from a hydrocarbon fuel (in the form of CO_2), leaving hydrogen that can then be combusted to generate heat and power. Post-combustion capture involves use of solvents, such as amines, to remove CO_2 from flue gas generated from traditional combustion of hydrocarbon fuels. And oxycombustion, which is characterized by removal of nitrogen (N_2) from the combustion air and use of relatively pure oxygen (O_2) as the oxidant, resulting in mainly CO_2 and water (H_2O) in the flue gas. All these technologies have been demonstrated in large-scale pilot projects or are being commercially used, and they can be applied to processes ranging from power generation to cement production.

2.2.1 Fermentation CO_2 Capture

Gaseous CO_2 generated during fermentation of sugars is highly concentrated with small impurities compared to the flue gas streams generated during fossil fuel combustion, which generally have lower CO_2 concentrations and non-condensable impurities [69].

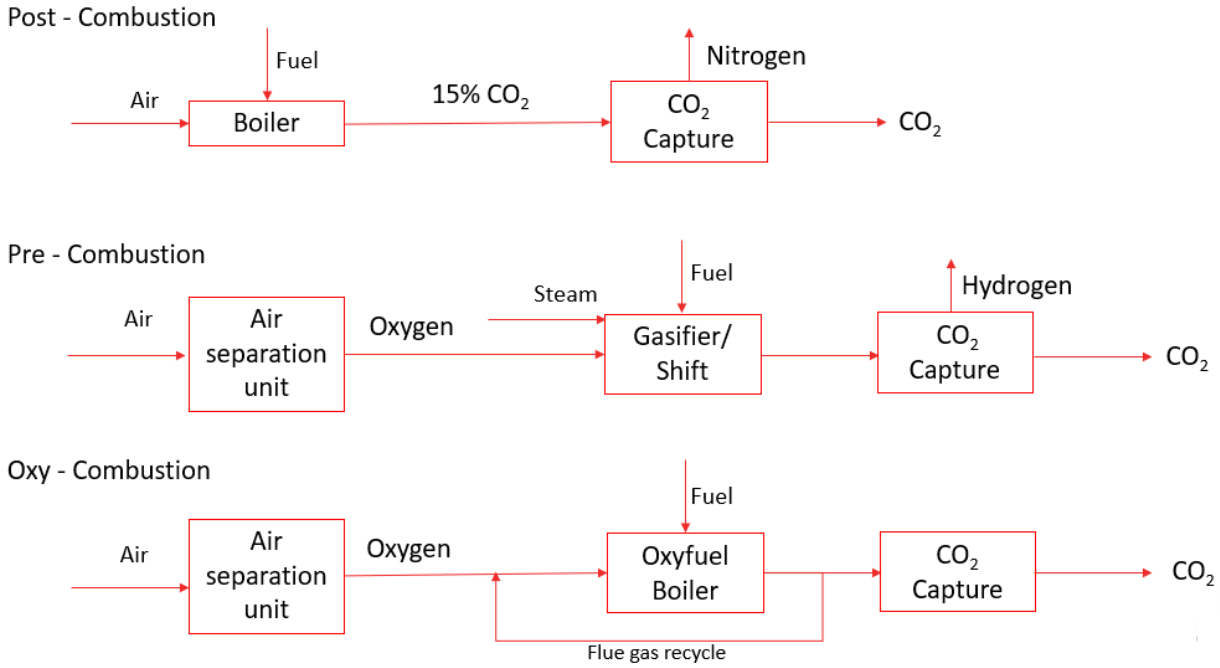

Figure 2-1: CO_2 capture processes flow diagram

Such high-purity CO_2 can be captured directly without separation, and requires only minimal downstream processing before sequestration [70]. Capture of CO_2 from fermentation has been previously investigated by several authors [70]–[74] and commercially demonstrated in the US. Sanchez *et al.* estimated that 45 Million tonnes per year of fermentation CO_2 were available from US ethanol plants in 2018 [75], and Moreira *et al.* estimated for Brazilian ethanol facilities at 28 Mt CO_2/y [76]. Carbon dioxide captured from the Arkalon and Bonanza biorefineries in Kansas, with respective capacities of 300,000 and 160,000 tonnes of CO_2 per year, has been used for enhanced oil recovery (EOR) for over a decade [77].

Furthermore, the Illinois Basin-Decatur Project successfully gathered and injected one million tonnes of CO_2 from biogenic sources over three years as part of a US Department of Energy demonstration project, and continues to capture and store CO_2 today [78]. Additionally, a project is currently underway to capture and store 180,000 tonnes of CO_2 per year from North Dakota's Red Trail Energy (RTE) 64 million gallons (240 million litres) per year ethanol facility [79]. Several other fermentation CCS projects are currently under development [80]–[82].

2.2.2 Oxycombustion CO_2 Capture

Multiple ethanol production processes require utility steam, including distillation, liquefaction and saccharification, evaporation, and drying [60]. Utility steam is typically supplied by a boiler using natural gas as a fuel and air as the oxidant. Combustion of natural gas in air produces flue gas with a low concentration of CO_2 and high nitrogen (N_2) because of the high nitrogen composition of air. Two previous studies have investigated the possibility of fermentation CCS with capture from fossil or biomass fired co-generation at ethanol refineries [72], [83]. Both studies examined post-combustion capture from on-site heat and electricity power generation using a monoethanolamine (MEA) solvent.

This work examines oxyfuel combustion an alternative option for steam generation that integrates CO_2 capture (Figure 2-1). Relatively high purity O_2 is generated by separating air into its components in an air separation unit (ASU). This O_2 is suppled to a modified boiler, along with natural gas, which is combusted to produce a flue gas largely composed of CO_2 and H_2O. A portion of the flue gas is recycled to the burner to control the combustion temperature and facilitate better heat transfer. Due to a lack of gaseous nitrogen in the combustion air, the NOx generation is often significantly lower than in a traditional combustion process. Oxyfuel combustion is an appealing capture option for two reasons. Firstly, it is based on commercially

proven cryogenic air separation technology and avoids the needs for solvents (and their management). Secondly, as demonstrated in the Total Lacq and Callide projects [84], [85], oxyfuel combustion technology may be retrofitted to currently operating boilers of the size utilised in conventional ethanol mills with minor modifications.

TOTAL Energies' 30 MW_{th} gas fired oxyfuel pilot plant was the first end-to-end industrial CCS project, comprising the capture, transport and injection of CO_2 into the depleted gas reservoir of Rousse in the southwest of France [85]. The project retrofitted an existing air-gas combustion boiler for steam generation into an oxygen-gas combustion boiler, using oxygen delivered by an ASU. The Lacq Project recorded more than 11,000 operating hours with about 51,000 tonnes of CO_2 transported and stored. Additionally, the Callide Oxyfuel Project in Queensland State Australia, demonstrated retrofitting an existing out-of-service coal fired power plant with oxyfuel combustion technology [84]. Likewise, Vattenfall's Schwarze Pumpe pilot plant (Figure 2-2) located in Brandenburg, Germany and the CIUDEN's CCS Technology Development Plant at Ponferrada, northwest of Spain demonstrated pulverized coal and circulating fluidized bed coal oxyfuel technologies [86], [87]. Oxyfuel technology also applies to other industries: iron and steel, cement, petrochemical and pulp and paper industries [88].

Air separation unit

High purity oxygen >95% is a requirement of the oxyfuel combustion technology. Air components (oxygen, nitrogen, and argon) are essential to many industries, including

Figure 2-2: Vattenfall's Schwarze Pumpe pilot plant

petrochemical, steel, food processing, and healthcare. Typically, cryogenic separation is employed for large-scale air separation. Low-temperature distillation is the foundation of the cryogenic air separation, which can provide significant quantities of high-purity liquid and gas phase products. Non-cryogenic procedures, on the other hand, rely on adsorption and membrane separation. This work models the cryogenic air separation because of its commercially mature status and economic performance for large scale production [89]. Many research outline descriptions of cryogenic air separation process configurations focusing on minimizing the parasitic power consumption [90]–[93]. A conventional dual column cycle consists of fundamental stages of air compression: ambient air is filtered to remove dust and other particles and compressed, air purification: impurities such as water vapour and CO_2 is removed, heat exchange: compressed air is cooled with the cold distillation product, distillation: air constituents are separated based on difference in boiling point, and product compression and/or retrieval.

CO_2 Compression and Purification Unit (CPU)

The CPU captures and purifies the CO_2 from combustion flue gases to the required specifications, i.e., pipeline transport for enhanced oil recovery (EOR) or sequestration. CPU schemes includes steps such as scrubbing, compression, drying and distillation and pumping of the condensed product to pipeline pressure [89], [94], [95].

2.3 Aspen Plus® Process Simulator

Aspen Plus® is a chemical process simulator developed by AspenTech, which is used for process modelling, design, and optimization. It uses fundamental engineering relationships like mass and energy balances, phase, and chemical equilibrium to predict process performance. It can replicate real plant behaviour using accurate thermodynamic data, practical operating conditions, and equipment models [96]. Its application includes but is not limited to bulk

chemical process improvement, energy management, environmental and safety analysis, heat exchanger design, solid process optimization can be raised. Process simulation is helpful in a project lifecycle from research and development to process design and production to design better plants and increase profitability. All process modelling in this thesis is carried out in Aspen Plus®.

2.4 Total Plant Energy Requirement

As reviewed in section 1.6.1, several sources have reported the energy use for corn ethanol biorefinery. Mueller (2008) reported the thermal energy requirements of a dry grind ethanol mill in US as 8.08 MJ/L (HHV) and the electricity requirement as 0.192 kWh/L [57]. This reported number is applied in this modelling (even though the survey is dated) to be conservative. This thermal energy requirement is modelled to be supplied by oxycombustion of natural gas, capturing the CO_2 produced during the combustion using ASPEN plus V11. Peng-Robinson (PENG-ROB) equations of state is the selected property method. There are two CCS cases investigated. Case 1 is a plant that uses direct gas drying for DDGS, wherein 3.09 MJ/L is needed for drying, and the rest 4.99 MJ/L is supplied by steam from the boiler. Case 2 uses steam drying for DDGS, wherein all the plant energy is assumed to be supplied by steam; therefore, 8.08 MJ/L is modelled to be supplied by the utility boiler.

2.5 CO_2 Capture Process Description and Modelling

Figure 2-3 shows the overall block flow representation of the process modelling. First, oxygen is separated from air by cryogenic distillation in the air separation unit (ASU) and supplied to the oxy-combustion unit along with natural gas for combustion and steam generation. Then, the flue gas (along with fermentation CO_2) is then sent to the CO_2 purification unit (CPU) for final cleanup before pipeline transportation.

2.5.1 Fermentation Material Balance

The material balance of the quantity of CO_2 capturable from a 40 million gallons (151 million litres) per year denatured (2.5 vol%) ethanol plant, running 358 days/year, is stated below. The composition of corn used is reviewed from several literature sources [60], [62], [97], [98]

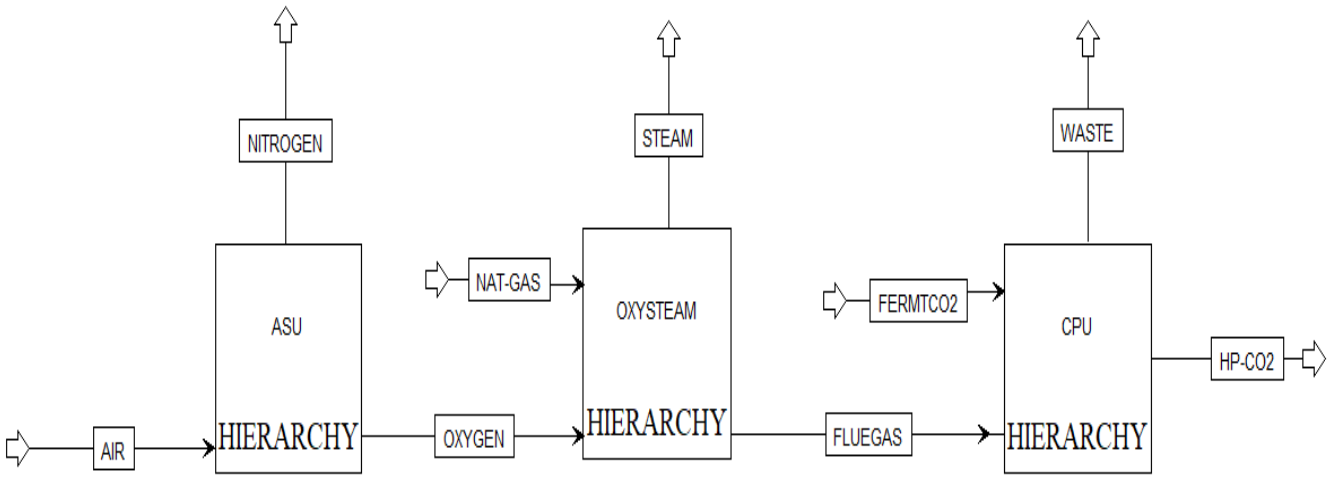

Figure 2-3: Aspen plus Block flow representation of the CCS addition

and given in Table 2-1. Shelled corn density is 56 lb/bu. The reaction equations are stated below.

Liquefaction of starch to maltose

$$2(C_6H_{10}O_5)_n + nH_2O \xrightarrow{\alpha-amylase} nC_{12}H_{22}O_{11}$$

Saccharification of maltose to glucose

$$C_{12}H_{22}O_{11} + H_2O \xrightarrow{glucoamylase} 2C_6H_{12}O_6$$

Fermentation of glucose to ethanol

$$C_6H_{12}O_6 \xrightarrow{yeast} 2C_2H_6O + 2CO_2$$

Table 2-1: Corn composition

Component	Wt% (Dry)
Starch	74.0
Glucose	2.0
Cellulose/Hemicellulose	8.5
Protein	9.5
Oil	4.5
Ash/Other solids	1.5

From the above equations, 1kg of starch produces up to 1.06 kg of maltose and 1kg of maltose produce up to 1.05 kg of glucose. From 1kg of glucose, up to 0.51 kg of ethanol and 0.49 kg of CO_2 are produced. Additionally, distillers' dry grains with soluble (DDGS) and corn oil are produced as by-products. Fermentation is assumed to have 93.2% glucose conversion efficiency, while the conversion efficiency of primary reactant is 99% for liquefaction and saccharification. Ethanol recovery is assumed to be 99% with its density taken as 0.79 kg/L.

2.5.2 Air Separation Unit Modelling

The first requirement for oxycombustion is high purity oxygen, which is separated from air cryogenically. A standard air composition of 78.1% N_2 and 21% O_2, and 0.9% argon at 15 ℃ and 1 atm was used.[1] In this unit, the air is compressed to 4.2 bar, cooled to atmospheric conditions, then subcooled to near dew point in a heat exchanger and sent to the last stage of the high-pressure column (HPC), shown in Figure 2-4. The overhead product of HPC is liquid N_2, and the bottom product is an O_2-N_2 liquid mixture. Both products are subcooled by 5 ℃, de-pressured and fed to the low-pressure column (LPC). High-purity liquid O_2 and high-purity gaseous N_2 are the bottom and distillate products of the LPC, respectively. These products are warmed against the incoming compressed air to ambient temperature, with the pure O_2 sent to the combustion

[1] All concentrations are reported in mol% unless otherwise stated

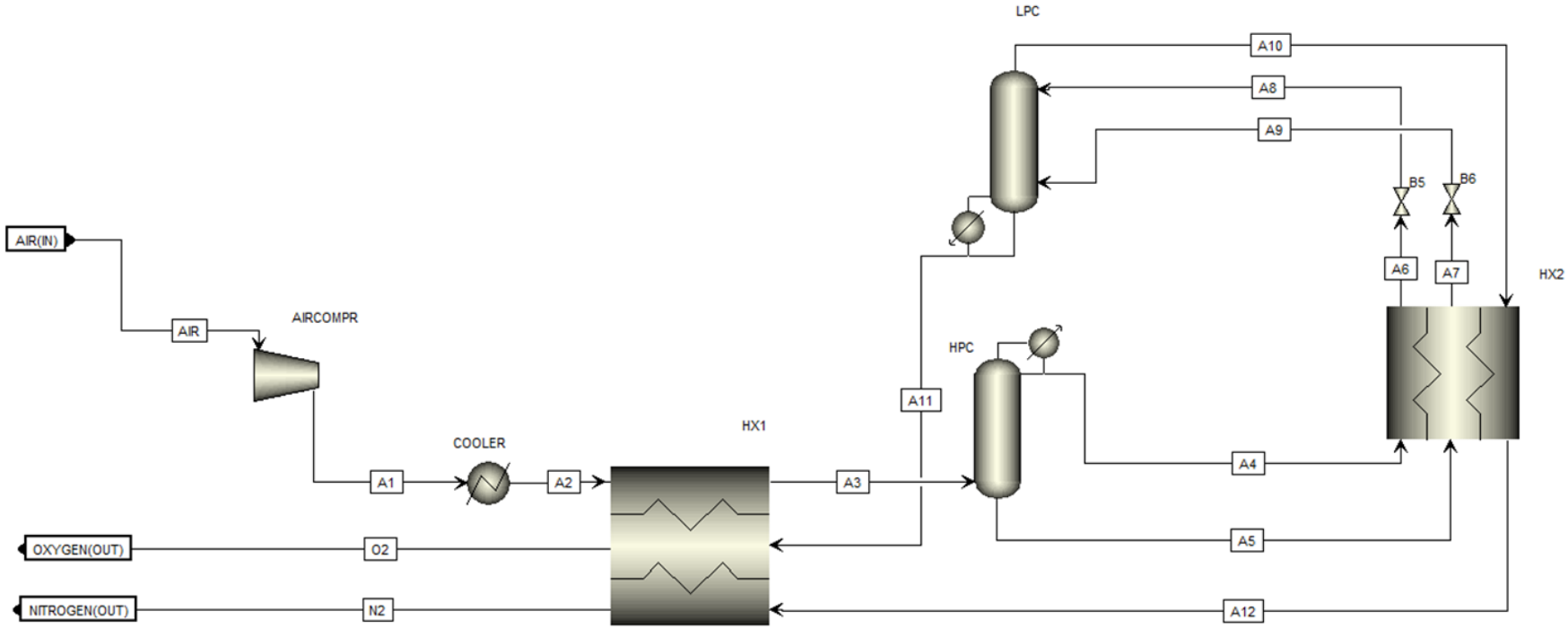

Figure 2-4: Aspen Plus flowsheet of the cryogenic air separation process

unit. The two distillation columns are thermally linked by exchanging the latent heat of vaporization via the HPC condenser and the LPC reboiler. Other modelling parameters are shown in Table 2-2. The distillation column is modelled using an Aspen RadFrac column. Table 2-3 shows the column conditions for the ASU. HX1 and HX2 are modelled using an Aspen MHeatX block. Other ASU modelling assumptions include:

- The pressure drop across the LPC and HPC is 0.1 bar
- 5kW and 10kW are lost during the thermal integration of the two columns in cases 1 and 2, respectively.

Table 2-2: ASU modelling parameters

	Case 1 (direct gas DDGS dryer)	Case 2 (steam DDGS dryer)	
Parameter	Value	Value	Unit
Air Flowrate	25100	40635	Nm^3/hr
Pressure	1	1	bar
Temperature	15	15	^oC
Compressor efficiency	85	85	%
O_2 purity	95	95	%
O_2 pressure	1.2	1.2	bar

2.5.3 Oxyfuel Combustion and Steam Generation Unit

Natural gas is supplied at 29 °C and 27 bar and depressurized to 1.2 bar before it is sent to the combustor (Figure 2-5). The composition of natural gas as specified by US National Energy Technology Laboratory (NETL) Quality Guidelines for Energy System Studies QGESS-

Specification for Selected Feedstocks [99] (which is representative of pipeline quality natural gas in USA) is given in Table 2-4.

Table 2-3: Cryogenic distillation column conditions of the ASU

	Case 1 (direct gas DDGS dryer)		Case 2 (steam DDGS dryer)	
Parameter	LPC	HPC	LPC	HPC
No of stages	20	15	20	15
Reboiler Duty	1206 kW	-	1952 kW	-
Condenser Duty	-	1212 kW	-	1962 kW
Boilup ratio	2.65	1.20	2.65	1.20
Stage 1 Pressure	1.1	4.1	1.1	4.1

The boiler is modelled as an RGibbs reactor with no pressure drop and adiabatic operation. The hot flue gas from the combustor is cooled to 138 °C, exchanging heat with cooling water to produce superheated steam, then split with parts recycled to the boiler. The flue gas recycle ratio (FGRR) is the percentage of total flue gas recycled into the boiler. Higher values indicate a lower oxygen concentration in the O_2/CO_2 oxidant entering the boiler, whereas zero FGRR is the case with no recycle. FGRR is necessary to control high combustion temperature by making up the volume of the missing N_2, thereby matching air combustion characteristics and allowing retrofitting air combustion boilers.

Excess O_2 is set at 2.7% to ensure complete combustion. The second part is sent to the CO_2 purification unit for cleanup and compression. Steam is produced at 190 °C and 12 bar.

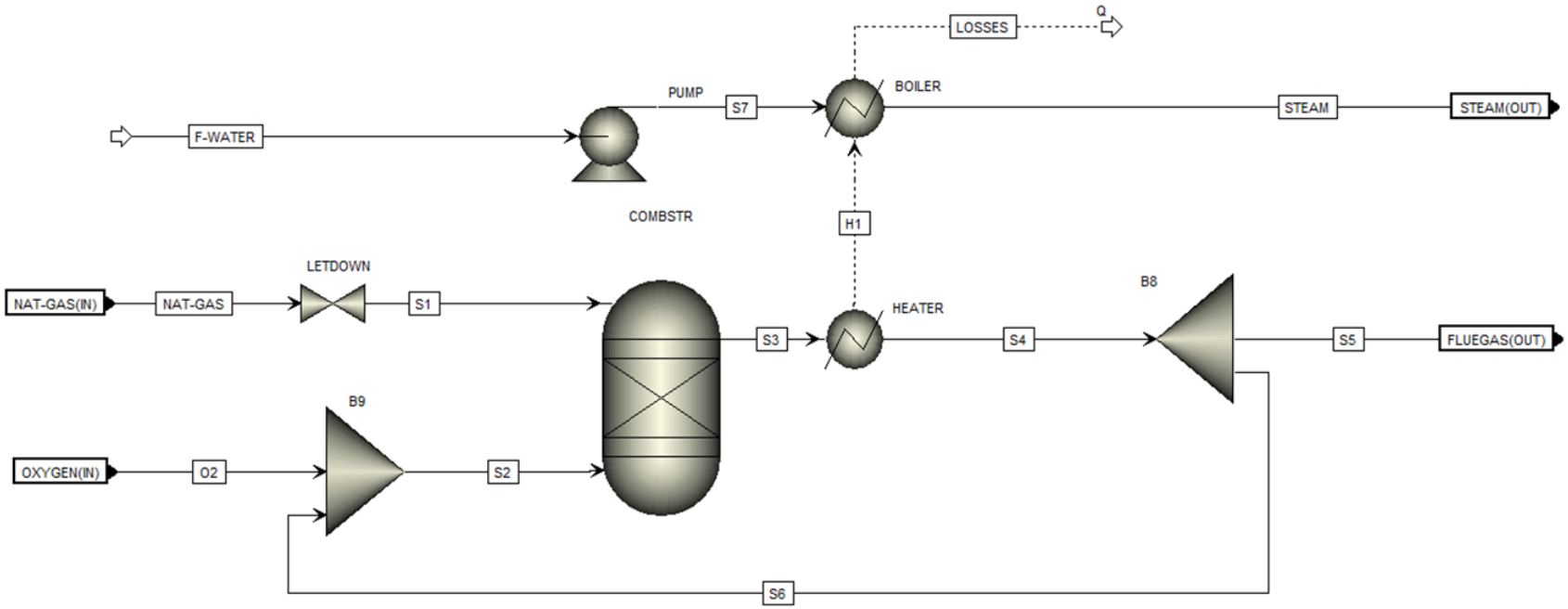

Figure 2-5: Aspen model of the combustion and steam generation unit

Table 2-4: Natural gas composition

Component	Volume Percentage	
Methane, CH_4	93.1	
Ethane, C_2H_6	3.2	
Propane, C_3H_8	0.7	
n-Butane, C_4H_{10}	0.4	
Carbon Dioxide, CO_2	1	
Nitrogen, N_2	1.6	
Methanethiol	$5.75x10^{-6}$	
Total	100.0	
	LHV	HHV
MJ/scm	34.52	38.25
kJ/kg	47,201	52,295
Btu/scf	927	1,027
Btu/lb	20,293	22,483

The water flow rate is calculated using a design specification for accounting for the heat transferred and 1% heat loss. Table 2-5 shows the boiler parameters and specifications.

Table 2-5: Boiler parameters and specification

	Case 1 (direct gas DDGS dryer)	Case 2 (steam DDGS dryer)	
Parameter	Value	Value	Unit
Boiler duty	24676	39949	kW
FGRR	84	84	%
Natural gas flow rate	1915	3100	kg/hr
Combustion temperature	1053	1053	^oC

2.5.4 CO_2 Purification and Compression Modelling

Although there are typically no significant technological obstacles to providing high purity captured CO_2, such requirements are likely to increase parasitic energy requirements and costs [94]. Therefore, the specification for transport, storage, environmental regulations, and other criteria determines the final composition of CO_2.

There are two sources of CO_2 in the process, from the fermentation and oxycombustion flue gas stream. The fermentation CO_2 is assumed to be at 100% purity and 32 °C, whereas the flue gas composition at the boiler outlet is about 32% CO_2 and 62% water with the remainder being nitrogen, argon, and oxygen.

Direct contact water scrubbing of the flue gas removes majority of the water content prior to the compressor leaving the composition at about 82% CO_2. There are two design options at this point. One is to compress and dry the streams (fermentation and combustion CO_2) separately before mixing the streams before pumping to pipeline pressure specification. The other design option is to mix the streams, then compress prior to subsequent purification. The latter means only one compression train but means the purification system will need to be sized to accommodate the additional CO_2 from fermentation. On a first run, the former had a higher associated energy consumption and two separate compression trains leading to potential higher operating and capital costs of compressors. The mixed stream is compressed to 15 bar, cooled, and flashed to remove free water, then further compressed to 30 bar before drying to remove water content, to prevent hydrates formation (Figure 2-6). Where the fermentation CO_2 stream alone is captured, that stream alone is sent to the compression train without cryogenic distillation (see Figure 2-7).

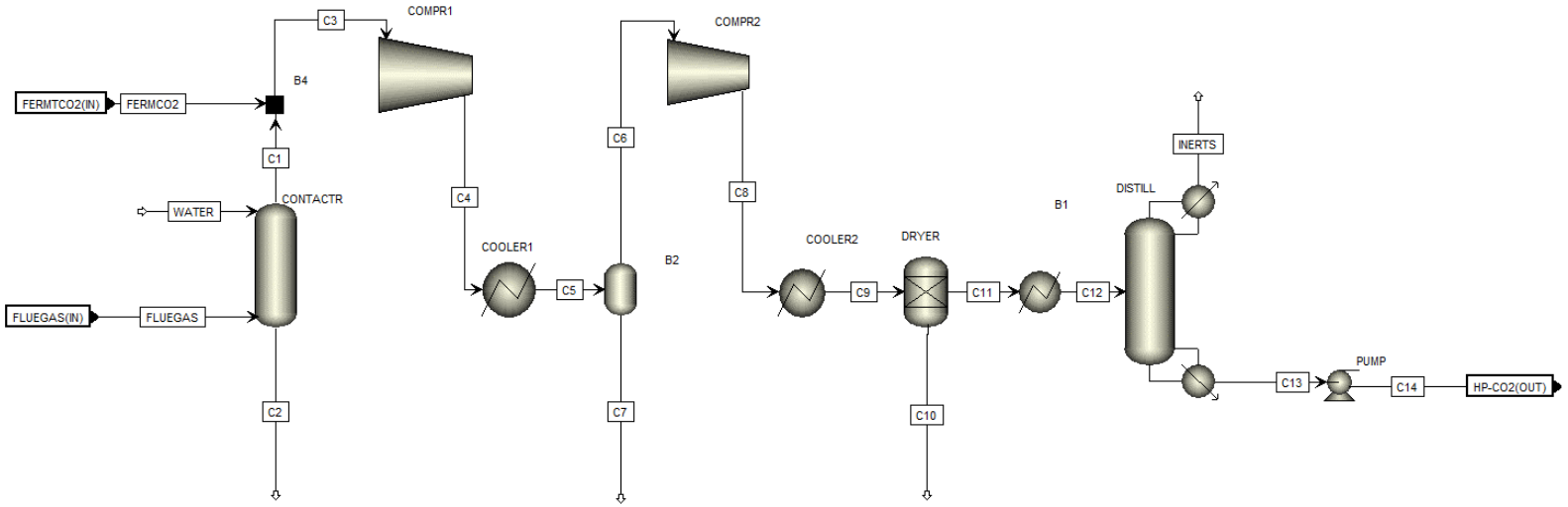

Figure 2-6: Aspen Plus flowsheet of CO_2 purification and compression process

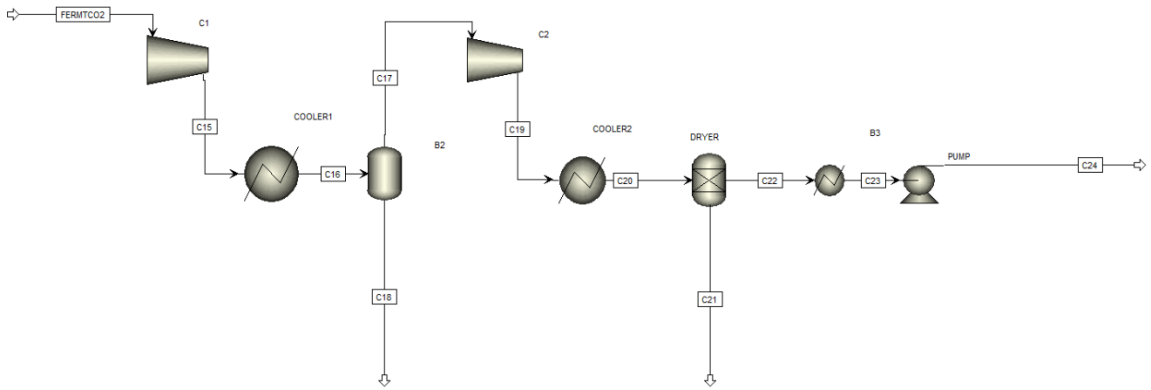

Figure 2-7: Aspen Plus flowsheet of CO_2 purification and compression process (fermentation only)

Interstage cooling is assumed to be provided by cooling water and low temperature cooling by a refrigerant. Drying is modelled using an Aspen separator block, which could represent either solid desiccant (molecular sieve) adsorption or liquid absorption (e.g., triethylene glycol dehydration) processes. However, the drying process energy consumption is not explicitly modeled, as its energy consumption is assumed to be small relative to compression energy. Finally, the dried CO_2 stream is distilled cryogenically to remove non-condensable gases and pumped to 150 bar to meet Alberta Carbon Trunk Line (ACTL) pipeline specification [100]. Other CO_2 purification methods such as double flashing as opposed to cryogenic distillation achieves 95% CO_2 with higher concentrations of O_2 [89] which does not meet ACTL specification. Additional reviewed pipeline composition are given in Appendix A.1.

2.6 CCS Process Modelling Results and Discussion

The Aspen flow sheet converges with no errors. The summary of results for both cases is shown in Table 2-6. From material balance, fermentation emissions from a 40 million gallon per year (MGY) ethanol plant is about 112 kt/year with 313 kg/hr and 11514 kg/hr corn oil and DDGS respectively. Corn input rate is 40,951 kg/hr which applicable to both Cases. Corn is calculated to be composed of 40.52% carbon. The carbon balances for both Cases are shown in Table 2-7.

Total CO_2 captured from the entire process is 159 kt/year and 187 kt/year of 99.9% CO_2 at a temperature of 10^{o}C and 150 bar for Cases 1 and 2, respectively, with an overall recovery of 99.6%. Based on 95% O_2 purity, the ASU specific energy requirement (SER) is 196 kWh/t O_2, which compares well with the 160 - 200 kWh/t O_2 estimated by Darde *et al*. [89] and 195 kWh/t O_2 reported by NETL [101]. Darde *et al.* defined ASU SER as “the power required to produce 1 metric ton of a gaseous oxygen stream at a given oxygen purity at atmospheric pressure” [89].

Table 2-6: CCS Results summary

Parameter	Case 1 (direct gas DDGS dryer)	Case 2 (steam DDGS dryer)
Air flow rate (t/d)	776	1256
O_2 flow rate (t/d)	189	306
N_2 flow rate (t/d)	873	950
Natural gas flow rate (t/d)	46	74
Steam flow rate (t/d)	779	1265
CO_2 product flow rate (t/d)	435	511
ASU SER (kWh/t O_2)	196	196
CPU SER (kWh/t CO_2)	115	117
Combustion temperature (^oC)	1053	1053

Efficiency of the compressor motors, heat of regeneration of driers and power consumption of the cooling system are not included in this definition. Furthermore, the CPU SER is 115 and 117 kWh/t CO_2 for Case 1 and Case 2, respectively, which compares well with 118 kWh/t CO_2 for 95.35 mol% CO_2 estimated by Aneke and Wang [95] and 110-140 kWh/t CO_2 by Darde et al. [89]). The fermentation only CPU SER is 110 kWh/t CO_2. This number is much smaller because it doesn't require cryogenic distillation and the stream is 100% CO_2. All stream boundary results are listed in Appendix A.2.

2.7 Sensitivity Analysis

This study changes in critical operating and design variables, and the model behaviour is examined and predicted using the sensitivity analysis tool. The effects of process factors such as oxygen purity, CO_2 pressure and FGRR on the intended output are examined in this sensitivity

analysis. These results explore "what-if" questions and give a sense of the variability that can be expected in real-world operation.

Table 2-7: Carbon balance for both CCS cases

Case 1	**Carbon in**				**Carbon out**			
Source		Flowrate	%C	C in kg/hr		Flowrate	%C	C in kg/hr
Fermentation	Corn	40951	40.52%	16595	EtOH	13701	52%	7143
					DDGS	11514	49%	5642
					Corn oil	313	76%	238
Oxyfuel	Natural gas			1383	Oxy vents	5.5	27%	1.5
					Ferment vents	6.5	27%	1.8
					CO_2 product	18145	27%	4952
Total				**17978**				**17978**
Case 2	**Carbon in**				**Carbon out**			
Source		Flowrate	%C	C in kg/hr		Flowrate	%C	C in kg/hr
Fermentation	Corn	40951	40.52%	16595	EtOH	13701	52%	7143
					DDGS	11514	49%	5642
					Corn oil	313	76%	238
Oxyfuel	Natural gas			2239	Oxy vents	9.2	27%	2.52
					Ferment vents	6.5	27%	1.78
					CO_2 product	21278	27%	5807
Total				**18834**				**18834**

2.7.1 Effects of Oxygen Purity on Process Variables

To produce the same amount of steam, the CPU SER, natural gas, and CO_2 product flow rate are equal for 95% and 99.8% purity oxygen, with substantial increase to the ASU SER, nitrogen

flow rate and feed air input (Figure 2-8). 99.8% purity O_2 has ASU SER of 316 kWh/tonne compared with 196 kWh/tonne for 95% O_2 due to additional energy compressing more feed air flowrate. As stated by Darde *et al.* [89], and confirmed in this work, the lower purity O_2 is adequate for this design as it requires less energy for the ASU.

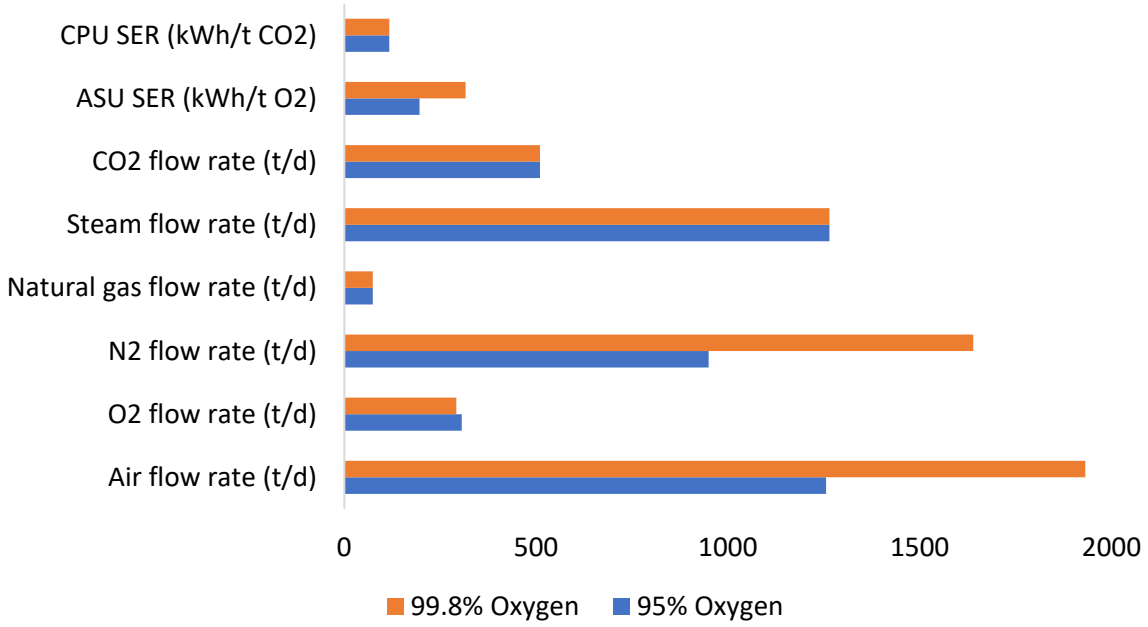

Figure 2-8: Effects of ASU oxygen purity on key process variables

2.7.2 Effects of Final CO_2 Pressure on CPU SER

As the pressure of final CO_2 product increases (Figure 2-9), the CPU SER increases because of additional energy to pump CO_2. For different product end use and location, the final CO_2 pressure may vary from 80 bar to 180 bar [102].

2.7.3 Effects of FGRR on Combustion Temperature and O_2 Concentration

It can be seen from Figure 2-10 that as the FGRR increases, the combustion temperature decreases drastically and O_2 concentration in the O_2/CO_2 oxidant to boiler increases until it

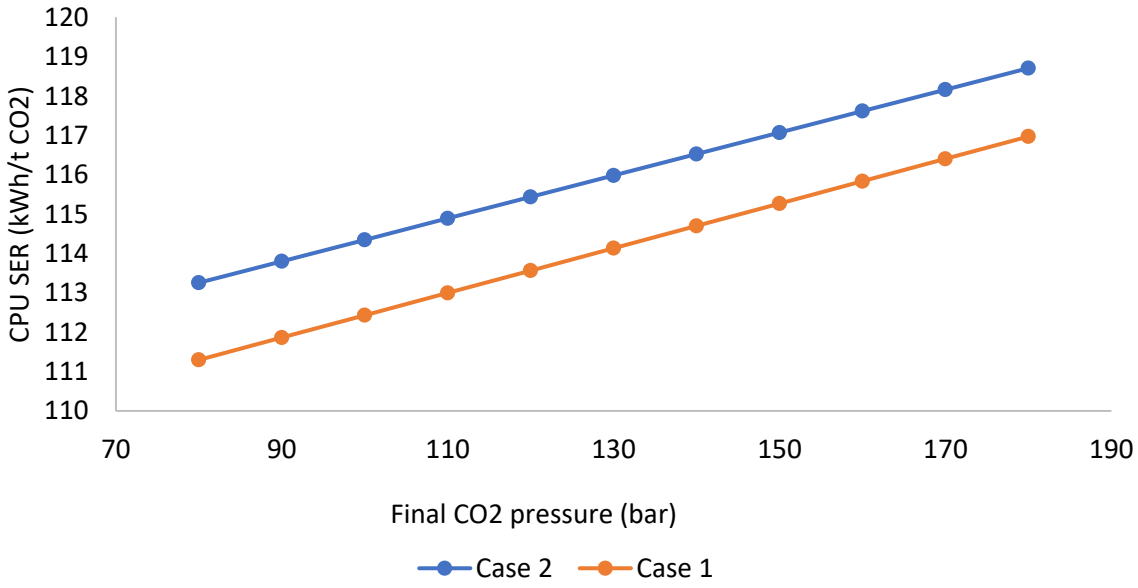

Figure 2-9: Effects of final CO_2 pressure on CPU specific energy requirement

remains constant at 0.75 FGRR. The operating point of the FGRR, combustion temperature and O_2 concentration in the O_2/CO_2 oxidant to boiler are 0.84, 1053 and 0.32 respectively, which provide results similar to those from the Total Lacq project [85].

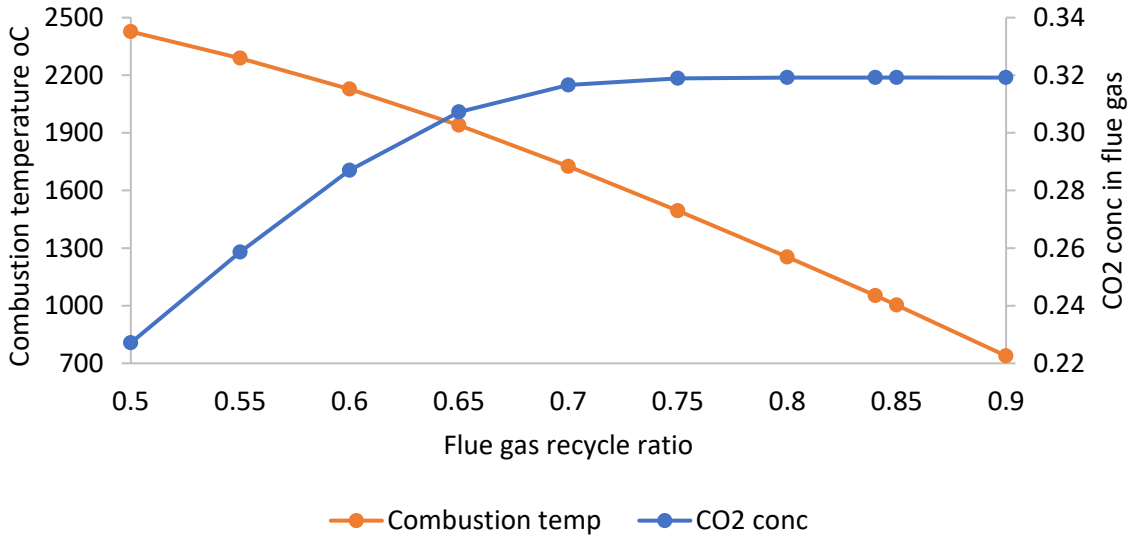

Figure 2-10: Effects of FGRR on combustion temperature and O_2 concentration in the O_2/CO_2 oxidant

2.8 CCS Equipment Cost Evaluation

The purchased cost of the CCS equipment is estimated here by scaling reported purchased costs of individual pieces of equipment or modules from existing facilities (or detailed engineering studies) to meet the capacity required for this facility. Such cost-capacity scaling methods are commonly used for concept screening at the start of a project and are associated with Class 4 or 5 cost estimates as specified by the Association for the Advancement of Cost Engineering (AACE) International [103]. According to AACE, the estimated class is determined by the maturity level of a project. Cost estimates range from Class 5 for 0 - 2% of the project completely defined to Class 1 for 65 - 100% of the project completely defined. Cost-capacity scaling methods assume typically that the unit cost of equipment or facilities decreases as the installed capacity of equipment increases, which reflects economies of scale. The governing equation is given below [104].

$$C_2 = C_1 \left[\frac{S_2}{S_1}\right]^n \qquad 2.1$$

Where, C_1 = known capital cost of the plant 1

C_2 = Required capital cost of the plant 2

S_1 = Capacity of the plant 1

S_2 = Capacity of the plant 2

n = Scaling exponent, where n is usually less than 1.

This work evaluates the equipment cost of cryogenic air separation units (ASU), oxycombustion boiler and CO_2 purification unit (CPU). The equipment cost is the purchased cost of the process equipment, excluding labour, material, installation, other direct and indirect costs. Several

sources in the literature were examined and shown in Table 2-8 and Table 2-9. The reference cost has been updated to 2020 dollars using the Chemical Engineering Plant Cost Index (CEPCI).

The relationship is given as [104]:

$$C_2 = C_1 \left[\frac{Cost\ Index\ in\ year\ 2}{Cost\ Index\ in\ year\ 1}\right] \qquad 2.2$$

For references with currencies given in non-USD, the OECD exchange rate for the particular year was utilized for conversion to USD [105].

2.8.1 Air Separation Unit Cost

The reviewed literature ASU equipment costs with corresponding base years are listed in Table 2-8 (see also Appendix A.3). The technology for O_2 separation from the air is cryogenic distillation. Figure 2-11 shows the cost per unit capacity decline as plant capacity increases for data points from Table 2-8, which shows that the economics of scale applies to ASUs. A power law scaling curve of cost vs capacity is plotted to determine the ASU's scaling exponent.

Figure 2-12 shows the plot of smaller-sized ASU from the references. The exponent is calculated as 0.71. The suggested scaling exponent for ASUs given by "Quality Guideline for Energy System Studies – Capital Cost Scaling Methodology" QGESS [106] and Hamelinck *et al.* [107] are 0.70 and 0.75, respectively. Therefore, the governing scaling equation for calculating the cost of cryogenic ASU using the capacity of oxygen produced as a scaling parameter is:

$$\text{ASU Equipment Cost } (M_{2020}\ \text{USD}) = 0.4489 \left[Capacity\left(\frac{tonne\ O_2}{day}\right)\right]^{0.71} \qquad 2.3$$

Table 2-8: Reviewed ASU equipment cost (2020) and capacities

Label	Source	Cost year	Capacity ($tonnesO_2$/day)	Updated Equipment Cost EC (M_{2020}$)	EC/Capacity (M$/$tonnesO_2$/day)
1	C&EN[1] [108]	2008	250	$27.54	0.11
2	CEMCAP project [109]	2014	395	$27.34	0.07
3	Hamelinck *et al* 2004 [107]	2002	576	$37.83	0.07
4	Callide oxyfuel project [84]	2012	660	$56.66	0.09
5	C&EN[2] [108]	2008	1000	$52.96	0.05
6	CEMCAP project [109]	2014	1055	$56.01	0.05
7	CEMCAP project [109]	2014	1233	$61.50	0.05
8	Keith *et al.* [110]	2016	1500	$42.76	0.03
9	C&EN[3] [108]	2008	2800	$127.11	0.05
10	C&EN[4] [108]	2008	3000	$138.76	0.05
11	NETL 2011 [111]	2007	3653	$173.08	0.05
A	NETL-2019 [112]	2018	3665	$52.68	0.01
B	NETL-2019 [112]	2018	3687	$52.90	0.01
C	NETL-2019 [112]	2018	3954	$55.54	0.01
D	NETL-2019 [112]	2018	4186	$57.81	0.01
E	NETL-2019 [112]	2018	4288	$58.80	0.01
F	NETL-2012 [113]	2018	11681	$126.35	0.01
G	NETL-2017 [101]	2011	12617	$194.54	0.02
H	NETL-2012 [113]	2007	12798	$133.46	0.01
I	NETL-2012 [113]	2007	12955	$134.45	0.01

[1.] Chemical & Engineering News, 12/5/05, p. 36

[2]. Chemical & Engineering News, 8/31/1998, p. 10

[3]. Chemical & Engineering News, 1/19/04, p. 18

[4]. Chemical & Engineering News, 6/3/02, p. 11

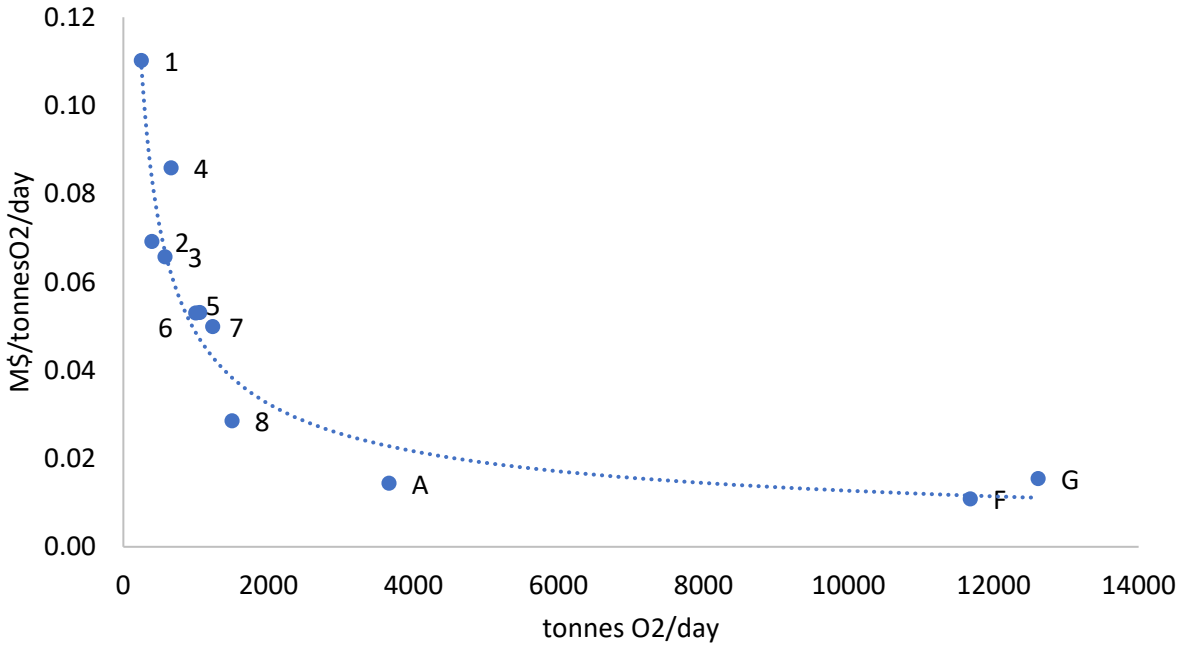

Figure 2-11: Plot of ASU cost per capacity vs capacity

The R^2 values measures how well the regression line fits the underlying data. The closer the value to 1, the better the fit and a value of 0.952 shows that the typical exponential form fits the data well Therefore, for a cryogenic ASU capacity of 377 tpd O_2, the equipment cost is $30.3M.

Figure 2-13 shows the plot of larger-sized ASU from the references. However, for larger capacity ASUs, the exponent is 0.75, and the governing equation is:

$$ASU\ Equipment\ Cost\ (M_{2020}\ USD) = 0.1126\left[Capacity\left(\frac{tonne\ O_2}{day}\right)\right]^{0.75} \qquad 2.4$$

Therefore, for a cryogenic ASU capacity of 377 tpd O_2, the equipment cost is $9.63M. According to Air Liquide Engineering and Construction Technology 2021 handbook [114], the cost of a Sigma–Standard Air Separation Unit, which produces 110 to 380 tpd O_2 up to 99.8% purity, is between 5.37 – 9.67 $M\$_{2020}$. The calculated cost of ASU producing 189 and 306 tpd is $5.74M and $8.24M, respectively. An R^2 value of 0.999 shows an almost perfect fit. However, it

should be noted that the data points evaluated were two National Energy Technology Laboratory (NETL) reports with different capacities.

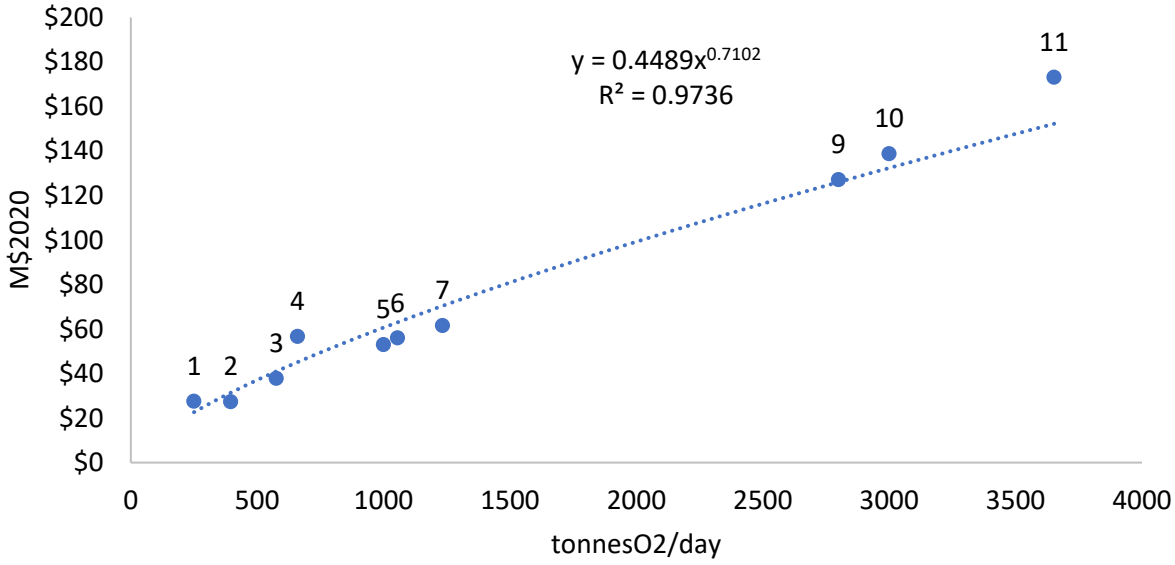

Figure 2-12: Cost versus capacity power regression analysis for smaller ASU capacities

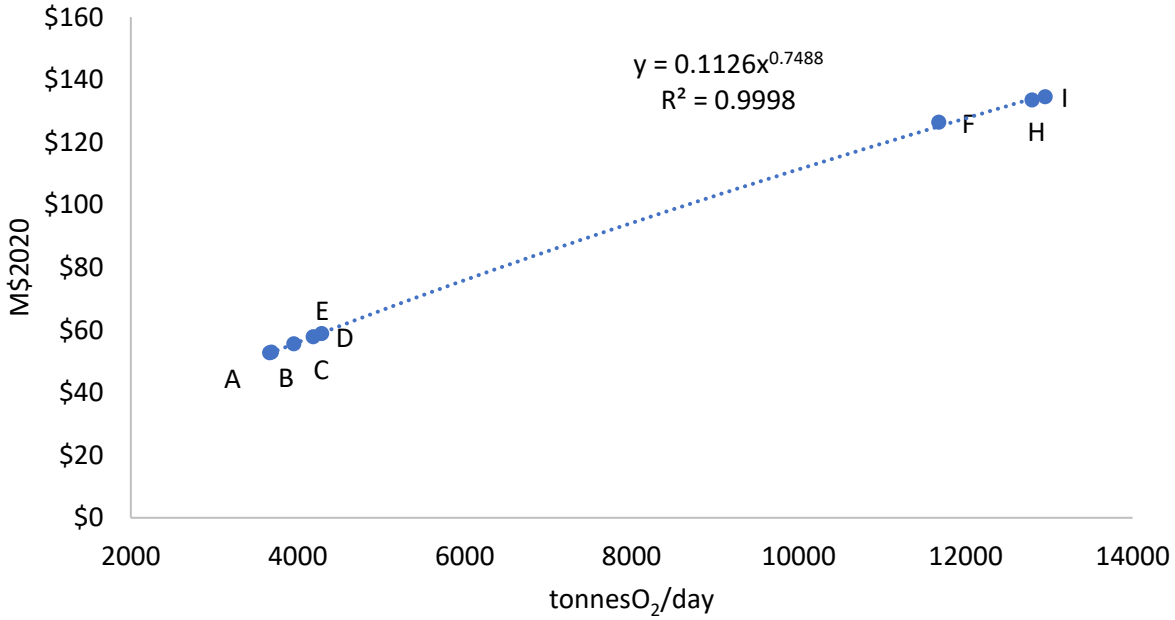

Figure 2-13: Cost versus capacity power regression analysis for larger ASU capacities

2.8.2 CO_2 Purification Unit Cost

The reviewed literature CPU equipment cost is listed in Table 2-9. The range of sources includes compression to >138.8 bar, cooling, drying and distillation. Figure 2-14 shows the cost per unit capacity decline as plant capacity increases for some data points from Table 2-9.

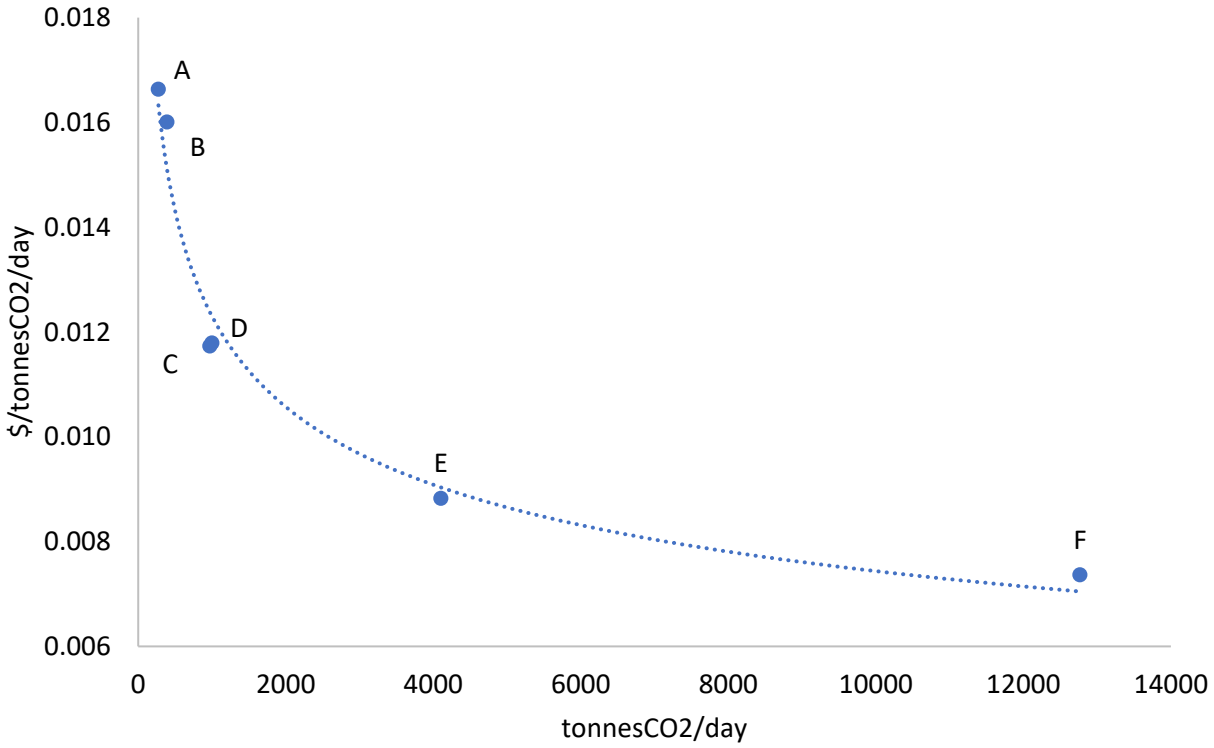

Figure 2-14: Plot of CPU cost per capacity vs capacity

This shows that the economics of scale applies to CPUs. To determine the scaling exponent of the CPU, a power law scaling curve of cost vs capacity is plotted. Figure 2-15 shows the plot of the CPU from the references. The exponent is calculated as 0.78. The suggested scaling exponent for CO_2 compression and drying given by QGESS [106] is 0.77 when using CO_2 flow rate as the scaling parameter.

The governing scaling equation for calculating the cost of CPU using the capacity of CO_2 compressed as a scaling parameter is:

$$CPU\ Equipment\ cost\ (M_{2020}\ USD)\ = 0.0557\left[Capacity(\frac{tonne\ CO_2}{day})\right]^{0.78} \qquad 2.5$$

Table 2-9: Reviewed CPU equipment cost (2020) and capacities

Tag	Source	Other Information	Cost year	Capacity (tonnesCO_2/ day)	Updated Equipment Cost EC (M$$_{2020}$)	EC/Capacity (M$/tonnes CO_2/day)
A	McKaskle [115]	Compression and cooling to 138.8 bar, mol sieve dryer, distillation	2014	274	$4.56	0.0166
B	NETL* 2014 [71]	Compression and cooling to 153 bar.	2011	392	$6.27	0.0160
C	McKaskle [115]	Compression and cooling to 138.8 bar, mol sieve dryer, distillation	2014	972	$11.40	0.0117
D	IBDP* [78]	Compression and cooling to 135bar, TEG, intercooler, and scrubbers	2009	1000	$11.79	0.0118
E	APS* [116]	Compression only to 100atm	2009	4104	$36.20	0.0088
F	NETL 2017 [101]	Compression, drying and distillation 152.7bar	2011	12769	$94.00	0.0074

*Does not include distillation for non-condensable gases.

The R^2 values of 0.9983 shows a good fit of the data to the exponential form. Using equation 5, the equipment cost is calculated as $6.37M and $7.22M for 435 and 511 tpd CO_2 CPUs respectively.

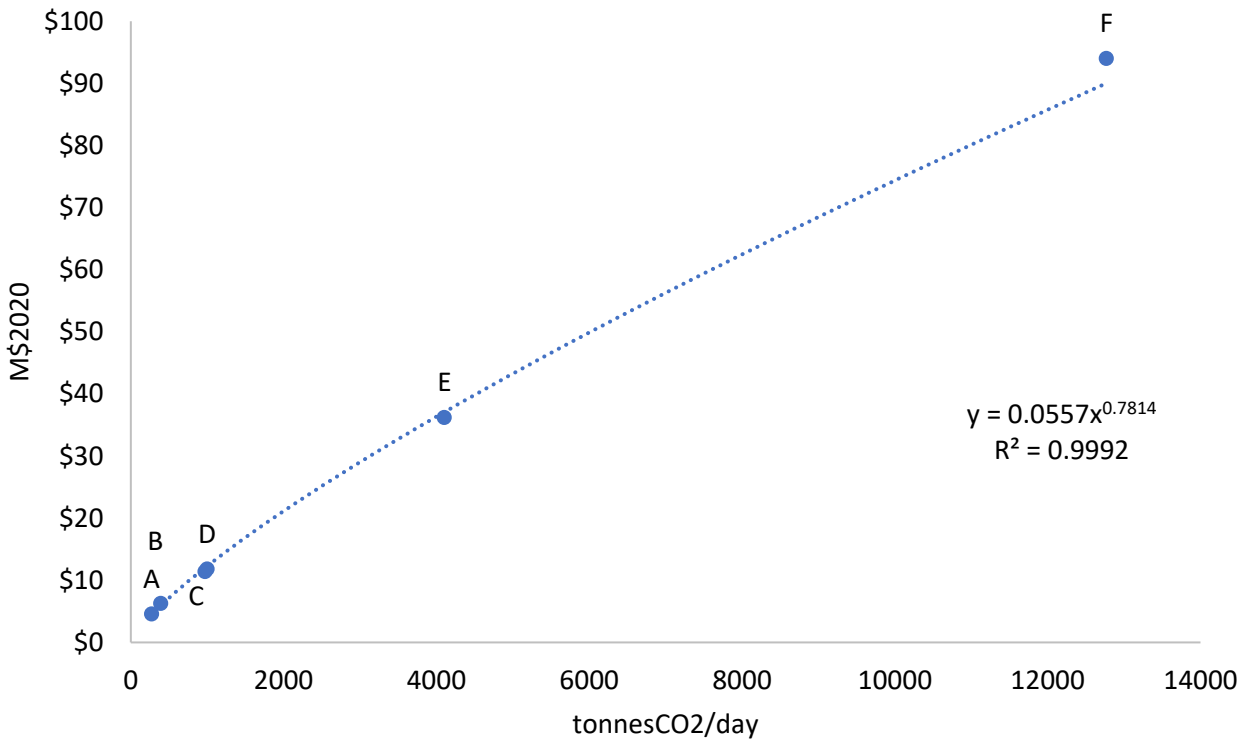

Figure 2-15: CPU Cost versus capacity power regression analysis

2.8.3 Oxyfuel Boiler Cost

Little literature reports the cost of new oxyfuel utility boilers or for retrofit of existing boilers. Lacking better data, the cost of an air combustion utility boiler is assumed to be comparable to that of an oxyfuel boiler. However, an installation factor was included to account for specific modifications for oxycombustion, including [84] :

- Burners optimized for oxycombustion
- Flue gas recycling ducts and fans
- Air preheater replaced by the economizer
- Superheater and attemperators

2.9 Conclusions

Applying oxyfuel combustion for steam generation in a 40 MGY dry grind ethanol mill utilizing direct-fired gas drying for DDGS has the potential to capture about 47 $ktCO_2$ annually. When combined with the fermentation CO_2, the total increases to 159 $ktCO_2$. For the plant utilizing steam drying of DDGS, there is a potential to capture 75 $ktCO_2$ annually. When combined with the fermentation CO_2, the total increases to 187 $ktCO_2$. The composition of the compressed CO_2 meets the ACTL pipeline requirement [100] which can be used for enhanced oil recovery or direct sequestration.

A 40 MGY ethanol plant utilizing steam DDGS drying requires an ASU producing 306 tpd O_2 and CPU producing 511 tpd CO_2. The purchased equipment costs are $8.24M and $7.22M respectively. The ASU requirement is 189 tpd O_2 and CPU 435 tpd CO_2 for the same capacity ethanol plant using direct gas grain drying. The purchased equipment costs are $5.74 M and $6.37M respectively. The summarized Costs results is given in Table 2-10. The installation factor is assumed to account for cost of material, direct and indirect labour, engineering, construction fees, and process contingency (if required). Oxyboiler has double the installation factor as the ASU and CPU). Outside battery limit (OSBL) costs is assumed as 10.5% of the Inside battery limit (ISBL) costs.

The equipment cost estimated here are inputs to the TEA conducted in a collaborative research effort to calculate the MESP and MAC. Additional TEA assumptions are given in Section 4.2 and Appendix C.1.

Table 2-10: Summarized TEA cost inputs and assumptions

		Equipment cost (M_{2020}$)	Installation factor (M_{2020}$)	Total installed equipment cost (ISBL) (M_{2020}$)	Outside battery limit (OSBL) costs (M_{2020}$)	Total installed cost (ISBL+OSBL) (M_{2020}$)
Case 1	ASU	5.74	2	11.5	1.2	12.7
	CPU	6.37	2	12.7	1.3	14.1
	Oxyboiler	0.75	4	3.0	0.3	3.3
	Total	12.86		27.2	2.9	30.1
Case 2	ASU	8.24	2	16.5	1.7	18.2
	CPU	7.22	2	14.4	1.5	16.0
	Oxyboiler	1.05	4	4.2	0.4	4.6
	Total	16.51		35.1	3.7	38.8

Chapter 3 Electrification: Heat Pumps Design

This chapter evaluates the potential of electrification to reduce the contribution of ethanol production to the life cycle carbon intensity of bioethanol. The goal of electrification is, thus, to replace heating based on fossil fuels with electricity by integrating heat pumps, thereby changing the process' energy structure but leaving the process design untouched. The process is directly electrified to reduce the heating required at the expense of additional mechanical work. Electrification is employed in various contexts to significantly reduce CO_2 emissions for industrial heating [117]. Schoeneberger *et al.* [118] explored GHG impacts of the replacement of US industrial boiler with electric boilers, while Chen *et al.* assessed the direct and indirect electrification in methanol production [119]. Atuonwu and Tassou [120] analysed electrified technologies for food processing such as radiofrequency heating, high voltage electric field processing and heat pumps. Cui *et al*. [121] examined potential cost and CO_2 reduction measures for azeotropic pressure swing distillation emissions by electrification based self-heated recovery in a water-tetrahydrofuran system. Rispoli *et al.* evaluated electrification's economic, environmental, and energetic effects on waste-to-ethanol production [122]. This is the first study investigating heat pump use to electrify corn ethanol biorefinery.

3.1 Heat Pump Principles and Applications

Heat pumps are devices capable of transferring energy from a low temperature heat source to a high temperature heat sink using an external (mechanical or thermal) energy source [123]. This is the working principle behind refrigerators and air conditioners. First, the pressure and temperature of the working fluid is increased to a superheated vapour phase through compression using an amount of work input, W in Step 1 (Figure 3-1). Next, heat, Q_h is delivered by condensing the

working fluid in the condenser in Step 2. Finally, the condensed fluid is expanded to low pressure in the expansion valve, Step 3, and sent to the evaporator.

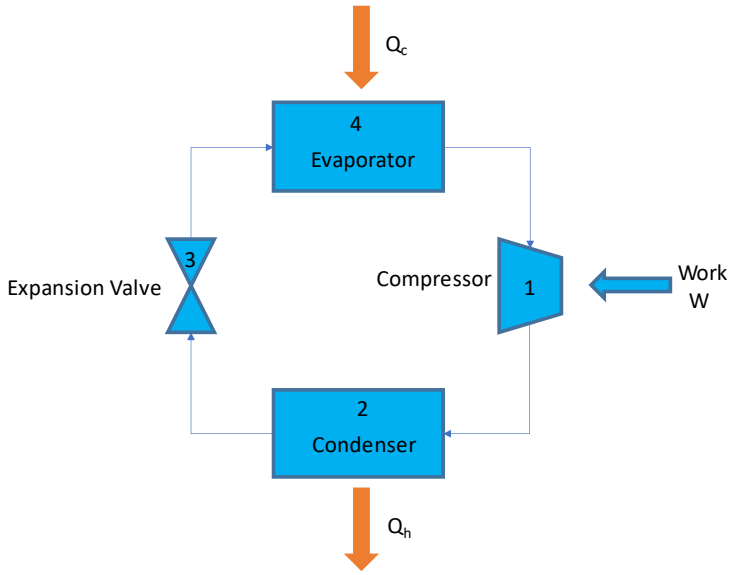

Figure 3-1: Schematic of a closed loop mechanical heat pump

In the evaporator, Step 4, the working fluid absorbs heat Q_c, and the cycle then continues in Step 1. The performance of heat pumps is expressed as coefficient of performance (COP) which is the ratio of heat transferred at high temperature divided by the work in from the compressor.

$$COP = \frac{Q_h}{W} \tag{3.1}$$

The COP for a heat pump is larger than one and can approach 12 for industrially relevant applications depending on the configuration and type of the heat pumps, and process conditions [124]. Common heat pump types include closed cycle mechanical heat pumps, which uses mechanical compression of an isolated common refrigerant as working fluid to achieve temperature lift; open cycle mechanical vapor recompression (MVR) heat pumps, which use a process stream as working fluid; open cycle thermocompression heat pumps, which use steam jet

ejector to increase the pressure of waste vapor; and, closed cycle absorption heat pumps, which use the principles of boiling point elevation and heat of absorption of two component working fluid to output useful temperature lifts [123]. These common heat pumps can be applied to unit operations such as distillation, evaporation and drying in different configurations to improve energy savings relative to use of utility steam [125]–[131]. In some literature, MVR is also called vapour recompression (VR).

3.1.1 Heat Pump Assisted Distillation (HPAD)

In distillation, a heat pump's goal is to utilize the heat of condensation released at the condenser for reboiler evaporation. Jana [125] reviewed heat pump-assisted distillation as an energy-efficient separation technique with a wide range of potential applications in the chemical, refinery, petrochemical, pharmaceutical, and biochemical industries. Furthermore, the simplicity of their introduction, structure, and operation allow heat pump systems to be considered in "grassroots" or retrofitting design in addition to decreasing energy consumption and, consequently, overall cost [125]. Different configurations for heat pump assisted distillation are shown in Figure 3-2. Configuration C is a closed cycle mechanical heat pump while B and D are open cycle mechanical vapor recompression (MVR) heat pumps.

Kiss *et al.* proposed a novel selection criteria for designing low-energy intensive distillation by efficiently reducing the number of technological options that may result in large energy savings, considering the unique process characteristics [124]. Plesu *et al.* presented a straightforward criterion based on the Carnot efficiency to determine if a heat pump is worth considering in a distillation column [132].

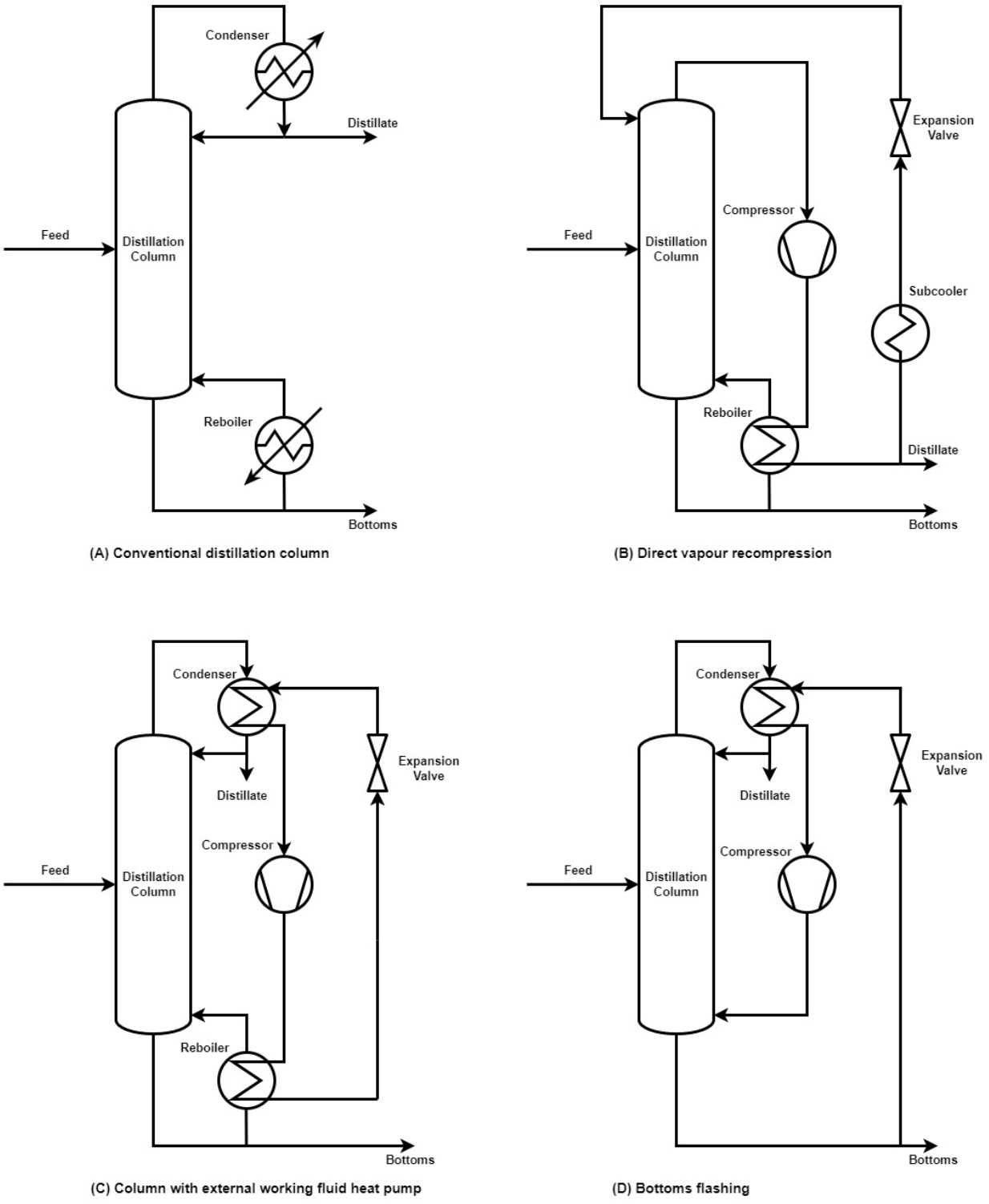

Figure 3-2: Schematic representations of (a) conventional distillation, and (b–d) other common heat-pump assisted distillation configurations (adapted from [133].

$$\frac{Q}{W} = \frac{1}{\eta} = \frac{T_c}{T_r - T_c} > 10 \quad 3.2$$

Where Q = reboiler duty,

W = work input

η = Carnot efficiency

T_r= reboiler temperature

T_c=condenser temperature.

Using this criterion, if $\frac{Q}{W}$ is greater than 10, then a heat pump should be considered. For ethanol-water separation, the ratio $\frac{Q}{W}$ is 16 (where T_r is 100 °C, and T_c is 78 °C).

There is a considerable amount of published studies which investigated HPAD systems [133]–[135], with some specifically for ethanol water mixture [131], [136]. For example, Kazemi *et al.* evaluated the performance of heat pump assisted distillation of an ethanol–water mixture [127] while Luo *et al.* proposed a heat pump extractive distillation for ethanol water mixture [126].

All these studies assume an ethanol-water mixture feed and do not consider some intricacies on the process level, such as the interaction between unit operations upstream and downstream of distillation, distillation feed temperature, final product condition: liquid or vapour distillate, presence of other components in distillation column like non-fermentable solids, oil, etc.

3.1.2 MVR Assisted Drying and Evaporation

Low-grade heat sources are widely available in the food and manufacturing industry due to the prevalence of low-temperature process heating like drying and pasteurization [120]. So, typical low-grade heat sources include the exhaust streams from these operations (sometimes after heat exchange for feed preheating) and related final cooling streams. No supplementary working fluid is employed in MVR systems. Instead, the evaporator is usually part of the main process. To reuse

the stream or water vapour that has been emitted, it is compressed to a higher temperature before or after heat exchange (Figure 3-3).

Patel and Kar [128] reviewed in heat pump assisted drying's principle, types and application for agricultural produce drying. Palacios-Bereche *et al.* [137] incorporated the MVR to multi effect evaporation MEE of juice for ethanol production from sugarcane. Other heat pump assisted drying and evaporation process have been studied including in: energy efficient milk powder production [138], superheated steam drying for food industry [139] ; pulp and/or paper drying in pulp refining industry [140]; wastewater desalination [141].

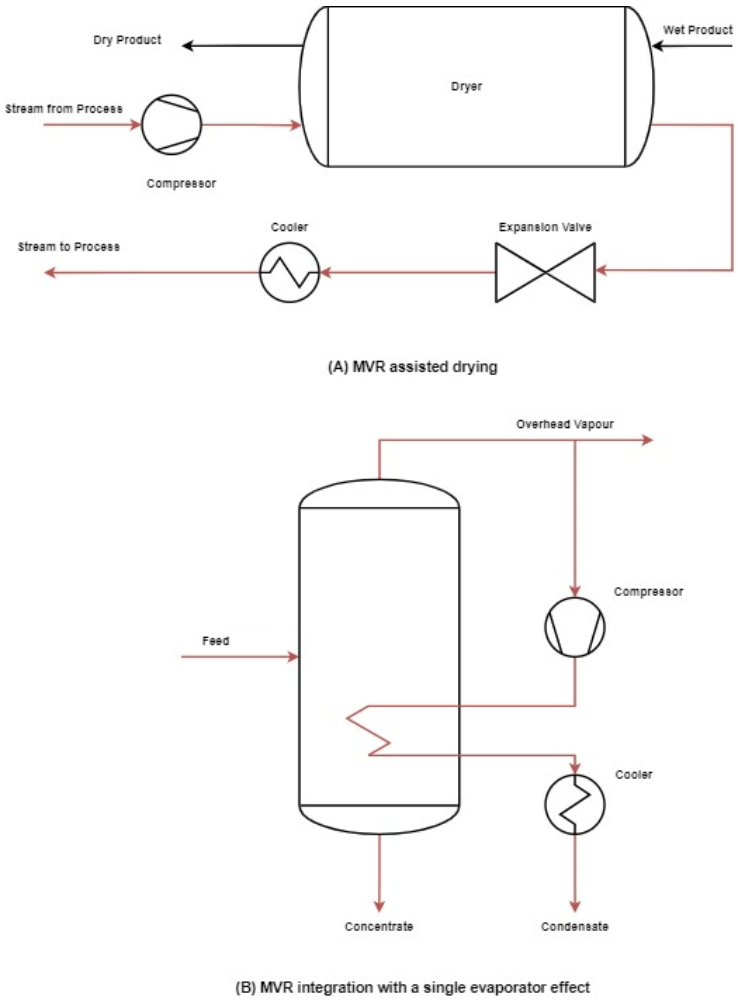

Figure 3-3 : MVR assisted drying and evaporation.

3.2 Material and Methods

Unlike the previous chapter where CO_2 capture is treated as a simple add-on to the process plant (necessitating, perhaps replacement of existing boiler components), integration of heat pump modelling requires detailed interaction of the biorefinery unit operations, i.e., each conversion step. Therefore, a comprehensive process model representing a standard dry mill biorefinery was used to model electrification.

3.2.1 Model Plant Description

A model for dry grind production of ethanol from corn was developed by the USDA Agricultural Research Service (ARS) [60], [97] and a version of this model is available as an example from AspenTech. The process design, and parameters (e.g., product specifications, feedstock composition) are based on information from ethanol producers, engineering firms, and equipment manufacturers [142]. Process modelling was conducted in ASPEN Plus V11, and the non-random two liquid (NRTL) property model was selected.

The base plant (described in detail in Section 2.1) is also 40 million gallons per year (151 million litres per year) dry grind ethanol mill that is representative of a modern biorefinery, located in the midwestern US because of proximity to existing high corn production, ethanol refineries, and geologic formation for sequestration of CO_2 such as the Forest City and Illinois Basins [143], [144]. It uses corn grains as feedstock, producing corn oil, CO_2, and distiller's dried grains with solubles (DDGS) as coproducts. Kwaitchowski *et al* [97] assumed 70% starch content on a dry basis, however, in this chapter, that fraction was increased to 73.5% to be consistent with other assumptions, keeping other components fractions proportional, given that ethanol yield has increased over the years. The main assumptions in this chapter and the previous one remains the same such as ethanol purity, plant size, corn oil extraction. The major differences are the assumed

corn composition and thermal energy requirement. Final assumed corn composition here is given in Table 3-1. There is a slightly higher component fraction here except ash or other solids.

Table 3-1: Modified corn composition

Component	wt% (Dry)
Starch	73.4%
Hemicellulose	4.6%
Cellulose	2.7%
Soluble Protein	3.5%
Insoluble Protein	5.1%
Oil	3.5%
Other Solids	7.1%

The ARS/ASPEN Plus model shown in *Figure 3-4* assumes that the four-effect evaporator's utility need is supplied by the heat of condensation of the second distillation column, therefore, process steam is supplied in only seven major places: liquefaction of ground corn with process water and enzymes to 88 °C (BLOCK EM01DUTY), cooking of backset from stillage and the previously liquefied stream to 110 °C (BLOCK EM03), beer column reboiler (BLOCK BEERCOL), second distillation column reboiler (BLOCK RECTIFY), molecular sieve package to increase ethanol purity to 100 wt% (BLOCK ED03), pre evaporator to 16.25 wt% solids (BLOCK PRE-EVAP) and drying of DDGS to 9 wt% (BLOCK DRYDDGS).

Features of the ARS/ASPEN plus Model

This subsection is a brief description adapted from the ASPEN plus example file. The model is described as a guide for understanding ethanol economics and a starting point for more sophisticated modelling. Components which represent chemical species include water, ethanol,

CO_2, glucose, NFDS (nonfermentable dissolved solids), Xylose (C5 sugars) and Protsol (soluble protein) are selected as CONV while starch, C5poly, C6poly, PROTSOL (insoluble proteins) and oil are selected as Solid components. Solid component types are non-library chemicals with user specified property parameters. The selected physical property method is Non-Random Two Liquid (NRTL) to estimate the chemical and thermodynamic equilibrium, and the physical properties of all streams. The reliability of results and the predicted cost of process equipment are significantly influenced by how accurately physical property calculations are performed.

Simplified chemical reactions includes saccharification (99% conversion of starch), fermentation (100% conversion of glucose to ethanol, CO_2 and NFDS). Saccharification and fermentation reactors are assumed to continuous processes and are modelled with RSTOIC reactors with stoichiometric reactions. Conversions and molar extents may also be adjusted. The effect of acid, enzymes and yeast in the reactors are not modelled but represented by NFDS, water and water respectively. Dehydration and dewatering are simplified separation blocks and not based on adsorption or centrifugation. Evaporation and DDGS drying are flash calculations for heat load requirement for desired moisture content.

3.2.2 Model Modification

The modifications to the ARS/ASPEN Plus example flowsheet include scaling the annual production from 189 million litres per year to 151 million litres per year (50MGY to 40MGY), modification of corn composition, detailed modelling of the multi-effect evaporator, addition of corn oil extraction and VOC thermal oxidizer, and integration of heat pumps to the flowsheet. Other modifications include RADFRAC breakdown to allow heat integration in the distillation column i.e., condenser and reboiler are modelled as external heater blocks (*Figure 3-5*).

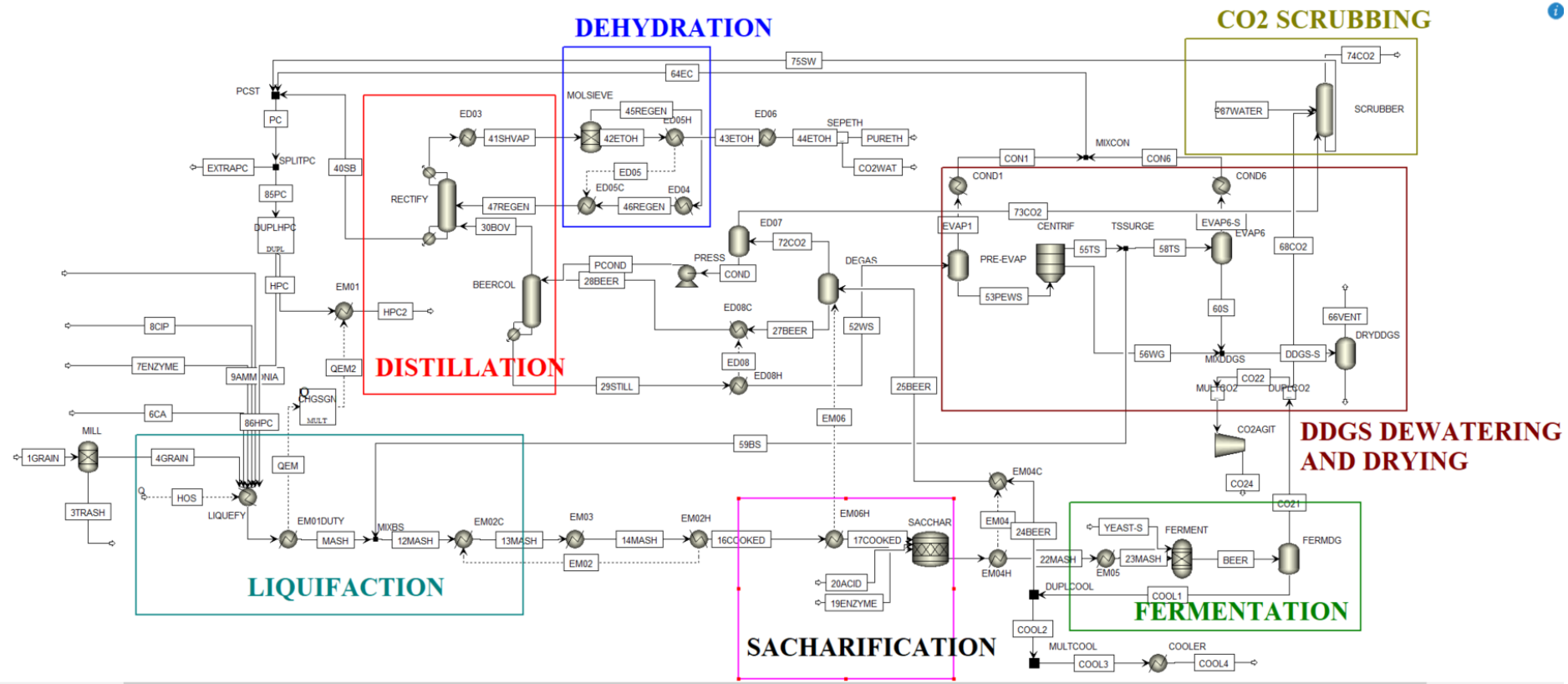

Figure 3-4: ARS/ASPEN PLUS model example of bioethanol from corn

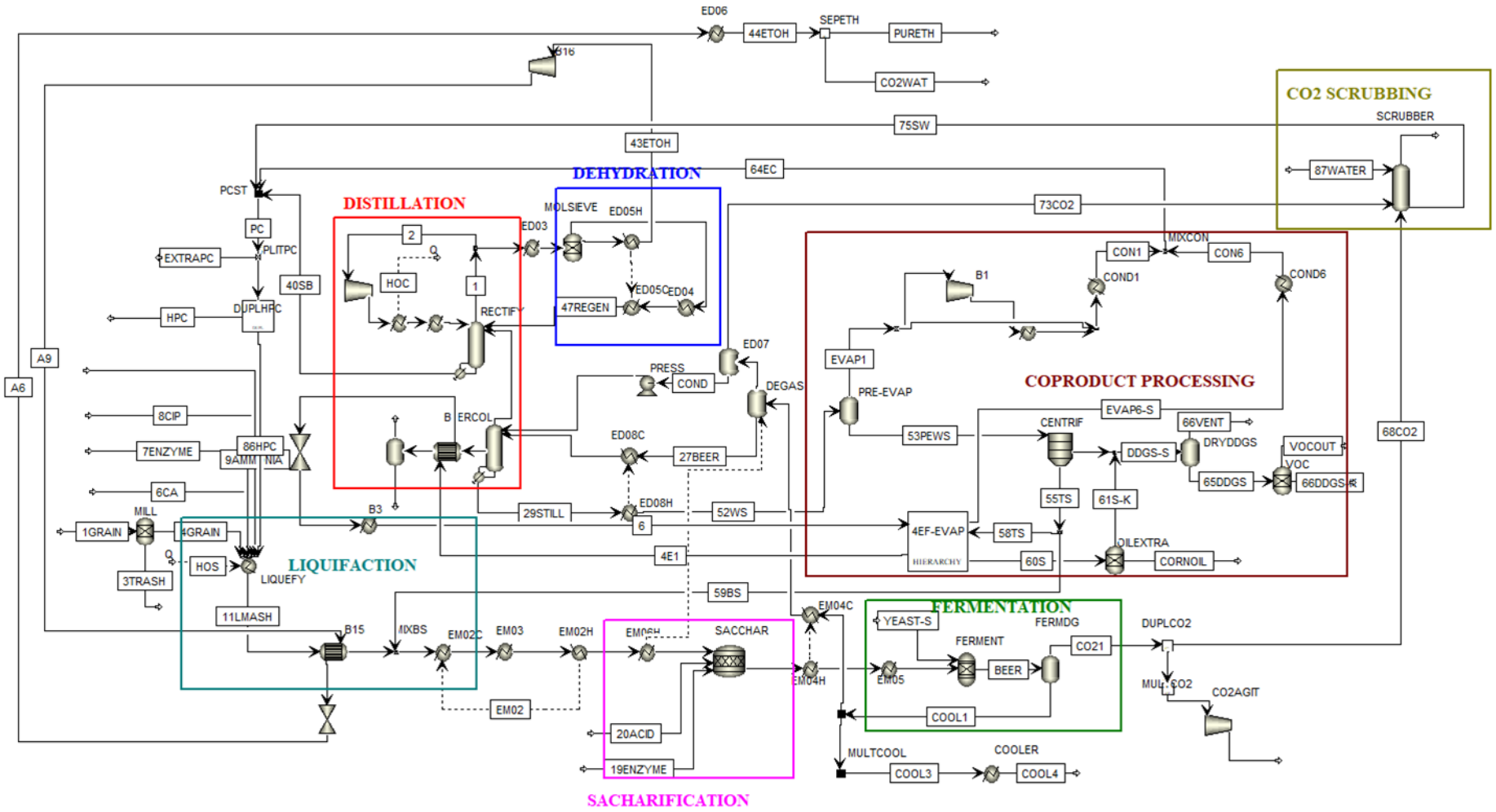

Figure 3-5: Final Flowsheet of modified ASPEN plus model.

MVR assisted 4-effect evaporation

This modification is shown in *Figure 3-6*. Each effect is modelled using a flash vessel and a condenser block. The heat of condensation from the Rectify column (HOC in *Figure 3-5*) is used in the first effect to evaporate water from the thin stillage in the tubes. The heat liberated by the condensing steam is delivered to the flash vessel of the next effect. This heat energy was reduced by 0.5%, regulated by a calculator block, to allow for heat losses. As a result, four coolers and four flash vessels were used to replicate the four-effect evaporation. The effects are assumed to have a pressure distributions at 1.6, 1.2, 0.6, 0.4 atm, respectively. A design specification adjusts the final concentration of syrup in the last effect to 55% solids. With this design specification, there is an excess energy after evaporation, which has been upgraded by MVR (i.e., compressed to a higher pressure to increase the temperature) and used to heat the reboiler of the BEERCOL BLOCK.

Corn oil extraction and VOC thermal oxidizer

Besides the standard DDGS coproduct, more corn oil is extracted from ethanol production. The extraction of corn oil, a biodiesel feedstock, is facilitated by installing corn oil extraction machinery in an existing ethanol plant, without impacting the amount of ethanol produced. After fermentation, distillation, and before drying of DDGS, corn oil is extracted from syrup from the evaporation step. It is modelled as a separator that removes 78% of oil in the syrup. In addition, the thermal oxidizer is modelled as a separator removing 2% of the DDGS as exhausts. *Figure 3-7* shows the corn oil extraction on the flowsheet and VOC thermal oxidizer from DDGS drying.

Integration of MVR heat pump

Open cycle MVR heat pumps recover waste heat in process streams that require cooling. Therefore, the MVR has a lower investment cost than the close loop cycle mechanical heat pumps

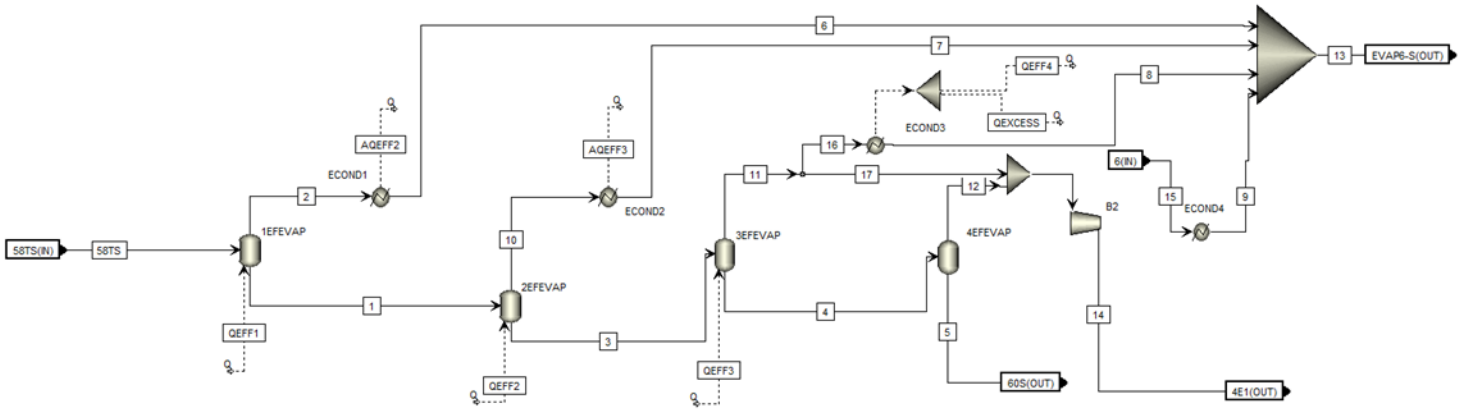

Figure 3-6: Detailed 4-effect evaporator process model

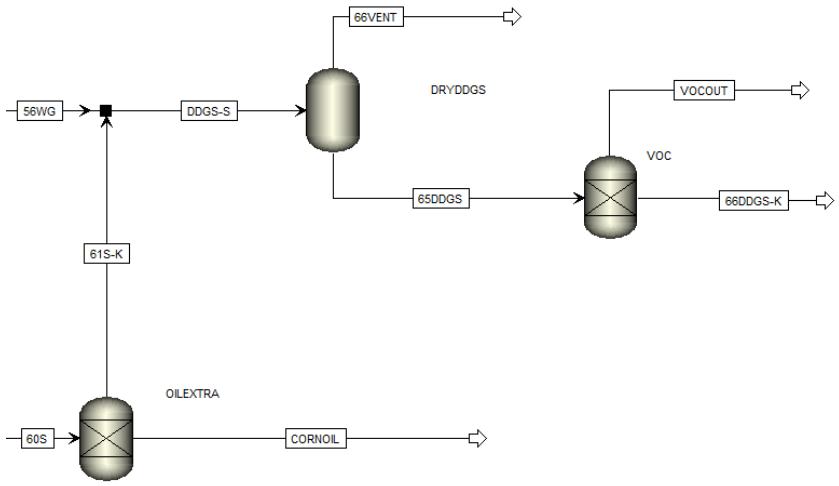

Figure 3-7: Corn oil extraction, DDGS drying, and VOC thermal oxidizer.

as one heat exchanger is eliminated. The process streams are compressed to higher pressure and temperature, then condensed as it exchanges heat with compatible process utility point of need in a heat exchanger. The pressure is dropped in an expansion valve and finally cooled to originally required point to continue the flowsheet as the base case, to avoid large scale changes to the downstream equipment duties.

There are two successful matches: a part of EVAP1 stream with PREEVAP block and 43ETOH stream with LIQUEFY block. The steam utility demand of the unit operation (block) is, thus, completely replaced by the electrical input of the compressors. The compressors are assumed to have an efficiency of 85%. Minimum temperature approach in the heat exchanger is 5^{o}C. The final modified flowsheet is shown in *Figure 3-5*.

3.2.3 Model Validation

To ensure the relative accuracy of the model, the result was validated with available real-life data/survey. For example, see comparison of results with Mueller and Kwik data in Table 3-2. Generally, the ARS Aspen Model has a better plant energy efficiency and better coproducts yield.

Table 3-2: Validation of results

Parameter	Chapter 2 CCS model	Mueller and Kwik [16]	Chapter 3 Model	% Difference (Aspen and Mueller & Kwik)
Thermal energy use (MJ/L)	8.08	7.38	7.55	2.3
Ethanol yield (gal/bu)	2.82	2.82	2.82	0
DDGS yield (lb/bu)	15.75	15.73	15.82	0.6
Corn oil yield (lb/bu)	0.43	0.53	0.53	0
CO_2 yield (lb/bu)	17.9	-	18.08	-

*bu= bushel, lb=pounds, gal=gallon, MJ= Megajoules, L= Litres.

3.3 Electrification Results and Discussion

The flowsheet converged with no errors. The modifications described in Section 3.2.2 result in a 63% reduction in the base plant heat demand when evaporation duty is excluded and 80% reduction when evaporation duty is included. The average calculated COP is 5.6. The final assumed carbon content of corn is 41.04%.

Table 3-3 shows the corresponding required heat duty for each stage. Table 3-4 shows the coefficient of performance of the heat pumps. Finally, the carbon balance is given in Table 3-5.

Table 3-3: Heat demand for the 40 MGY base plant

Point of use	Heat duty (kW)	% of total
Molecular sieve	261	1
Liquefaction	4394	13
Cooking	1654	5
DDGS drying	7114	21
Pre evaporation	4920	14
Beer column reboiler	12190	36
Second column reboiler	3507	10
Total	34071	100
Evaporation	29043	-

Table 3-4: Coefficient of performance results

Point of use	Q_h (kW)	W (kW)	COP
Liquefaction	4394	755	5.8
Pre evaporation	4920	514	9.6
Beer column reboiler	12190	4992	2.4
Evaporator	29043	2745	10.6

Table 3-5: Carbon balance for electrification case

	Carbon in			Carbon out			
Source	Flowrate	%C	C in kg/hr		Flowrate	%C	C in kg/hr
Corn	43075	41.04%	17678	EtOH	14343	52%	7478
				DDGS	12176	49%	5966
				Corn oil	406	76%	308
				CO_2	13705	27%	3740
Waste				Trash	129.2	41%	53
				CO_2wat	11.0	27%	3
				Vent	1.3	52%	1
				VOC	248.5	49%	122
				CO_2ethoh	13	52%	7
Total			17678				17678

3.3.1 Effects of Mechanical Compression Efficiency on Output Power

The basic assumption for the MVR compressors is 85%. The driver power varies inversely with the compression efficiency, as shown in *Figure 3-8*; the higher the efficiency, the lower the driver power. 100% is completely hypothetical.

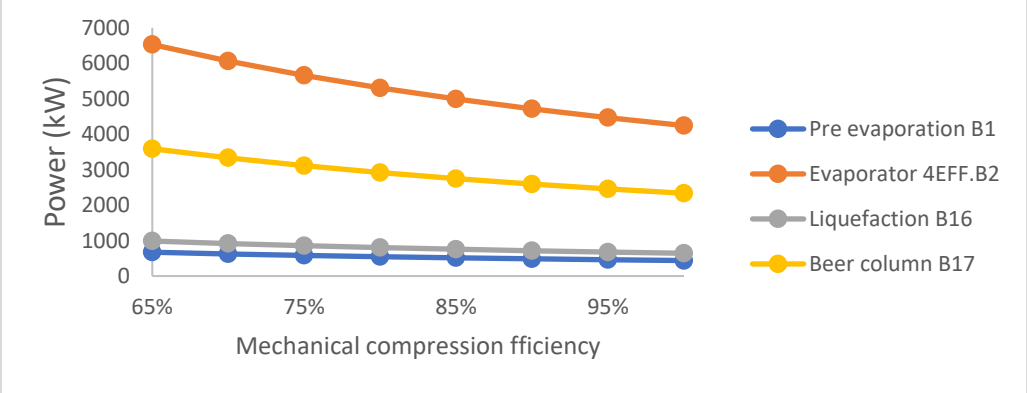

Figure 3-8: Effects of mechanical compression efficiency on output power

3.4 MVR Equipment Cost Evaluation

Without cost information for a reference plant with heat pumps, Aspen Process Economic Analyzer (APEA) evaluates the capital cost of upgrading a conventional ethanol dry mill with heat pumps. Using APEA, the installed capital cost of equipment, installation, and ancillary equipment costs can be estimated. Only the additional compressor cost to MVR unit operations added to the flowsheet was evaluated because of its share significance in the upgrade. It is assumed that the heat exchangers in base plant will be useful for the modifications. This analysis does not consider the cost of removal, disposal, or sale of unused/non-required equipment. The equipment cost is evaluated in the following steps:

- After the convergence of the flowsheet simulation, the economics tab in Aspen Plus is activated.
- Next, the model representing unit operations such as distillation, compression, absorption, and cooling is mapped for sizing physical equipment in the Aspen database by clicking "Send to APEA" in the Economics tab.
- The APEA software is launched, and the default mapping of all the designs in the flowsheet is loaded. The cost index was also adjusted to 2020 using the CEPCI (same as chapter 2 for consistency in cost model), with the base year in the APEA V12 database being 1st Quarter of 2019.
- The compressors are selected as reciprocating integral gas compressors, requiring actual gas flow rate inlet (cubic feet per minute CFM), design gauge inlet and outlet pressure (PSIG) and driver power (HP) as input to evaluate costs. Mckascle *et al.* [115] recommend a rotary screw compressor for CO_2 compression based on lower costs, but this type is

unavailable for selection in the database. Other selection for modification includes casing material (default carbon steel is used). The corresponding inputs and estimated cost in 2020 USD are summarized in Table 3-6 (results are rounded to 2 Significant figures). Installed cost is the ISBL which includes installation cost of piping, civil, electrical, and manpower costs. The detailed APEA results are given in Appendix B.2. The value estimated in this section is subjected to the same economic assumptions given in Appendix C.1 for the techno-economic analysis to evaluate the electrification MESP.

Table 3-6: APEA cost of MVR compressors in 2020 USD

Compressor	Purchased equipment cost	Installed cost (ISBL)	Capacity (CFM)
Liquefaction B16	$1,100,000	$1,300,000	5,981
Pre evaporation B1	$860,000	$1,100,000	17,782
Beer column B17	$1,400,000	$1,700,000	11,446
Evaporator 4EFF.B2	$5,300,000	$5,800,000	35,387
Total	$8,700,000	$9,800,000	

3.4.1 Effects of Mechanical Compression Efficiency on Cost.

Since the driver power is a required input to evaluate the costs of the compressors, the sensitivity of cost to mechanical compression efficiency is evaluated and displayed in Figure 3-9. Both equipment and installed costs decrease as the compression efficiency increases (driver power reduces). Therefore, the higher the compression efficiency, the better the price.

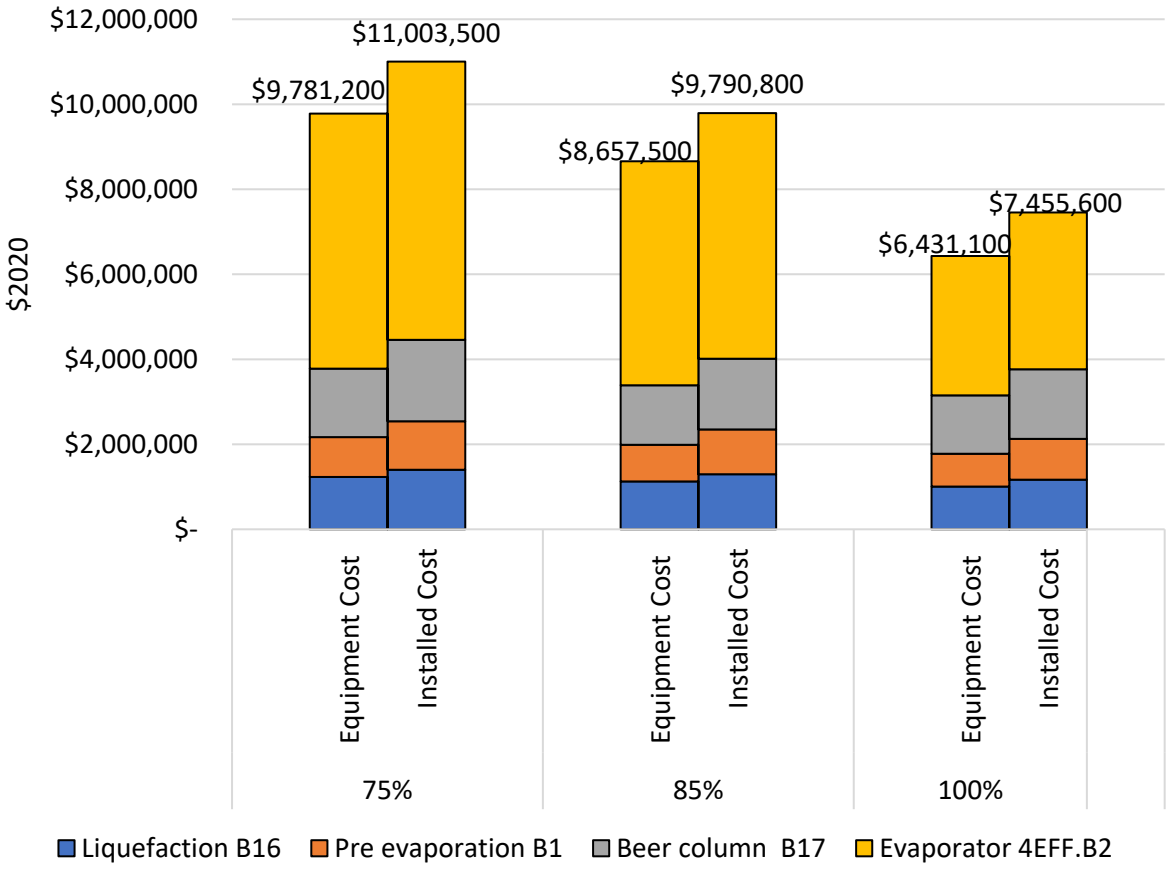

Figure 3-9: Effects of mechanical compression efficiency on costs

Chapter 4 Life Cycle and Technoeconomic Analysis

This chapter discusses the LCA and TEA analyses that allow the emissions reduction options modeled in the previous chapters to be compared. The approach taken follows that taken by Dees *et al.* [61], but the analysis is expanded to include both CCS and electrification options in this chapter. In addition, this chapter modifies Dees et al. reported lifecycle inventory and cost model.

4.1 Life Cycle Assessment (LCA)

The LCA's goal is to calculate the change in the well-to-wheel (WtW) carbon intensity of corn fuel ethanol from a dry mill ethanol refinery resulting from the incorporation of CCS, an oxyfuel combustion boiler, and heat pumps. In addition, these alterations' influence on a base refinery described earlier (Section 2.1) is compared. The Base case life cycle inventory is extracted from Argonne National Lab's GREET.net 2019 Model with some parameters adjusted with results in previous chapters. The adjusted parameters are ethanol, co-product yield, and baseline and intervention scenario thermal energy and power requirements.

The functional unit is based on 1 MJ (LHV) of ethanol ready for blending into gasoline. For this analysis, the system boundary includes farming of corn, transportation of corn from farm to refinery, production of ethanol from the corn starch feedstock, and transport of finished ethanol product to blending/denaturing facility. While the impact of blending and denaturing is not considered in this analysis, the final combustion of the ethanol is assumed to be embodied biogenic carbon, which returns to the atmosphere as CO_2. Additionally, no significant emissions are assumed to be associated with permanent storage in a saline aquifer. Electricity is supplied by the Midwestern Reliability Organization (MRO) with grid emission intensity of 625 gCO_2e/kWh. Corn travels about 50 miles by heavy diesel truck from the farm to the ethanol refinery while ethanol is transported 1800 miles by Diesel rail to denaturing and blending facility.

System expansion was used for the treatment of multifunctionality. Ethanol carries all environmental burdens (and benefits) of production, while co-products are assumed to substitute for equivalents in the market. This treatment is consistent with that applied to ethanol in the California LCFS program, in which DDGS is assumed to displace alternative agricultural feed. The type and mass of feed displaced relative to the total mass of DDGS are corn (78%), soybean meal (31%), and urea (2.3%). Because the displacement ratio of DDGS to feed is greater than 1, the sum of these weight percentages exceeds 100%. In contrast, corn oil displaces soy oil on a 1:1 basis. Similarly, system expansion is adopted to include land use change (LUC) impacts of corn production, as assumed in the most recent CA-GREET 3.0 Model under the LCFS program. More details available in Dees *et al* [61]. Biogenic CO_2 emissions are assumed to be "net zero"; short rotation crops such as corn will uptake equivalent quantities of CO_2 in the next growth cycle; thus, oxidization of carbon originating in corn feedstock adds no net CO_2 to the atmosphere.

The nomenclature of the cases considered in addition to the base case are summarized as:

- Case 1A: Fermentation CO_2 capture and storage
- Case 1B: Integration of oxyfuel boiler with fermentation CO_2 capture and storage
- Case 2: Integration of mechanical vapour recompression heat pumps
- Case 3A: Case 1A + Case 2
- Case 3B: Case 1B + Case 2

4.1.1 LCA Results and Discussion

The base case—representing corn ethanol produced from a modern, dry mill ethanol plant in the US—has a total CI of 55.4 gCO_2e/MJ (Figure 4-1). For comparison, the life cycle fuel pathways database for California's Low Carbon Fuel Standard (LCFS) reports GHG emissions intensities

(CI scores) for corn-only dry mill ethanol facilities ranging between 53 and 86 gCO_2e/MJ [145]. The US Department of Agriculture (USDA)'s 2019 data reports the CI of US corn ethanol using the GREET model as 56.6 gCO_2e/MJ, which includes a land use change (LUC) GHG value of 6.7 gCO_2e/MJ and project a CI of 51.7 gCO_2e/MJ for 2022 [14]. Lee *et al.*[15] estimates 52.4 gCO_2e/MJ in 2019 (including the LUC value of 7.4 gCO_2e/MJ) while Scully *et al* [17] estimated a CI of 51.4gCO_2e/MJ in 2020.

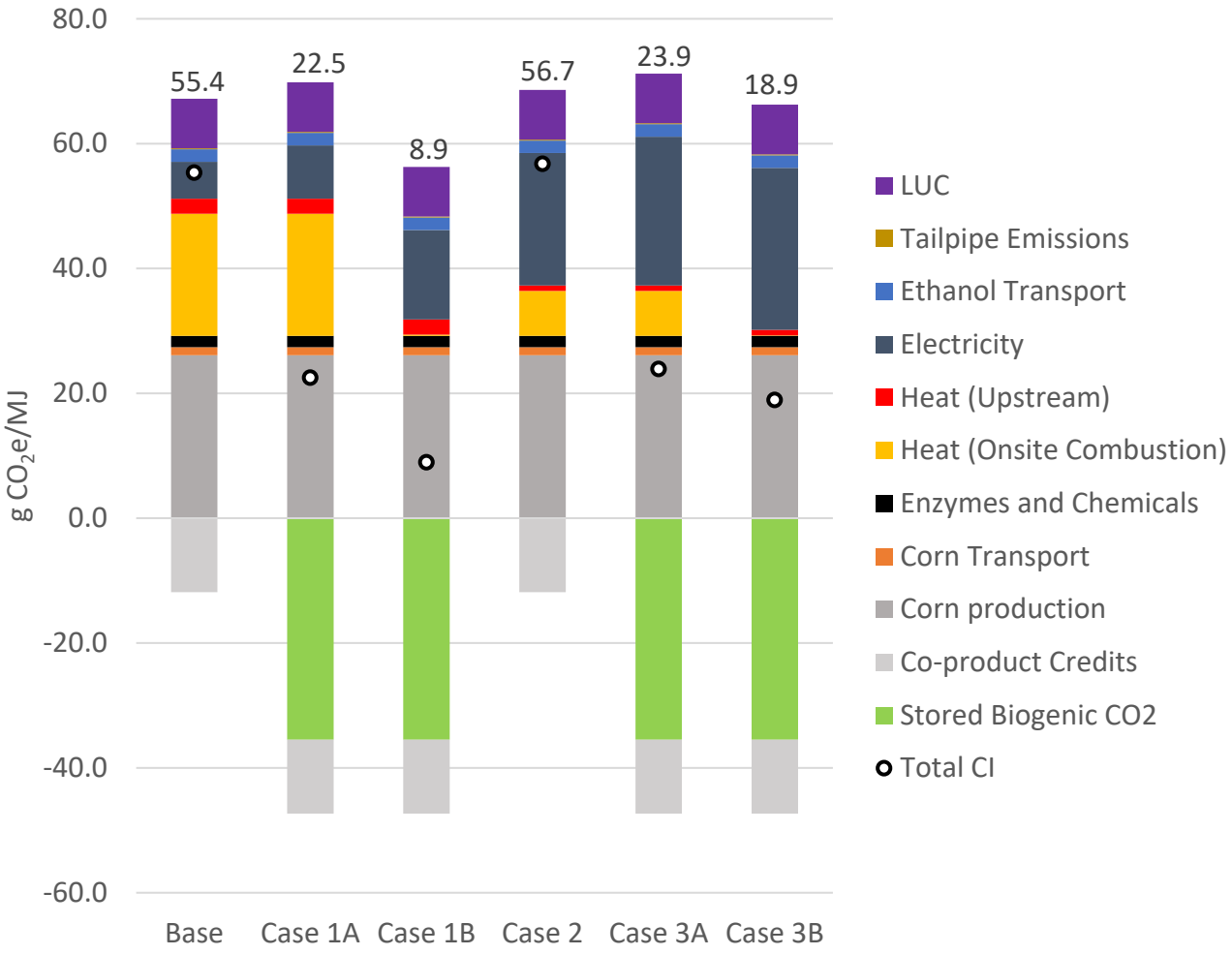

Figure 4-1: Life cycle carbon intensity of six cases examined. CCS = Carbon Capture and Sequestration, LUC = Land Use Change

Corn production accounts for the largest life cycle emissions, followed by onsite natural gas combustion in the boiler. LUC emissions are the next largest contributor at 8 gCO_2e/MJ followed by electricity generation. Co-product credits for emissions avoidance reduce the overall CI in all six scenarios by 11.9 gCO_2e/MJ. Tailpipe emissions are negligible and comprise only non-CO_2 GHGs, due to the biogenic origin of the carbon.

Case 1A—fermentation CO_2 capture and storage—yields a CI of 22.5 gCO_2e/MJ, a 59% reduction of the base case. Emissions from electricity generation increased by 44% due to the extra power required for the CPU. The CCS system captures approximately 35.5 gCO_2/MJ from the fermentation stage. Because the CO_2 captured from fermentation is solely of biogenic origin and, thus, originated from the atmosphere, its capture and storage is represented as a negative value (credit) in the lifecycle. Onsite combustion of natural gas remains the largest share of onsite facility emissions, accounting for 19.6 gCO_2e/MJ.

Case 1B targets CO_2 emissions from the fermentation column and the oxyfuel boiler. This scenario yields a CI of 8.9 gCO_2e/MJ, an 84% reduction from base case. Additional grid power required for the ASU and CPU results in a 142% increase in emissions associated with electricity generation. However, the boiler combustion emissions are reduced by 99% since almost all CO_2 is captured by oxyfuel CCS system.

Case 2 which uses heat pumps for electrification yields a CI of 56.7 gCO_2e/MJ, a 2% increase from the base case. Emissions from electricity generation increase by 259% due to the addition of electric power in the heat pump compressors which leads to a decrease 63% in onsite combustion emissions.

Case 3A and 3B have a CI of 23.9 gCO_2e/MJ and 18.9 gCO_2e/MJ respectively. Emissions from electricity generation increases substantially due to the addition of electric power in the heat pump

compressors, ASU, and CPU. However, because they both include the capture of fermentation CO_2, they also receive a credit in the lifecycle.

4.1.2 LCA Sensitivity Analysis

Figure 4-1 shows that electricity production emissions significantly contribute to lifecycle emissions, particularly in Cases 2, 3A and 3B. The GHG intensity of electricity generation can also vary depending on the composition of the electricity grid mix (or choice of stand-alone resource) from well below 100gCO_2e/kWh to close to 1 kgCO_2e/kWh. The impact of the GHG intensity of electricity generation on life cycle emissions is explored in this section.

Four cases were added to the Base case for electricity, in which GHG generation intensity represents that in the Midwest Reliability Organization (MRO) region. The four sensitivity cases are a hypothetical zero marginal emissions electricity source, a future hypothetical grid mix of 100 gCO_2e/kWh (e.g., a predominantly renewable grid mix), the current California grid intensity of 271 gCO_2e/kWh, and the current average U.S. Central/Southern Plains GHG intensity at 754 gCO_2e/kWh, keeping all other assumptions constant. Figure 4-2 shows the results of the sensitivity of CI to changes in grid electricity. In the zero-emissions grid, the CI of ethanol is reduced to -5.4 and -7.1 gCO_2e/MJ for Case 1B and 3B, respectively. The high-end test yields a maximum CI of ethanol of 61.1 gCO_2e/MJ for Case 2. For MVR to have the same CI as the base case, the grid emission intensity should be 584 gCO_2e/kWh i.e., 7% less than MRO grid intensity. Net zero is achieved at grid intensity of 170 gCO_2e/kWh for all interventions combined. Case 1B gives the most emission reduction benefits. The all-intervention Case 3B is most sensitive to electricity CI (the steepest slope).

Effects of Mechanical Compression Efficiency on Carbon Intensity

As the mechanical compression efficiency changes, the impact on overall carbon intensity is evaluated while keeping the electricity emissions intensity constant on the MRO grid. This efficiency is varied between a low 65% and a theoretical high of 100%. The base case assumption is not varied because it is assumed to be constant and not shown in Figure 4-3. The lowest and highest points are 7.7 gCO_2e/MJ and 58.8 gCO_2e/MJ.

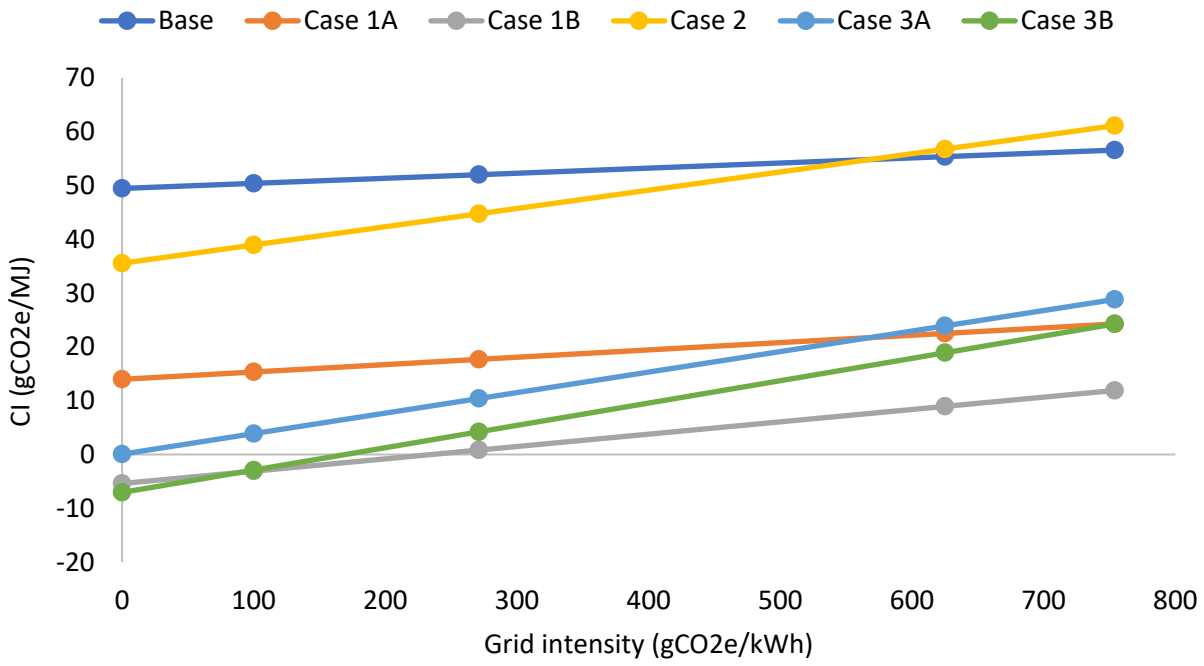

Figure 4-2: Sensitivity of CI to changes in grid electricity

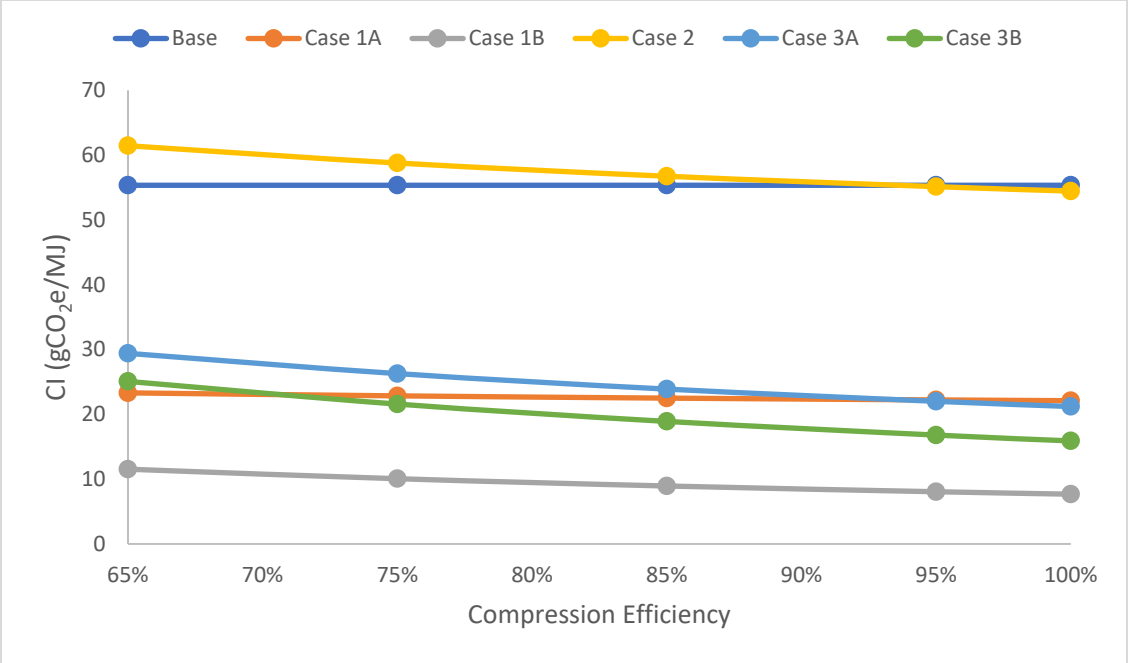

Figure 4-3: Effects of mechanical compression efficiency on carbon intensity

4.2 Techno-economic Assessment TEA

The techno-economic assessment TEA uses a discounted cash flow analysis to determine the minimum ethanol selling price (MESP) for each case described in Section 4.1. MESP is the least price ethanol must be sold for a net present value of zero, assuming a 10% after-tax return on equity. The TEA builds upon an in-house version of the United States Department of Agriculture (USDA) Dry Mill Ethanol Production [146], [147]. This model uses a cost-to-capacity method, as described in Section 2.5, to estimate the purchased equipment cost and applies an installation factor to arrive at the installed or inside battery limit (ISBL) capital cost. The financial assumptions such as outside battery limit (OSBL), project contingencies, and indirect costs, for the discounted cash flow analysis are shown Appendix C.1.

The reference costs are primarily based on the equipment costs reported in prior NREL cost assessments [146]–[150]. The cost evaluated in sections 2.5 and 3.4 are additional inputs for the

technological pathways assessed in this study. All costs are adjusted to 2020 U.S. dollars using the Chemical Engineering Plant Cost Index (CEPCI) [151], U.S. Bureau of Labor Statistics' Labour Cost Index [152] and Chemical Cost Index [153] for equipment, labour and feedstock respectively.

Table 4-1 shows estimated capital costs, operating costs, and product prices. It should be noted that these results does not include any policy incentive. The policy impacts were analysed separately and discussed in Section 4.2.2. One additional plant employee was assumed to run the plant under CCS intervention scenarios. The boiler installation factor increased from 3 to 4 for cases 1B and 3B. Other installed costs for all Cases have been explained previously.

4.2.1 TEA Results and Discussion

The MESP and marginal abatement cost (MAC) of the cases are shown in Figure 4-3. There is no abatement cost in the base case. The MAC is the ratio between the difference in production cost relative to the base case versus the difference in CI relative to the base case. The base case MESP is \$1.94/gallon, comparable with the production costs of \$1.81-\$2.03/gallon reported by Ethanol Profitability Model by Iowa State University Extension Office [154] between January 2020 and December 2021.

Case 1A yields a MESP of \$2.10/gallon, an 8% increase from base case. This results from additional CPU capital costs and increased OPEX costs associated with increased grid power demand and CO_2 transport and storage. As a result, the MAC is \$54/tCO_2e avoided.

Case 1B targets CO_2 emissions from the fermentation column and the oxyfuel boiler. This case yields an MESP of \$2.34/gallon, a 21% increase from base case. This is due to increased CPU, ASU, oxyfuel boiler, OPEX, and CO_2 handling costs. As a result, the MAC is \$95/tCO_2e avoided.

Table 4-1 CAPEX and OPEX estimates and coproducts prices (2020 USD basis)

Base Case CAPEX	Price
Total installed equipment cost (ISBL)	$77.8M
Total installed cost (TIC)	$86M
Total plant cost (TPC)	$133.3M
Total capital investment (TCI)	$146.6M
OPEX	
Fixed operation costs	$7M/yr
Corn	$3.30/bushel
Electricity (Midwest)	$0.072/kWh
Natural Gas	$4.20/mmBtu
Co-product selling price	
DDGS	$0.074/lb
Corn Oil	$0.28/lb

Case 2 which uses heat pumps for electrification has a MESP of $2.08/gallon, a 7% increase from the base case. This is also less than the case 1B because no additional plant employee is required (no ASU and CPU) and boiler type is a smaller conventional air fired. Because the CI of the fuel in Case 2 is larger than in the Base Case, marginal abatement cost is not calculated.

Case 3A and 3B have a MESP of $2.24/gallon and $2.34/gallon respectively with corresponding MAC of $107/t$CO_2$e and $122/t$CO_2$e respectively. Case 3B which is all scenarios investigated combined has the same MESP as case 1B (fermentation+ Oxyfuel combustion) because, even though there is additional cost incurred from MVR modification, the boiler, ASU, and CPU capacities are smaller, which results in a smaller CAPEX. In addition, a tradeoff between natural

gas and electricity prices in OPEX. For example, energy cost per gallon is constant, and an increase matches the reduction in thermal energy consumption in unit energy costs (i.e., electricity being more costly than natural gas).

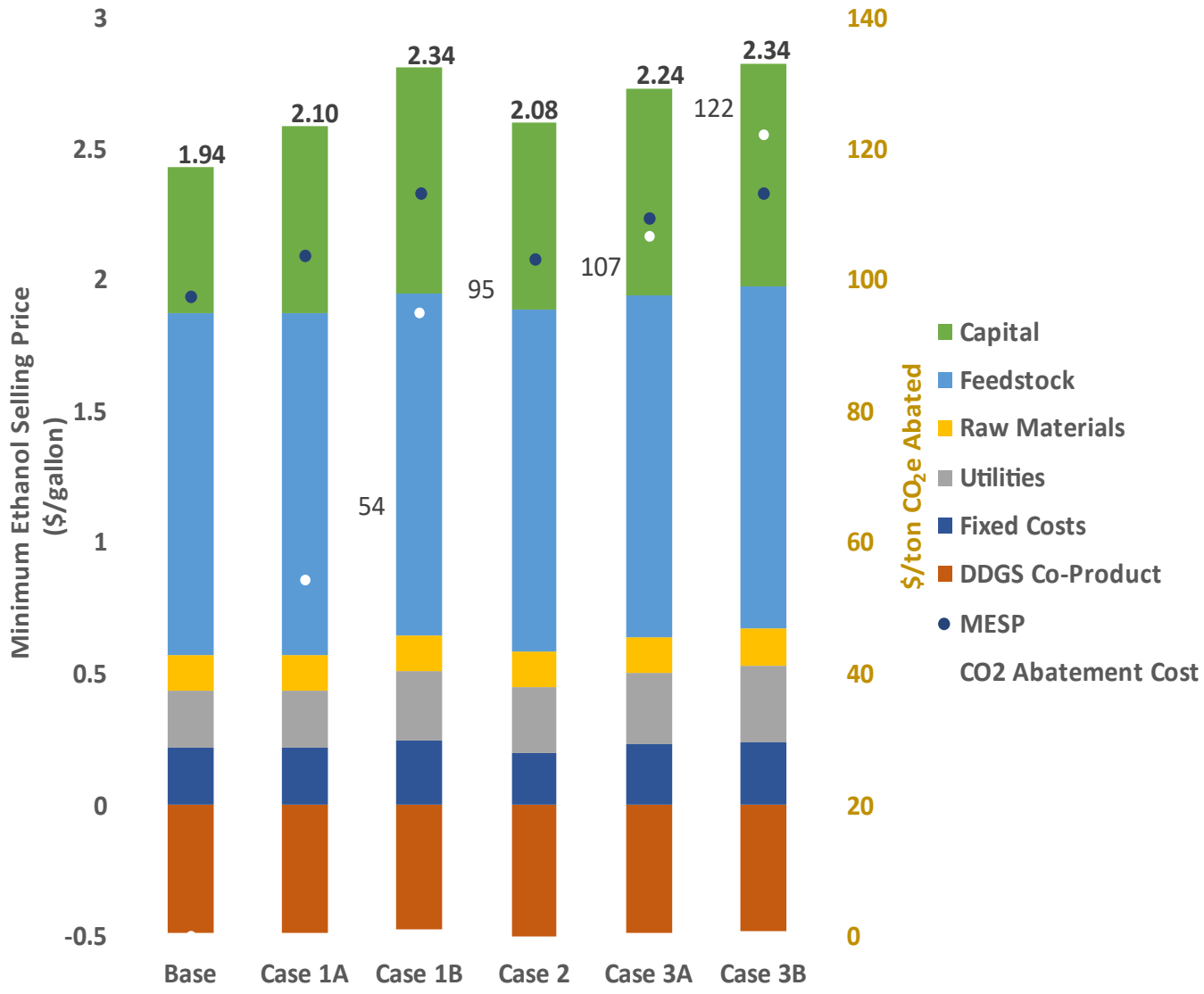

*Figure 4-4: MESP and cost of GHG abatement in the cases *Case 2 has no CI reduction, therefore, no abatement cost is calculated.*

4.2.2 TEA Sensitivity Analysis

Various sensitivities that may affect the ethanol facility, such as differences in process design configurations, location, and fuel, have been explored in Dees *et al.* As stated in section 4.1.2, carbon removal in an oxyfuel boiler and MVR upgrades require more considerable electricity use; a lower carbon-intensity grid could change the cost dynamics of the approaches.

Effects of grid electricity CI on MAC

Since changes to grid emission intensity affect the CI of the interventions case, these invariably affect the cost of carbon abatement. The sensitivity is shown in Figure 4-5. The MAC reduces to \$81/tCO_2e and \$95/tCO_2e in the zero emissions grid for cases 1B and 3B, respectively. There is no GHG emissions reduction in Case 2 in the MRO and US central/southern plains grid. The MAC is as high as \$217/tCO_2e in Case 2 as there is a smaller margin to emission reduction relative to base case.

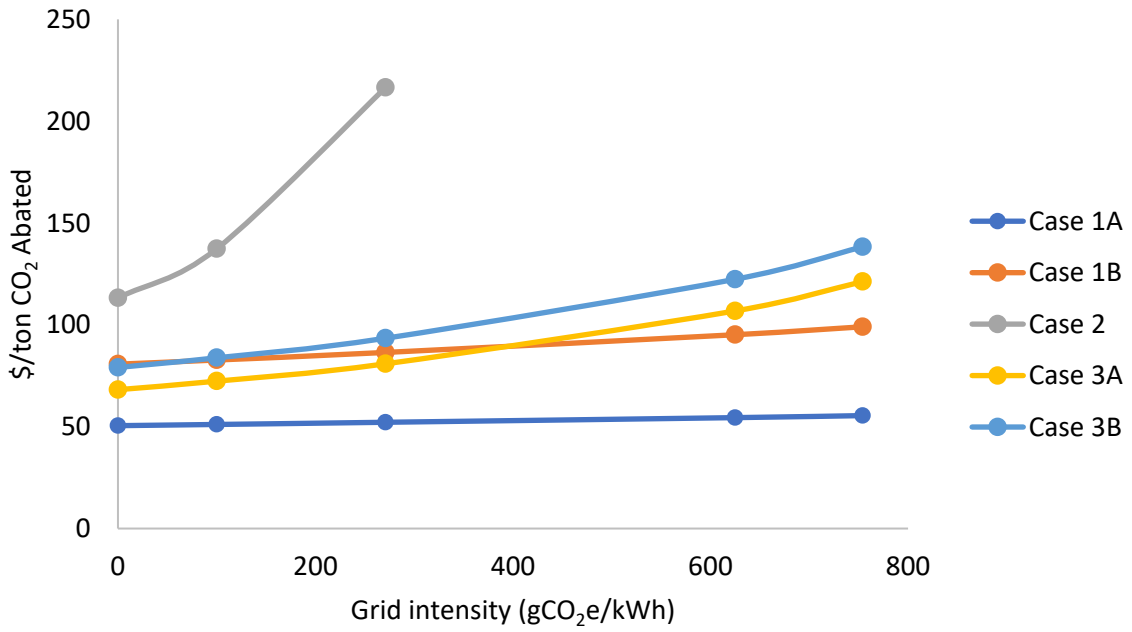

Figure 4-5: Effects of grid electricity CI on MAC

Effects of policy on MESP

As discussed in Section 1.5.1, policy support has enhanced the implementation of low carbon fuel usage, therefore sensitivities to US policy incentives (a combination of LCFS and 45Q) are assessed. The test range is $100/tonne to $200/tonne and $60/tonne to $85/tonne for LCFS and 45Q respectively. The 45Q tax credit is not applicable in Case 2 because CCS is not used. There are 103,992 and 223,836 LCFS credits generated in Case 2 and Case 3B respectively (see Appendix C.2 for calculations). The resulting MESP for a policy case where both the LCFS and 45Q values are at the low-end of the range is $1.81/gal and $1.59/gal for Cases 2 and 3B respectively, while the high end reduces to $1.54/gal and $0.93/gal (Figure 4-6). Assuming that the 45Q is fixed at $60/tonne, the calculated break even LCFS price (i.e., required to match the base case MESP of $1.94/gal) is $53/tonne and $41/tonne for Cases 2 and 3B, respectively. These are the lowest LCFS price to produce ethanol at the MESP of base case with those interventions. For example, at as low as $5/tonne LCFS price, fermentation only Case 1A has a MESP of $1.94/gal).

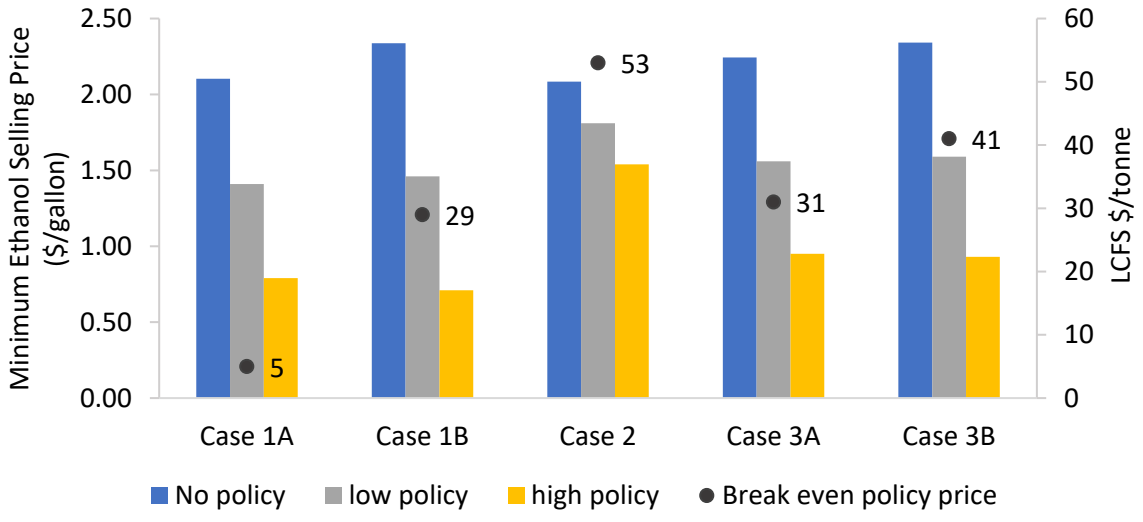

Figure 4-6: Effects of policy price on MESP

Chapter 5 Conclusions and Recommendations

Ethanol is widely used today as an oxygenate in gasoline and a low-emission alternative transportation fuel. Improving the carbon intensity of ethanol by integrating energy efficient technologies in its production could improve its competitiveness as a transportation fuel and expand options for its use as a feedstock for production of chemicals. Two alternative technologies that could reduce emissions from ethanol production were compared in this work: (1) carbon capture and storage (CCS) and (2) electrifying provision of heat to the production process. This chapter describes the conclusions drawn from this analysis and some recommendation for future work.

5.1 Conclusions

There is an opportunity to capture 99.6% CO_2 in a 40 million gallons (151 million litres) dry grind corn ethanol mill and this would result in a total of 187 ktCO_2 being captured (and stored) annually. Steam drying of DDGS is recommended for maximum CO_2 capture in the ethanol biorefinery baring no technology constraints. If both fermentation and oxycombustion capture is implemented across all existing US biorefinery capacity, there is a capture potential of approximately 70 million tonnes of CO_2 per year. The composition of the compressed CO_2 meets several pipelines requirements for enhanced oil recovery or direct sequestration in a saline aquifer. There is a net reduction of the life cycle carbon intensity by 84% to only 8.9 gCO_2eq/MJ when both biogenic and fossil CO_2 are captured at the cost of 95 USD/t_{CO2}.

Near atmospheric pressure 95% purity O_2 is adequate for oxyfuel utility boiler required in the plant because this has lower associated parasitic energy requirement. Corn ethanol biorefineries sizes vary from 12 – 400 million gallons per year. ASUs and CPUs benefits from economies of

scale therefore cost reduction advantages will become more obvious as plant capacities becomes larger.

The electrification configuration described resulted in a 63% reduction from 7.55 MJ/L in the base plant heat demand which is typically supplied by natural gas. For a modern US ethanol dry mill, the life cycle emissions reduction benefits are limited by the relatively high GHG intensity of electricity generation in much of the country. However, as the electricity grid decarbonizes, the electrification of ethanol mills will become a more attractive option, particularly when combined with the capture of CO_2 from fermentation. For the electrification alone (Case 2) to be adequate i.e., to have the same CI as the Base case, the grid emission intensity should be 584 gCO_2e/kWh i.e., 7% less than MRO grid intensity. The grid intensity needs to be 232 gCO_2e/kWh (14% less than California's grid intensity) for electrification and fermentation capture (Case 3A) to be equivalent to the full CCS option (Case 1B) in an MRO grid. Net zero is achieved at grid intensity of 170 gCO_2e/kWh for all interventions combined. Integrating fermentation with oxyfuel capture (Case 1B) provides the best emissions reduction benefit on the low emission electricity grid.

Ethanol is produced at the same cost of $2.34/gal for CCS alone case and when all intervention is applied. In the extreme case, when all 3 interventions (fermentation CCS, oxyfuel CCS, and MVR) are introduced whilst operating on a zero-emission grid electricity, life cycle emissions can be reduced by 113% to -7.1 gCO_2eq/MJ from the Base case at 122 USD/t_{CO2}. Sensitivity analysis has shown that conventional ethanol refineries can generate carbon neutral or even negative fuel, potentially at a profit given current policy support, when combined with additional interventions like renewable energy. Assuming that the 45Q is fixed at $60/tonne, MESP for fermentation Case 1A is same as Base case at as low as $5/tonne LCFS price. The four minimum criteria described

by Tanzer and Ramirez [155], for a technology to be tagged “negative emission technology” are met for the combination of CCS and electrification of an corn ethanol mill.

5.2 Recommendations

The results presented in this thesis are generally applicable to the manufacture of ethanol from various alternative feedstocks with lower sustainability risk and higher potential for CI reduction than corn. The carbon reduction potential of the ethanol industry is significant when employed in current sugarcane and developing cellulosic feedstock market.

The oxyfuel combustion CCS modelling are applicable to any industry for steam provision although applicable costs must be assessed on a case-by-case basis. Moreover, considering the geospatial concentration of ethanol mills, collated steam utility supply and gathering of fermentation off gas clean up, could provide additional economic benefit.

The implication of the complexity of coproduct displacement/system expansion on negative emission results should be further reviewed. Additionally, the potential of heat integration between the ASUs, oxyboiler, CPUs and MVR system should be assessed because this thesis considered each as a separate package unit. Likewise, the applicability of electric boilers and alternative heat pump technology such as heat pumps with external working fluid should be examined.

Considering that the sustainable production of fuel from food-based (first-generation) crops may have its restrictions, the potential for additional use of this ethanol will depend on whether cultivated yields can keep up with rising demand without negatively impacting the environment and food systems.

References

[1] IPCC, "Climate Change 2014: Synthesis Report. Contribution of Working Groups I, II and III to the Fifth Assessment Report of the Intergovernmental Panel on Climate Change [Core Writing Team, R.K. Pachauri and L.A. Meyer (eds.)]," IPCC, Geneva, Switzerland, 2014. Accessed: Aug. 12, 2022. [Online]. Available: https://archive.ipcc.ch/pdf/assessment-report/ar5/syr/SYR_AR5_FINAL_full_wcover.pdf

[2] B. Kovarik, "Henry Ford, Charles F. Kettering and the Fuel of the Future.," *Automotive History Review*, vol. 32, pp. 7–27.

[3] "Ford Predicts Fuel from Vegetation," *The New York Times*, p. 24, Sep. 20, 1925.

[4] D. D. Songstad, P. Lakshmanan, J. Chen, W. Gibbons, S. Hughes, and R. Nelson, "Historical perspective of biofuels: learning from the past to rediscover the future," *In Vitro Cell.Dev.Biol.-Plant*, vol. 45, no. 3, pp. 189–192, Jun. 2009, doi: 10.1007/s11627-009-9218-6.

[5] "Global Energy Review: CO2 Emissions in 2021," p. 14, 2021.

[6] S. J. Davis *et al.*, "Net-zero emissions energy systems," *Science*, vol. 360, no. 6396, p. eaas9793, Jun. 2018, doi: 10.1126/science.aas9793.

[7] J. L. Field *et al.*, "Robust paths to net greenhouse gas mitigation and negative emissions via advanced biofuels," *Proc. Natl. Acad. Sci. U.S.A.*, vol. 117, no. 36, pp. 21968–21977, Sep. 2020, doi: 10.1073/pnas.1920877117.

[8] S. N. Naik, V. V. Goud, P. K. Rout, and A. K. Dalai, "Production of first and second generation biofuels: A comprehensive review," *Renewable and Sustainable Energy Reviews*, vol. 14, no. 2, pp. 578–597, Feb. 2010, doi: 10.1016/j.rser.2009.10.003.

[9] B. Strohm, "Ethanol," in *Encyclopedia of Toxicology (Third Edition)*, P. Wexler, Ed., Oxford: Academic Press, 2014, pp. 488–491. doi: 10.1016/B978-0-12-386454-3.00379-1.

[10] J. E. Logsdon, "Ethanol," in *Kirk-Othmer Encyclopedia of Chemical Technology*, John Wiley & Sons, Inc, Ed., 1st ed.Wiley, 2004. doi: 10.1002/0471238961.0520080112150719.a01.pub2.

[11] K. Verschueren, *Handbook of environmental data on organic chemicals*, 4th ed. New York: Wiley, 2001.

[12] T. J. Lark *et al.*, "Environmental outcomes of the US Renewable Fuel Standard," *Proc. Natl. Acad. Sci. U.S.A.*, vol. 119, no. 9, p. e2101084119, Mar. 2022, doi: 10.1073/pnas.2101084119.

[13] T. Searchinger *et al.*, "Use of U.S. Croplands for Biofuels Increases Greenhouse Gases Through Emissions from Land-Use Change," *Science*, vol. 319, no. 5867, pp. 1238–1240, Feb. 2008, doi: 10.1126/science.1151861.

[14] J. Lewandrowski, J. Rosenfeld, D. Pape, T. Hendrickson, K. Jaglo, and K. Moffroid, "The greenhouse gas benefits of corn ethanol – assessing recent evidence," *Biofuels*, vol. 11, no. 3, pp. 361–375, Apr. 2020, doi: 10.1080/17597269.2018.1546488.

[15] U. Lee, H. Kwon, M. Wu, and M. Wang, “Retrospective analysis of the U.S. corn ethanol industry for 2005 – 2019 : implications for greenhouse gas emission reductions,” *Biofuels, Bioprod. Bioref.*, vol. 15, no. 5, pp. 1318–1331, Sep. 2021, doi: 10.1002/bbb.2225.

[16] S. Mueller and J. Kwik, “2012 Corn Ethanol: Emerging Plant Energy and Environmental Technologies,” p. 31.

[17] M. J. Scully, G. A. Norris, T. M. Alarcon Falconi, and D. L. MacIntosh, “Carbon intensity of corn ethanol in the United States: state of the science,” *Environ. Res. Lett.*, vol. 16, no. 4, p. 043001, Apr. 2021, doi: 10.1088/1748-9326/abde08.

[18] H. L. Chum *et al.*, “Understanding the evolution of environmental and energy performance of the US corn ethanol industry: evaluation of selected metrics,” *Biofuels, Bioprod. Bioref.*, vol. 8, no. 2, pp. 224–240, Mar. 2014, doi: 10.1002/bbb.1449.

[19] M. Wang, J. Han, J. B. Dunn, H. Cai, and A. Elgowainy, “Well-to-wheels energy use and greenhouse gas emissions of ethanol from corn, sugarcane and cellulosic biomass for US use,” *Environ. Res. Lett.*, vol. 7, no. 4, p. 045905, Dec. 2012, doi: 10.1088/1748-9326/7/4/045905.

[20] N. Eisberg, “Harvesting Energy,” *Chem Ind*, vol. No. 17, pp. 24–25, 2006.

[21] T. Raj *et al.*, “Recent advances in commercial biorefineries for lignocellulosic ethanol production: Current status, challenges and future perspectives,” *Bioresource Technology*, vol. 344, p. 126292, Jan. 2022, doi: 10.1016/j.biortech.2021.126292.

[22] Renewable Fuels Association RFA, “Annual Ethanol Production,” 2022. https://ethanolrfa.org/markets-and-statistics/annual-ethanol-production (accessed Nov. 09, 2022).

[23] US DOE ENERGY EFFICIENCY & RENEWABLE ENERGY, “Global Ethanol Production by Country or Region,” Jun. 2021. https://afdc.energy.gov/data/10331 (accessed Nov. 17, 2022).

[24] U.S. Energy Information Administration, “International biofuels data.” https://www.eia.gov/international/data/world (accessed Nov. 17, 2022).

[25] OECD/Food and Agriculture Organization of the United Nations, “‘Biofuels’, in OECD-FAO Agricultural Outlook 2022-2031,” OECD Publishing, Paris, 2022. Accessed: Nov. 15, 2022. [Online]. Available: https://www.oecd-ilibrary.org/agriculture-and-food/oecd-fao-agricultural-outlook-2022-2031_c90c6fa0-en

[26] Renewable Fuel Association RFA, “Zeroing in on new opportunities,” p. 40, 2022.

[27] U.S. Department of Agriculture Economic Research Service, “U.S. Bioenergy Statistics.,” Nov. 01, 2022. https://www.ers.usda.gov/data-products/u-s-bioenergy-statistics/ (accessed Nov. 13, 2022).

[28] S. Barros and N. Rubio, “Brazil Biofuel Annual Report 2022, Global Agricultural Information Network,” Foreign Agricultural Service, U.S. Department of Agriculture, Washington, DC, USA, BR2022-0047, Sep. 2022. Accessed: Nov. 13, 2022. [Online]. Available: https://www.fas.usda.gov/data/brazil-biofuels-annual-9

[29] B. Flach, S. Lieberz, S. Bolla, and E. Leonardi, “European Union Biofuel Annual Report 2022, Global Agricultural Information Network,” Foreign Agricultural Service, U.S. Department of Agriculture, Washington, DC, USA, E42022-0048, Jul. 2022. Accessed: Nov. 13, 2022. [Online]. Available: https://www.fas.usda.gov/data/european-union-biofuels-annual-2

[30] C. McGrath and A. Branson, “China Biofuel Annual Report 2022, Global Agricultural Information Network,” Foreign Agricultural Service, U.S. Department of Agriculture, Washington, DC, USA, CH2022-0089, Sep. 2022. Accessed: Nov. 13, 2022. [Online]. Available: https://www.fas.usda.gov/data/china-biofuels-annual-8

[31] A. Chandra and M. Rosmann, “India Biofuel Annual Report 2022, Global Agricultural Information Network,” Foreign Agricultural Service, U.S. Department of Agriculture, Washington, DC, USA, IN2022-0056, Jun. 2022. Accessed: Nov. 13, 2022. [Online]. Available: https://www.fas.usda.gov/data/india-biofuels-annual-7

[32] E. Danielson and P. Hayes, “Canada Biofuel Annual Report 2022, Global Agricultural Information Network,” Foreign Agricultural Service, U.S. Department of Agriculture, Washington, DC, USA, CA2022-0019, Aug. 2022. Accessed: Nov. 13, 2022. [Online]. Available: https://www.fas.usda.gov/data/canada-biofuels-annual-8

[33] D. Splitter, A. Pawlowski, and R. Wagner, “A Historical Analysis of the Co-evolution of Gasoline Octane Number and Spark-Ignition Engines,” *Front. Mech. Eng.*, vol. 1, Jan. 2016, doi: 10.3389/fmech.2015.00016.

[34] B. D. Solomon, J. R. Barnes, and K. E. Halvorsen, “Grain and cellulosic ethanol: History, economics, and energy policy,” *Biomass and Bioenergy*, vol. 31, no. 6, pp. 416–425, Jun. 2007, doi: 10.1016/j.biombioe.2007.01.023.

[35] C. Johnson, K. Moriarty, T. Alleman, and D. Santini, “History of Ethanol Fuel Adoption in the United States: Policy, Economics, and Logistics,” NREL/TP-5400-76260, 1832224, MainId:6072, Nov. 2021. doi: 10.2172/1832224.

[36] U.S Energy Information Administration, “Almost all U.S. gasoline is blended with 10% ethanol,” May 04, 2016. https://www.eia.gov/todayinenergy/detail.php?id=26092# (accessed Nov. 07, 2022).

[37] W. E. Tyner, “u.s. ethanol Policy— Possibilities for the Future,” p. 9.

[38] US Environmental Protection Agency, “Renewable Fuel Standard program,” 2022. https://www.epa.gov/renewable-fuel-standard-program/overview-renewable-fuel-standard (accessed Nov. 18, 2022).

[39] US Environmental Protection Agency, “Renewable Fuel Standard (RFS2): final rule,” 2022. https://www.epa.gov/renewable-fuel-standard-program/renewable-fuel-standard-rfs2-final-rule (accessed Nov. 18, 2022).

[40] Renewable Fuels Association RFA, “Essential Energy 2021 Ethanol Industry Outlook,” 2021. Accessed: Jan. 05, 2022. [Online]. Available: https://ethanolrfa.org/file/314/RFA_Outlook_2021_fin_low.pdf

[41] California Air Resources Board, “Low Carbon Fuel Standard,” 2022. https://ww2.arb.ca.gov/our-work/programs/low-carbon-fuel-standard (accessed Nov. 18, 2022).

[42] California Air Resources Board, “LCFS Data Dashboard,” 2022. https://ww2.arb.ca.gov/resources/documents/lcfs-data-dashboard (accessed Nov. 18, 2022).

[43] “U.S. Energy Information Administration Annual Fuel Ethanol Overview.” https://www.eia.gov/totalenergy/data/browser/?tbl=T10.03#/?f=A&start=1981&end=2021&charted=7-18 (accessed Mar. 02, 2023).

[44] International Energy Agency IEA, “Section 45Q Credit for Carbon Oxide Sequestration,” 2022. https://www.iea.org/policies/4986-section-45q-credit-for-carbon-oxide-sequestration

[45] G. Sorda, M. Banse, and C. Kemfert, “An overview of biofuel policies across the world,” *Energy Policy*, vol. 38, no. 11, pp. 6977–6988, Nov. 2010, doi: 10.1016/j.enpol.2010.06.066.

[46] J. A. M. Costa, “From Sugarcane To Ethanol: The Historical Process That Transformed Brazil Into A Biofuel Superpower,” p. 10, 2019.

[47] R. Abel, K. Coney, C. Johnson, M. Thornton, B. Zigler, and R. McCormick, “Global Ethanol-Blended-Fuel Vehicle Compatibility Study,” NREL/TP-5400-81252, 1832216, MainId:82025, Nov. 2021. doi: 10.2172/1832216.

[48] H. L. Chum, E. Warner, J. E. A. Seabra, and I. C. Macedo, “A comparison of commercial ethanol production systems from Brazilian sugarcane and US corn,” *Biofuels, Bioprod. Bioref.*, vol. 8, no. 2, pp. 205–223, Mar. 2014, doi: 10.1002/bbb.1448.

[49] Publications Office of the European Union, “Directive 2009/28/EC of the European Parliament and of the Council of 23 April 2009 on the promotion of the use of energy from renewable sources,” *OJ L 140, 5.6.2009*, pp. 16–62, 2009.

[50] Publications Office of the European Union, “DIRECTIVE 2018/2001 of the European Parliament and of the Council of 11 December 2018 on the promotion of the use of energy from renewable sources (recast),” *OJ L 328, 21.12.2018*, pp. 82–209, 2018.

[51] EUR-Lex Access to European Union law, “Summary of directive (EU) 2018/2001 on the promotion of the use of energy from renewable sources,” Apr. 21, 2022. https://eur-lex.europa.eu/legal-content/EN/LSU/?uri=uriserv:OJ.L_.2018.328.01.0082.01.ENG (accessed Nov. 21, 2022).

[52] H. Shapouri, J. A. Duffield, and M. Wang, “The Energy Balance of Corn Ethanol: An Update,” 1218357, Jul. 2002. doi: 10.2172/1218357.

[53] H. Shapouri, P. W. Gallagher, W. Nefstead, R. Schwartz, S. Noe, and R. Conway, “2008 Energy Balance for the Corn-Ethanol Industry,” p. 18.

[54] Renewable Fuels Association RFA, “RE-EXAMINING CORN ETHANOL’S ENERGY BALANCE RATIO,” Mar. 2016. https://d35t1syewk4d42.cloudfront.net/file/942/Re-examining-Corn-Ethanols-Energy-Balance.pdf (accessed Nov. 21, 2022).

[55] Renewable Fuels Association RFA, “CORN ETHANOL’S ENERGY BALANCE CONTINUES TO IMPROVE,” Apr. 2022.

https://d35t1syewk4d42.cloudfront.net/file/2214/Ethanol%20Energy%20Balance%20Update%20April%202022.pdf (accessed Nov. 21, 2022).

[56] A. R. Brandt, "How Does Energy Resource Depletion Affect Prosperity? Mathematics of a Minimum Energy Return on Investment (EROI)," *Biophys Econ Resour Qual*, vol. 2, no. 1, p. 2, Mar. 2017, doi: 10.1007/s41247-017-0019-y.

[57] S. Mueller, "2008 National dry mill corn ethanol survey," *Biotechnol Lett*, vol. 32, no. 9, pp. 1261–1264, Sep. 2010, doi: 10.1007/s10529-010-0296-7.

[58] P. W. Gallagher, J. A. Duffield, W. C. Yee, and H. Baumes, "2015 Energy Balance for the Corn-Ethanol Industry," p. 21.

[59] M. Wang *et al.*, "Greenhouse gases, Regulated Emissions, and Energy use in Transportation Model ® (2019 .Net)." Oct. 2019. doi: 10.11578/GREET-Net-2019/dc.20200706.2.

[60] A. McAloon, F. Taylor, and W. Yee, "Determining the Cost of Producing Ethanol from Corn Starch and Lignocellulosic Feedstocks," p. 44, 2000.

[61] J. Dees *et al.*, "Cost and Life Cycle Emissions of Ethanol Produced with an Oxyfuel Boiler and Carbon Capture and Storage," *Environ. Sci. Technol.*, vol. 57, no. 13, pp. 5391–5403, Apr. 2023, doi: 10.1021/acs.est.2c04784.

[62] R. Karuppiah, A. Peschel, I. E. Grossmann, M. Martín, W. Martinson, and L. Zullo, "Energy optimization for the design of corn-based ethanol plants," *AIChE J.*, vol. 54, no. 6, pp. 1499–1525, Jun. 2008, doi: 10.1002/aic.11480.

[63] M. J. De Kam, R. Vance Morey, and D. G. Tiffany, "Biomass Integrated Gasification Combined Cycle for heat and power at ethanol plants," *Energy Conversion and Management*, vol. 50, no. 7, pp. 1682–1690, Jul. 2009, doi: 10.1016/j.enconman.2009.03.031.

[64] M. J. D. Kam, R. V. Morey, and D. G. Tiffany, "INTEGRATING BIOMASS TO PRODUCE HEAT AND POWER AT ETHANOL PLANTS," *APPLIED ENGINEERING IN AGRICULTURE*, vol. 25, p. 18.

[65] H. Zheng, N. Kaliyan, and R. V. Morey, "Aspen Plus simulation of biomass integrated gasification combined cycle systems at corn ethanol plants," *Biomass and Bioenergy*, vol. 56, pp. 197–210, Sep. 2013, doi: 10.1016/j.biombioe.2013.04.032.

[66] M. Wang, M. Wu, and H. Huo, "Life-cycle energy and greenhouse gas emission impacts of different corn ethanol plant types," *Environ. Res. Lett.*, vol. 2, no. 2, p. 024001, Apr. 2007, doi: 10.1088/1748-9326/2/2/024001.

[67] N. Kaliyan, R. V. Morey, and D. G. Tiffany, "Reducing life cycle greenhouse gas emissions of corn ethanol by integrating biomass to produce heat and power at ethanol plants," *Biomass and Bioenergy*, vol. 35, no. 3, pp. 1103–1113, Mar. 2011, doi: 10.1016/j.biombioe.2010.11.035.

[68] U. Lee, T. R Hawkins, E. Yoo, M. Wang, Z. Huang, and L. Tao, "Using waste CO_2 from corn ethanol biorefineries for additional ethanol production: life-cycle analysis," *Biofuels, Bioprod. Bioref.*, vol. 15, no. 2, pp. 468–480, Mar. 2021, doi: 10.1002/bbb.2175.

[69] "exhibit 64a to revised petition for review ...12.64a.pdf."

[70] H. S. Kheshgi and R. C. Prince, "Sequestration of fermentation CO2 from ethanol production," *Energy*, vol. 30, no. 10, pp. 1865–1871, Jul. 2005, doi: 10.1016/j.energy.2004.11.004.

[71] W. M. Summers, S. E. Herron, and A. Zoelle, "Cost of Capturing CO2 from Industrial Sources," National Energy Technology Laboratory, DOE/NETL-2013/1602, Jan. 2014.

[72] A. Laude, O. Ricci, G. Bureau, J. Royer-Adnot, and A. Fabbri, "CO2 capture and storage from a bioethanol plant: Carbon and energy footprint and economic assessment," *International Journal of Greenhouse Gas Control*, vol. 5, no. 5, pp. 1220–1231, Sep. 2011, doi: 10.1016/j.ijggc.2011.06.004.

[73] Y. Xu, L. Isom, and M. A. Hanna, "Adding value to carbon dioxide from ethanol fermentations," *Bioresource Technology*, vol. 101, no. 10, pp. 3311–3319, May 2010, doi: 10.1016/j.biortech.2010.01.006.

[74] H. Xu, U. Lee, and M. Wang, "Life-cycle greenhouse gas emissions reduction potential for corn ethanol refining in the USA," *Biofuels, Bioprod. Bioref.*, vol. 16, no. 2, pp. 671–681, Apr. 2022, doi: 10.1002/bbb.2348.

[75] D. L. Sanchez, N. Johnson, S. T. McCoy, P. A. Turner, and K. J. Mach, "Near-term deployment of carbon capture and sequestration from biorefineries in the United States," *Proc. Natl. Acad. Sci. U.S.A.*, vol. 115, no. 19, pp. 4875–4880, May 2018, doi: 10.1073/pnas.1719695115.

[76] J. R. Moreira, V. Romeiro, S. Fuss, F. Kraxner, and S. A. Pacca, "BECCS potential in Brazil: Achieving negative emissions in ethanol and electricity production based on sugar cane bagasse and other residues," *Applied Energy*, vol. 179, pp. 55–63, Oct. 2016, doi: 10.1016/j.apenergy.2016.06.044.

[77] L. Gibson, "Enhanced Oilfield Opportunities," *Ethanol Producer Magazine*, Apr. 23, 2018. https://ethanolproducer.com/articles/15185/enhanced-oilfield-opportunities (accessed Nov. 26, 2022).

[78] S. Greenberg, K. Canaday, A. Vance, R. McKaskle, and J. Koenig, "A Detailed Approach for Cost Analysis for Early CCS Projects: A Case Study from the Illinois Basin - Decatur Project," *SSRN Journal*, 2019, doi: 10.2139/ssrn.3365964.

[79] K. Leroux *et al.*, "First North Dakota CCS Project: Advancing North Dakota Ethanol Economics," *SSRN Journal*, 2021, doi: 10.2139/ssrn.3812021.

[80] E. Voegele, "Large-scale CCS project will sequester CO2 from ethanol plants," *Ethanol Producer Magazine*, Feb. 18, 2021. https://ethanolproducer.com/articles/18001/large-scale-ccs-project-will-sequester-co2-from-ethanol-plants (accessed Nov. 26, 2022).

[81] E. Voegele, "Aemetis cuts carbon score of Keyes ethanol plant," *Ethanol Producer Magazine*, Aug. 08, 2019. https://ethanolproducer.com/articles/16435/aemetis-cuts-carbon-score-of-keyes-ethanol-plant (accessed Nov. 26, 2022).

[82] Navigator CO2 Ventures LLC, "Navigator CO2, Big River announce CCUS agreement," *Ethanol Producer Magazine*, May 10, 2022.

https://ethanolproducer.com/articles/19249/navigator-co2-big-river-announce-ccus-agreement (accessed Nov. 26, 2022).

[83] S. Kim *et al.*, "Carbon-Negative Biofuel Production," *Environ. Sci. Technol.*, vol. 54, no. 17, pp. 10797–10807, Sep. 2020, doi: 10.1021/acs.est.0c01097.

[84] T. Uchida, T. Goto, T. Yamada, T. Kiga, and C. Spero, "Oxyfuel Combustion as CO2 Capture Technology Advancing for Practical use - callide Oxyfuel Project -," *Energy Procedia*, vol. 37, pp. 1471–1479, 2013, doi: 10.1016/j.egypro.2013.06.022.

[85] "Carbon capture and storage: the Lacq pilot. Project and injection period 2006-2013," p. 276.

[86] M. Lupion, R. Diego, L. Loubeau, and B. Navarrete, "CIUDEN CCS Project: Status of the CO2 capture technology development plant in power generation," *Energy Procedia*, vol. 4, pp. 5639–5646, 2011, doi: 10.1016/j.egypro.2011.02.555.

[87] V. White, A. Wright, S. Tappe, and J. Yan, "The Air Products Vattenfall Oxyfuel CO2 Compression and Purification Pilot Plant at Schwarze Pumpe," *Energy Procedia*, vol. 37, pp. 1490–1499, 2013, doi: 10.1016/j.egypro.2013.06.024.

[88] D. Leeson, N. Mac Dowell, N. Shah, C. Petit, and P. S. Fennell, "A Techno-economic analysis and systematic review of carbon capture and storage (CCS) applied to the iron and steel, cement, oil refining and pulp and paper industries, as well as other high purity sources," *International Journal of Greenhouse Gas Control*, vol. 61, pp. 71–84, Jun. 2017, doi: 10.1016/j.ijggc.2017.03.020.

[89] A. Darde, R. Prabhakar, J.-P. Tranier, and N. Perrin, "Air separation and flue gas compression and purification units for oxy-coal combustion systems," *Energy Procedia*, vol. 1, no. 1, pp. 527–534, Feb. 2009, doi: 10.1016/j.egypro.2009.01.070.

[90] Y. Kansha, A. Kishimoto, T. Nakagawa, and A. Tsutsumi, "A novel cryogenic air separation process based on self-heat recuperation," *Separation and Purification Technology*, vol. 77, no. 3, pp. 389–396, Mar. 2011, doi: 10.1016/j.seppur.2011.01.012.

[91] P. Higginbotham, V. White, K. Fogash, and G. Guvelioglu, "Oxygen supply for oxyfuel CO2 capture," *International Journal of Greenhouse Gas Control*, vol. 5, pp. S194–S203, Jul. 2011, doi: 10.1016/j.ijggc.2011.03.007.

[92] Z. A. M. Khalel, A. A. Rabah, and T. A. M. Barakat, "A New Cryogenic Air Separation Process with Flash Separator," *ISRN Thermodynamics*, vol. 2013, pp. 1–4, Jun. 2013, doi: 10.1155/2013/253437.

[93] V. N. Raibhole and S. N. Sapali, "Simulation and Parametric Analysis of Cryogenic Oxygen Plant for Biomass Gasification," *MER*, vol. 2, no. 2, p. p97, Nov. 2012, doi: 10.5539/mer.v2n2p97.

[94] G. Pipitone and O. Bolland, "Power generation with CO2 capture: Technology for CO2 purification," *International Journal of Greenhouse Gas Control*, vol. 3, no. 5, pp. 528–534, Sep. 2009, doi: 10.1016/j.ijggc.2009.03.001.

[95] M. Aneke and M. Wang, "Process analysis of pressurized oxy-coal power cycle for carbon capture application integrated with liquid air power generation and binary cycle

engines," *Applied Energy*, vol. 154, pp. 556–566, Sep. 2015, doi: 10.1016/j.apenergy.2015.05.030.

[96] "AspenPlus20041GettingStartedProcessModel.pdf."

[97] J. R. Kwiatkowski, A. J. McAloon, F. Taylor, and D. B. Johnston, "Modeling the process and costs of fuel ethanol production by the corn dry-grind process," *Industrial Crops and Products*, vol. 23, no. 3, pp. 288–296, May 2006, doi: 10.1016/j.indcrop.2005.08.004.

[98] BBI International, "Corn Ethanol Industry Process Data: September 27, 2007 - January 27, 2008," NREL/SR-6A1-45152, 948744, Feb. 2009. doi: 10.2172/948744.

[99] W. M. Summers, "Quality Guidelines for Energy System Studies: Specification for Selected Feedstocks," NETL-PUB-22460, 1557271, Jan. 2019. doi: 10.2172/1557271.

[100] "NWR, Wolf & Enhance- ACTL Knowledge Sharing Report 2018.pdf."

[101] A. Iyengar, N. Kuehn, V. Shah, M. J. Turner, M. Woods, and D. Keairns, "Advanced Oxy-combustion Technology for Pulverized Bituminous Coal Power Plants," National Energy Technology Laboratory (NETL)., NETL-PUB-21545, 1560803, Oct. 2017. doi: 10.2172/1560803.

[102] "Carbon Dioxide Enhanced Oil Recovery: Untapped Domestic Energy Supply and Long Term Carbon Storage Solution," U.S. DOE/NETL, Pittsburgh, Pennsylvania, Mar. 2010. Accessed: Jan. 05, 2023. [Online]. Available: https://www.netl.doe.gov/sites/default/files/netl-file/co2_eor_primer.pdf

[103] "18R-97: Cost Estimate Classification System – As Applied in Engineering, Procurement, and Construction for the Process Industries," p. 7, 2020.

[104] G. P. Towler and R. K. Sinnott, *Chemical engineering design: principles, practice, and economics of plant and process design*, 2nd ed. Boston, MA: Butterworth-Heinemann, 2013.

[105] OECD, "Exchange rates (indicator)." https://data.oecd.org/conversion/exchange-rates.htm (accessed Nov. 04, 2021).

[106] Marc J. Turner, Lora L. Pinkerton, "Quality Guideline for Energy System Studies – Capital Cost Scaling Methodology" QGESS," National Energy Technology Laboratory (NETL)., DOE/NETL-341/013113, Jan. 2013.

[107] C. Hamelinck, A. Faaij, H. Denuil, and H. Boerrigter, "Production of FT transportation fuels from biomass; technical options, process analysis and optimisation, and development potential," *Energy*, vol. 29, no. 11, pp. 1743–1771, Sep. 2004, doi: 10.1016/j.energy.2004.01.002.

[108] K. P. Kostroski and P. C. Wankat, "Potential Hybrid Methods for Oxygen Production," *Sep. Sci. Technol., 45, 1171, 2010. Referenced in Oxygen- Enhanced Combustion, Second Edition, edited by Charles E. Baukal Jr.*, p. 20.

[109] S. Gardarsdottir *et al.*, "Comparison of Technologies for CO2 Capture from Cement Production—Part 2: Cost Analysis," *Energies*, vol. 12, no. 3, p. 542, Feb. 2019, doi: 10.3390/en12030542.

[110] D. W. Keith, G. Holmes, D. St. Angelo, and K. Heidel, “A Process for Capturing CO2 from the Atmosphere,” *Joule*, vol. 2, no. 8, pp. 1573–1594, Aug. 2018, doi: 10.1016/j.joule.2018.05.006.

[111] “Cost and Performance Baseline for Fossil Energy Plants; Volume 3a: Low Rank Coal to Electricity: IGCC Cases,” vol. National Energy Technology Laboratory (NETL), p. 487.

[112] R. E. James III PhD, D. Kearins, M. Turner, M. Woods, N. Kuehn, and A. Zoelle, “Cost and Performance Baseline for Fossil Energy Plants Volume 1: Bituminous Coal and Natural Gas to Electricity,” NETL-PUB-22638, 1569246, Sep. 2019. doi: 10.2172/1569246.

[113] Marc J. Turner, Mark Woods, Scott Chen, Robert D. Brasington, John L. Haslbeck, Charlie Zhang, “Advancing Oxycombustion Technology for Bituminous Coal Power Plants: An R&D Guide,” National Energy Technology Laboratory (NETL)., DOE/NETL-2010/1405, Apr. 2012.

[114] Air Liquide Engineering and Construction, “Technology Handbook,” Jun. 2021. Accessed: Oct. 21, 2021. [Online]. Available: https://www.engineering-airliquide.com/technology-handbook

[115] R. McKaskle, K. Fisher, P. Selz, and Y. Lu, “Evaluation of Carbon Dioxide Capture Options from Ethanol Plants,” Champaign, Illinois State Geological Survey, Circular 595, 2018.

[116] R. Socolow *et al.*, “Direct Air Capture of CO2 with Chemicals,” American Physical Society APS Panel on Public Affairs (POPA)., Jun. 2011.

[117] G. P. Thiel and A. K. Stark, “To decarbonize industry, we must decarbonize heat,” *Joule*, vol. 5, no. 3, pp. 531–550, Mar. 2021, doi: 10.1016/j.joule.2020.12.007.

[118] C. Schoeneberger, J. Zhang, C. McMillan, J. B. Dunn, and E. Masanet, “Electrification potential of U.S. industrial boilers and assessment of the GHG emissions impact,” *Advances in Applied Energy*, vol. 5, p. 100089, Feb. 2022, doi: 10.1016/j.adapen.2022.100089.

[119] C. Chen, Y. Lu, and R. Banares-Alcantara, “Direct and indirect electrification of chemical industry using methanol production as a case study,” *Applied Energy*, vol. 243, pp. 71–90, Jun. 2019, doi: 10.1016/j.apenergy.2019.03.184.

[120] J. Atuonwu and S. Tassou, “Decarbonisation of food manufacturing by the electrification of heat: A review of developments, technology options and future directions,” *Trends in Food Science & Technology*, vol. 107, pp. 168–182, Jan. 2021, doi: 10.1016/j.tifs.2020.10.011.

[121] C. Cui, N. V. D. Long, J. Sun, and M. Lee, “Electrical-driven self-heat recuperative pressure-swing azeotropic distillation to minimize process cost and CO2 emission: Process electrification and simultaneous optimization,” *Energy*, vol. 195, p. 116998, Mar. 2020, doi: 10.1016/j.energy.2020.116998.

[122] A. L. Rispoli *et al.*, “The Electrification of Conventional Industrial Processes: The Use of Mechanical Vapor Compression in an EtOH–Water Distillation Tower,” *Energies*, vol. 14, no. 21, p. 7267, Nov. 2021, doi: 10.3390/en14217267.

[123] Department of Energy (DOE), “Industrial heat pumps for steam and fuel savings,” DOE EERE Industrial Technologies Program: 4, 2014. Accessed: Sep. 20, 2021. [Online]. Available: https://www.energy.gov/si tes/prod/files/2014/05/f15/heatpump.pdf

[124] A. Kiss, S. J. Landaeta, and C. A. Ferreira, “Towards energy efficient distillation technologies e Making the right choice,” *Energy*, vol. 47, pp. 531–542, 2012, doi: 10.1016/j.energy.2012.09.038.

[125] A. K. Jana, “Advances in heat pump assisted distillation column: A review,” *Energy Conversion and Management*, vol. 77, pp. 287–297, 2014, doi: DOI:10.1016/J.ENCONMAN.2013.09.055.

[126] H. Luo, C. S. Bildea, and A. A. Kiss, “Novel Heat-Pump-Assisted Extractive Distillation for Bioethanol Purification,” *Ind. Eng. Chem. Res.*, vol. 54, no. 7, pp. 2208–2213, Feb. 2015, doi: 10.1021/ie504459c.

[127] A. Kazemi, V. Faizi, A. Mehrabani-Zeinabad, and M. Hosseini, “Evaluation of the performance of heat pump-assisted distillation of an ethanol–water mixture,” *Separation Science and Technology*, vol. 52, no. 8, pp. 1387–1396, May 2017, doi: 10.1080/01496395.2017.1281306.

[128] K. K. Patel and A. Kar, “Heat pump assisted drying of agricultural produce—an overview,” *J Food Sci Technol*, vol. 49, no. 2, pp. 142–160, Apr. 2012, doi: 10.1007/s13197-011-0334-z.

[129] M. Madoumier, C. Azzaro-Pantel, G. Tanguy, and G. Gésan-Guiziou, “Modelling the properties of liquid foods for use of process flowsheeting simulators: Application to milk concentration,” *Journal of Food Engineering*, vol. 164, pp. 70–89, Nov. 2015, doi: 10.1016/j.jfoodeng.2015.04.023.

[130] Gonzalez Cortes M., Verelst H., and Gonzales E., “Energy integration of multiple effect evaporators in sugar process production,” *Chemical Engineering Transactions*, vol. 21, pp. 277–282, Sep. 2010, doi: 10.3303/CET1021047.

[131] M. A. Collura and W. L. Luyben, “Energy-saving distillation designs in ethanol production,” *Ind. Eng. Chem. Res.*, vol. 27, no. 9, pp. 1686–1696, Sep. 1988, doi: 10.1021/ie00081a021.

[132] V. Plesu, A. E. Bonet Ruiz, J. Bonet, and J. Llorens, “Simple equation for suitability of heat pump use in distillation,” *Comput.-Aided Chem. Eng.*, vol. 33, p. 1327−1332, 2014, doi: 10.1016/B978-0-444-63455-9.50056-8.

[133] N. Felbab, B. Patel, M. M. El-Halwagi, D. Hildebrandt, and D. Glasser, “Vapor recompression for efficient distillation. 1. A new synthesis perspective on standard configurations,” *AIChE J.*, vol. 59, pp. 2977–2992, 2013, doi: 10.1002/aic.14070.

[134] A. Harwardt and W. Marquardt, “Heat-Integrated Distillation Columns: Vapor Recompression or Internal Heat Integration?,” *AIChE J.*, vol. 58, pp. 3740–3750, 2012, doi: 10.1002/aic.13775.

[135] M. Usman, T. Ajayi, and K. Famoriyo, “Comparison of Vapor Recompression and Thermal Coupling for Energy Reduction in Binary Distillation,” *j. emerg. trends eng. appl. sci.*, vol. 3, no. 1, pp. 188–194, 2012.

[136] A. Kiss, H. Luo, and C. S. Bildea, “Energy Efficient Bioethanol Purification by Heat Pump Assisted Extractive Distillation,” *Computer Aided Chemical Engineering*, 2015, doi: 10.1016/B978-0-444-63577-8.50063-2.

[137] Palacios-Bereche R., Ensinas A.V., Modesto M., and Nebra S.A., “Mechanical vapour recompression incorporated to the ethanol production from sugarcane and thermal integration to the overall process applying pinch analysis,” *Chemical Engineering Transactions*, vol. 39, pp. 397–402, Aug. 2014, doi: 10.3303/CET1439067.

[138] S. N. Moejes, Q. Visser, J. H. Bitter, and A. J. B. van Boxtel, “Closed-loop spray drying solutions for energy efficient powder production,” *Innovative Food Science & Emerging Technologies*, vol. 47, pp. 24–37, Jun. 2018, doi: 10.1016/j.ifset.2018.01.005.

[139] M. Bantle, “Turbo-compressors: Prototype tests of mechanical vapour re- compression for steam driers,” p. 8, 2017.

[140] Y. Kim, J. Lim, H. Cho, and J. Kim, “Novel mechanical vapor recompression-assisted evaporation process for improving energy efficiency in pulp and paper industry,” *Int J Energy Res*, vol. 46, no. 3, pp. 3409–3427, 2022, doi: 10.1002/er.7390.

[141] H. Dahmardeh, H. A. Akhlaghi Amiri, and S. M. Nowee, “Evaluation of mechanical vapor recompression crystallization process for treatment of high salinity wastewater,” *Chemical Engineering and Processing - Process Intensification*, vol. 145, p. 107682, Nov. 2019, doi: 10.1016/j.cep.2019.107682.

[142] USDA Agricultural Research Service, “Dry Grind Production of Ethanol from Corn,” Jul. 25, 2019. https://www.ars.usda.gov/northeast-area/wyndmoor-pa/eastern-regional-research-center/docs/engineering-super-support-group/dry-grind-production-of-ethanol-from-corn/ (accessed Aug. 02, 2022).

[143] S. Gollakota and S. McDonald, “CO 2 capture from ethanol production and storage into the Mt Simon Sandstone,” *Greenhouse Gases: Science and Technology*, vol. 2, no. 5, pp. 346–351, Oct. 2012, doi: 10.1002/ghg.1305.

[144] C. R. Burrows and M. S. Appold, “Hydrology of the Forest City basin, Mid-Continent, USA: implications for CO2 sequestration in the St. Peter Sandstone,” *Environ Earth Sci*, vol. 73, no. 4, pp. 1409–1425, Feb. 2015, doi: 10.1007/s12665-014-3494-0.

[145] California Air Resources Board (CARB), “Current Fuel Pathways [Spreadsheet].” CARB LCFS Program, 2022.

[146] H. E. Grethlein, T. B. Nelson, and J. C. Craig, “Projected process economics for ethanol production from corn.” Food and Argiculture Organization of the United Nations AGRIS Archive, 1992. Accessed: Jun. 15, 2022. [Online]. Available: https://agris.fao.org/agris-search/search.do?recordID=US19940081595

[147] A. McAloon, F. Taylor, and W. Yee, “Determining the Cost of Producing Ethanol from Corn Starch and Lignocellulosic Feedstocks,” National Renewable Energy Laboratory (NREL), Technical Report NREL/TP-580-28893, 2000. [Online]. Available: https://www.nrel.gov/docs/fy01osti/28893.pdf

[148] S. D. Phillips, J. K. Tarud, M. J. Biddy, and A. Dutta, “Gasoline from Woody Biomass via Thermochemical Gasification, Methanol Synthesis, and Methanol-to-Gasoline

Technologies: A Technoeconomic Analysis," *Ind. Eng. Chem. Res.*, vol. 50, no. 20, pp. 11734–11745, Oct. 2011, doi: 10.1021/ie2010675.

[149] S. Jones *et al.*, "Process Design and Economics for the Conversion of Algal Biomass to Hydrocarbons: Whole Algae Hydrothermal Liquefaction and Upgrading," Pacific Northwest National Laboratory, Mar. 2014.

[150] R. Davis, J. Markham, C. Kinchin, N. Grundl, E. Tan, and D. Humbird, "Process Design and Economics for the Production of Algal Biomass: Algal Biomass Production in Open Pond Systems and Processing Through Dewatering for Downstream Conversion," National Renewable Energy Laboratory (NREL), Feb. 2016. Accessed: Mar. 01, 2022. [Online]. Available: https://www.nrel.gov/docs/fy16osti/64772.pdf

[151] Chemical Engineering Magazine, "Chemical Engineering Plant Cost Index," Dec. 2021.

[152] U.S. Bureau of Labor Statistics, "Average hourly earnings of production and nonsupervisory employees, chemicals, not seasonally adjusted," U.S. Bureau of Labor Statistics, 2022. Accessed: Mar. 01, 2022. [Online]. Available: https://beta.bls.gov/dataViewer/view/timeseries/CEU3232500008

[153] U.S. Bureau of Labor Statistics, "Producer Price Index by Commodity: Chemicals and Allied Products: Basic Inorganic Chemicals," U.S. Bureau of Labor Statistics, 2022. Accessed: Mar. 01, 2022. [Online]. Available: https://fred.stlouisfed.org/series/WPU0613#0

[154] D. Hofstrand, "Ag Decision Maker D1-10: Ethanol Profitability." Iowa State University Extension and Outreach, Mar. 21, 2022. Accessed: Feb. 15, 2022. [Online]. Available: https://www.extension.iastate.edu/agdm/energy/html/d1-10.html

[155] S. E. Tanzer and A. Ramírez, "When are negative emissions negative emissions?," *Energy Environ. Sci.*, vol. 12, no. 4, pp. 1210–1218, 2019, doi: 10.1039/C8EE03338B.

[156] "Quest Carbon Capture and Storage Project ANNUAL SUMMARY REPORT : 2020," ALBERTA DEPARTMENT OF ENERGY, Aug. 2021.

[157] IPCC, *IPCC Special Report on Carbon Dioxide Capture and Storage Prepared by Working Group III of the Intergovernmental Panel on Climate Change [Metz, B., O. Davidson, H. C. de Coninck, M. Loos, and L. A. Meyer (eds.)]*. Cambridge University Press, Cambridge, United Kingdom and New York, NY, USA, 2005.

[158] "CO2 Supply Report by by Elsam A/S, Kinder Morgan CO2 Company L.P. and New Energy Statoil," Oct. 2003. Accessed: Dec. 16, 2022. [Online]. Available: https://co2.no/wp-content/uploads/2020/07/CO2-Supply_Report-Rev1.pdf

[159] P. Shirley and P. Myles, "Quality Guidelines for Energy System Studies: CO2 Impurity Design Parameters," NETL-PUB-22529, 1566771, Jan. 2019. doi: 10.2172/1566771.

Appendix A.1 Pipeline CO_2 Specification

Component	ACTL 2019 [100]	Quest CCS Project [156]	Canyon Reef [157]	Weyburn Pipeline [157]	Gullfaks [158]	QGESS (EOR) [159]
CO_2	> 95%	≥ 99.23%	> 95%	96%	99.5%	≥ 95%
Hydrocarbon	≤ 2%	-	< 5%	-	100 ppm	-
Glycol	≤ 63 ppmv (3 lb/mmscf)	-	4 x 10^{-5} L m^{-3}	-	-	46 ppbv
H_2O	≤ 210 ppmv (10 lb/mmscf)	-	No free water < 0.489 m^{-3} in the vapour phase	< 20 ppm	Water vapour content equivalent to saturation at -5ºC	500 ppmv
H_2S	≤ 10 ppmv	-	< 1500 ppmw	0.9%	-	< 0.01%
Total sulphur	≤16 ppmv	-	< 1450 ppmw	-	-	-
N_2	< 1%	0	4%	< 300 ppm	< 0.48%	< 1%
H_2	< 1%	≤ 0.65%				< 1%
CO	< 1%	≤ 0.02%	-	0.1%	< 10 ppm	35 ppmv
Ar	< 1%	-				< 1%
CH_4	< 1%	≤ 0.09%	-	0.7%	-	< 1%
O_2	< 0.1%	-	< 10 ppmw	< 50 ppm	< 10 ppm	< 0.001%
SOx	< 100 ppmv	-	-	-	10 ppm	< 100 ppm
NOx	< 100 ppmv	-	-	-	< 50 ppm	< 100 ppm
Hg	< 100ppbv	-				-
C_2^+	-	-	-	2.3%	-	-
Temperature (ºC)	< 25	43	< 48.9	-	-	-
Pressure (MPa)	<17.93	10	-	15.2	-	15.2

Appendix A.2 Result Summary for Stream Boundary CCS

	Units	AIR	FERMTCO2	FLUEGAS	HP-CO2	NAT-GAS	NITROGEN	OXYGEN	STEAM
Description									
From				OXYSTEAM	CPU		ASU	ASU	OXYSTEAM
To		ASU	CPU	CPU		OXYSTEAM		OXYSTEAM	
Stream Class		CONVEN	CONVEN	CONVEN	CONVEN	CONVEN	CONVEN	CONVEN	CONVEN
Maximum Relative Error									
Cost Flow	$/hr								
− **MIXED Substream**									
Phase		Vapor Phase	Vapor Phase	Vapor Phase	Liquid Phase	Vapor Phase	Vapor Phase	Vapor Phase	Vapor Phase
Temperature	C	15	32	138	9.91455	29	13.4313	13.4313	190
Pressure	bar	1.01	1.2	1.2	150	27	1.1	1.2	12
Molar Vapor Fraction		1	1	1	0	1	1	1	1
Molar Liquid Fraction		0	0	0	1	0	0	0	0
Average MW		28.8681	44.0098	27.1129	44.0093	17.3275	28.0262	31.8422	18.0153
+ **Mole Flows**	**kmol/hr**	**1812.95**	**297.4**	**584.072**	**483.5**	**178.923**	**1412.99**	**399.96**	**2926.42**
− **Mole Fractions**									
H2O		0	0	0.614514	2.70126e-06	0	0	0	1
N2		0.787378	0	0.036651	6.1185e-07	0.016	0.99712	0.0463939	0
O2		0.211715	0	0.0271533	3.64004e-05	0	0.00272343	0.950046	0
AR		0.00090735	0	0.00243801	2.53418e-06	0	0.00015641	0.00356029	0
CO		0	0	4.4707e-07	5.77988e-12	0	0	0	0
CO2		0	1	0.319204	0.999958	0.01	0	0	0
NO2		0	0	1.45362e-07	1.6841e-10	0	0	0	0
NO		0	0	3.95089e-05	1.24981e-08	0	0	0	0
N2O		0	0	5.32429e-10	6.42088e-10	0	0	0	0
C1		0	0	4.96744e-30	0	0.931	0	0	0
C2		0	0	0	0	0.032	0	0	0
C3		0	0	0	0	0.007	0	0	0
C4		0	0	0	0	0.004	0	0	0
TEG		0	0	0	0	0	0	0	0
+ **Mass Flows**	**tonne/day**	**1256.07**	**314.124**	**380.062**	**510.684**	**74.4072**	**950.418**	**305.655**	**1265.29**

Appendix A.3 Description of the ASU and CPU Layout and Operating Parameters of Different Studies for Equipment Cost Estimation

Air Separation Unit dataset

Chemical & Engineering News (C&EN) [108]

Description: A conventional dual-pressure double column cryogenic ASU

Source of information: Reprinted from another paper. (The exact cost aggregate not specified)

ASU conditions: Only plant capacity specified.

Reported Cost Year: 2008 (updated using CEPCI)

Reported cost currency: $

European Cement Research Academy (ERCA) CEMCAP Project [109]

Description: The report is based on ASU required for oxyfuel and calcium looping CO_2 capture technologies from cement production.

Source of information: Scaled from another report with 40bar O_2 and removed O_2 compression cost. Cost used in analysis is the reported equipment and installation cost.

ASU conditions: 95% oxygen at 1.5 bar, sizes; 436 ton/d, 1163.4 ton/day and 1359.9 ton/d

Conversion: 1 ton = 0.907 tonne

Reported Cost Year: 2014 (updated using CEPCI)

Reported cost currency: € (OECD year conversion 0.753 € = 1 $)

Hamelinck *et al* paper [107]

Description: Oxygen required for Fischer–Tropsch diesel production from biomass gasification system.

Source of information: Cost reported from another source with best oxygen cost price fit. (The exact aggregate not specified)

ASU conditions: 99.5% oxygen at 1 bar; 576 tonne/day

Reported Cost Year: 2002 (updated using CEPCI)

Reported cost currency: € (OECD year conversion 0.88 € = 1 $)

Callide Oxyfuel Project [84]

Description: Oxygen required for oxyfuel combustion of coal for electricity generation

Source of Information: the project capital cost was reported, (the exact aggregate not specified)

ASU conditions: 98% oxygen at 1.8 bar; 660 tonne/day

Reported Cost Year: 2012 (updated using CEPCI)

Reported cost currency: AUD (OECD year conversion 0.966 AUD = 1 $)

NETL 2011 report [111]

Description: Oxygen required for Integrated Gasification Combined Cycle

Source of Information: Cost estimated from a combination of vendor quotes and simulation results. Cost used in analysis is the reported equipment cost, with material and labour costs, excluding engineering and contingencies fees.

ASU conditions: 95% oxygen at 8.6 bar; 152,191 kg/hr (2 trains)

Reported Cost Year: 2007 (updated using CEPCI)

NETL 2019 report [112]

Description: Oxygen required for different Integrated Gasification Combined Cycle configurations

Source of Information: Estimated from previous published data and vendor in house data. Cost used in analysis is the reported equipment cost, excludes material and labour costs, engineering, and contingencies.

ASU conditions: 95% oxygen at 51bar; 152710, 153619, 164733, 174406, 178678 kg/hr (2 trains)

Reported Cost Year: 2018 (updated using CEPCI)

Reported cost currency: US$

NETL 2012 report [113]

Description: Oxygen required for Oxycombustion Technology for Bituminous Coal Power Plants

Source of Information: ASU cost scaled from quote from Air Liquide. Cost used in analysis is the reported equipment cost, excludes material and labour costs, engineering, and contingencies.

ASU conditions: 95% oxygen at 1.6 bar; 486703, 533240, and 539798 kg/hr (2 trains)

Reported Cost Year: 2007 (updated using CEPCI)

Reported cost currency: US$

NETL 2017 report [101]

Description: Oxygen required for oxycombustion pulverized coal plant

Source of Information: Cost estimated from existing quote. Cost used in this analysis is the reported equipment cost, excludes material and labour costs, engineering, and contingencies.

ASU conditions: 95% oxygen at 1.6 bar; 525695 kg/hr (2 trains)

Reported Cost Year: 2011 (updated using CEPCI)

Reported cost currency: US$

CO_2 Purification Unit dataset

McKaskle *et al* [115]

Description: CO_2 compression of fermentation emissions from ethanol plants

Source of Information: Reported cost includes purchased equipment based only on vendor quotes for similar projects and in-house bottom-up cost estimation.

CPU conditions: Compression to 21.3 bar, cooling and pumping to 138.8 bar, molecular sieve dryer for dehydration, distillation for non condensable gas separation.

Reported Cost Year: 2014 (updated using CEPCI)

Reported cost currency: US$

NETL 2014 [71]

Description: CO_2 compression of fermentation emissions from ethanol plants

Source of Information: Vendor quote for 5 stage reciprocating compressor. Ductwork, piping, and instruments cost also included. Cost used in this analysis is the reported bare erect cost.

CPU conditions: compression and cooling only of 100% fermentation CO_2 to 153 bar

Reported Cost Year: 2011 (updated using CEPCI)

Reported cost currency: US$

Illinois Basin – Decatur Project (IBDP) [78]

Description: CO_2 compression of fermentation emissions from ethanol plants

Source of Information: Cost reported for equipment cost in project execution. Cost used in this analysis includes the purchased equipment cost of compression and dehydration, instrumentation and controls, and electrical systems.

CPU conditions: Compression and cooling to 97 bar, TEG dehydration, intercooler, and scrubbers and pumping to 135 bar.

Reported Cost Year: 2009 (updated using CEPCI)

Reported cost currency: US$

American Physics Society (APS) report [116]

Description: CO_2 compression from Direct air capture (DAC)

Source of Information: The cost reported is purchased equipment cost of compression equipment based on industrial experience.

CPU conditions: Compression only to 100atm

Reported Cost Year: 2009 (updated using CEPCI)

Reported cost currency: US$

NETL 2017 report [101]

Description: CO_2 capture from oxycombustion pulverized coal plant

Source of Information: Cost estimated from existing quote. Cost used in this analysis is the reported equipment cost, excludes material and labour costs, engineering, and contingencies.

CPU conditions: Compression to 30 bar, drying and distillation and pumping to 152.7 bar

Reported Cost Year: 2011 (updated using CEPCI)

Reported cost currency: US$

Appendix B.1 APEA Detailed Cost Estimation

The detailed cost estimation from Aspen Process Economic Analyzer is given here. Direct cost includes installation cost of piping, civil, electrical, etc. and man hours and manpower costs

```
Equipment mapped from '4EF-EVAP.B2'.

       Evaporator 4Eff.B2           GC -    8 A2

              COMPONENT  DATA  SHEET

                   RECIP GAS

CODE OF ACCOUNT:     152

COMPONENT DESIGN DATA:
        Material                                  CS
        Actual gas flow rate Inlet          35386.76 CFM
        Design gauge pressure Outlet          141.81 PSIG
        Design temperature Inlet              182.18 DEG F
        Design gauge pressure Inlet           -8.818 PSIG
        Driver power                         6692.00 HP
        Total weight                          439900 LBS

COST DATA:
        ESTIMATED PURCHASE COST USD    5267600.
```

	---MATERIAL---	*** M A N P O W E R ***		L/M RATIO
	USD	USD	MANHOURS	USD/USD
EQUIPMENT&SETTING	5267600.	112084.	3238	0.021
PIPING	104735.	21789.	641	0.208
CIVIL	128210.	70817.	2546	0.552
STRUCTURAL STEEL	0.	0.	0	0.000
INSTRUMENTATION	43986.	11141.	323	0.253
ELECTRICAL	0.	0.	0	0.000
INSULATION	8094.	6053.	236	0.748
PAINT	916.	2281.	89	2.490
SUBTOTAL	5553542.	224165.	7073	0.040

INSTALLED DIRECT COST 5777700. INST'L COST/PE RATIO 1.097

Equipment mapped from 'B1'.

PreEvaporation B1 GC - 10 A

COMPONENT DATA SHEET

RECIP GAS

CODE OF ACCOUNT: 152

COMPONENT DESIGN DATA:

Material	CS
Actual gas flow rate Inlet	17782.40 CFM
Design gauge pressure Outlet	-0.000600 PSIG
Design temperature Inlet	171.30 DEG F
Design gauge pressure Inlet	-8.587 PSIG
Driver power	688.60 HP
Total weight	45900 LBS

COST DATA:

ESTIMATED PURCHASE COST USD 861200.

	MATERIAL	*** MANPOWER ***		L/M RATIO
	USD	USD	MANHOURS	USD/USD
EQUIPMENT&SETTING	861200.	18263.	528	0.021
PIPING	68657.	17881.	527	0.260
CIVIL	13378.	7599.	275	0.568
STRUCTURAL STEEL	0.	0.	0	0.000
INSTRUMENTATION	43445.	11141.	323	0.256
ELECTRICAL	0.	0.	0	0.000
INSULATION	7179.	5390.	210	0.751
PAINT	801.	2084.	82	2.602
SUBTOTAL	994660.	62358.	1945	0.063

INSTALLED DIRECT COST 1057000. INST'L COST/PE RATIO 1.227

Equipment mapped from 'B16'.

Liquefaction B16 GC - 12 A

COMPONENT DATA SHEET

RECIP GAS

CODE OF ACCOUNT: 152

COMPONENT DESIGN DATA:

Material	CS	
Actual gas flow rate Inlet	5981.06	CFM
Design gauge pressure Outlet	60.10	PSIG
Design temperature Inlet	184.17	DEG F
Design gauge pressure Inlet	-0.00100	PSIG
Driver power	1012.00	HP
Total weight	62600	LBS

COST DATA:

ESTIMATED PURCHASE COST USD 1127200.

	MATERIAL	*** MANPOWER ***		L/M RATIO
	USD	USD	MANHOURS	USD/USD
EQUIPMENT&SETTING	1127200.	23429.	677	0.021
PIPING	35584.	12602.	371	0.354
CIVIL	18245.	10175.	367	0.558
STRUCTURAL STEEL	0.	0.	0	0.000
INSTRUMENTATION	43986.	11141.	323	0.253
ELECTRICAL	0.	0.	0	0.000
INSULATION	5263.	4156.	162	0.790
PAINT	564.	1476.	58	2.616
SUBTOTAL	1230842.	62980.	1958	0.051

INSTALLED DIRECT COST 1293800. INST'L COST/PE RATIO 1.148

Equipment mapped from 'B17'.

BeerColumn B17 GC - 39 a

COMPONENT DATA SHEET

RECIP GAS

CODE OF ACCOUNT: 152

COMPONENT DESIGN DATA:

Material	CS	
Actual gas flow rate Inlet	11445.86	CFM
Design gauge pressure Outlet	161.65	PSIG
Design temperature Inlet	187.40	DEG F
Design gauge pressure Inlet	5.303	PSIG
Driver power	3680.00	HP
Total weight	261200	LBS

	:---MATERIAL---:	*** M A N P O W E R ***:		L/M RATIO :
	: USD :	USD	MANHOURS	:USD/USD :
EQUIPMENT&SETTING	: 1401500. :	25774.	743	: 0.018 :
PIPING	: 73072. :	22127.	652	: 0.303 :
CIVIL	: 17073. :	9862.	358	: 0.578 :
STRUCTURAL STEEL	: 0. :	0.	0	: 0.000 :
INSTRUMENTATION	: 54596. :	27771.	806	: 0.509 :
ELECTRICAL	: 7391. :	8099.	243	: 1.096 :
INSULATION	: 3119. :	2023.	79	: 0.649 :
PAINT	: 2533. :	7385.	301	: 2.915 :
SUBTOTAL	: 1559283. :	103041.	3182	: 0.066 :

INSTALLED DIRECT COST 1662300. INST'L COST/PE RATIO 1.186

Appendix C.1 Main Assumptions of Economic Analysis

Economic parameters	Assumed basis
Basis year for analysis	2020
Debt/equity for plant financing	60%/40%
Interest rate and term for debt financing	8%/10 years
Internal rate of return for equity financing	10%
Total income tax rate	21%
Plant life	20 years
Construction period	3 years
Fixed capital expenditure schedule (years 1–3)	32% in year 1, 60% in year 2, 8% in year 3
Start-up time	0.5 year
Revenues during startup	50%
Variable costs during startup	75%
Fixed costs during startup	100%
Outside battery limit (OSBL) costs	10.5% of ISBL
Total installed cost (TIC)	Total of ISBL and OSBL costs
Indirect costs	% TIC
Prorated expenses	10%
Home office and construction fees	25%
Field expenses	10%
Project contingency	10%
Total plant cost (TPC)	TIC + Indirect Costs
Other costs (start-up and permitting)	10 % TPC
Total capital investment (TCI)	TPC + Other costs
Working capital	5% TPI

Appendix C.2 LCFS Credits Calculation

The credits generated under California's LCFS program is calculated using the following formula (See Dees *et al.* [61])

$$Credits\ (MT) = \left(CI_{standard} - CI_{reported}\right) \times E_{displaced}\ \times \mathrm{C}$$

Where:

$Credits\ (MT)$ is the number of LCFS credits generated

$CI_{standard}$ is the average carbon intensity requirement of the reference fuel (gasoline)

$CI_{reported}$ is the carbon intensity value of EtOH in gCO_2e/MJ

$E_{displaced}$ is the total quantity of gasoline displaced in MJ

C is a factor used to convert credits to units of tonnes from gCO_2e and has the value of:

$$C = 1.0 \times\ 10^{-6}\ \frac{(MT)}{(gCO2e)}$$